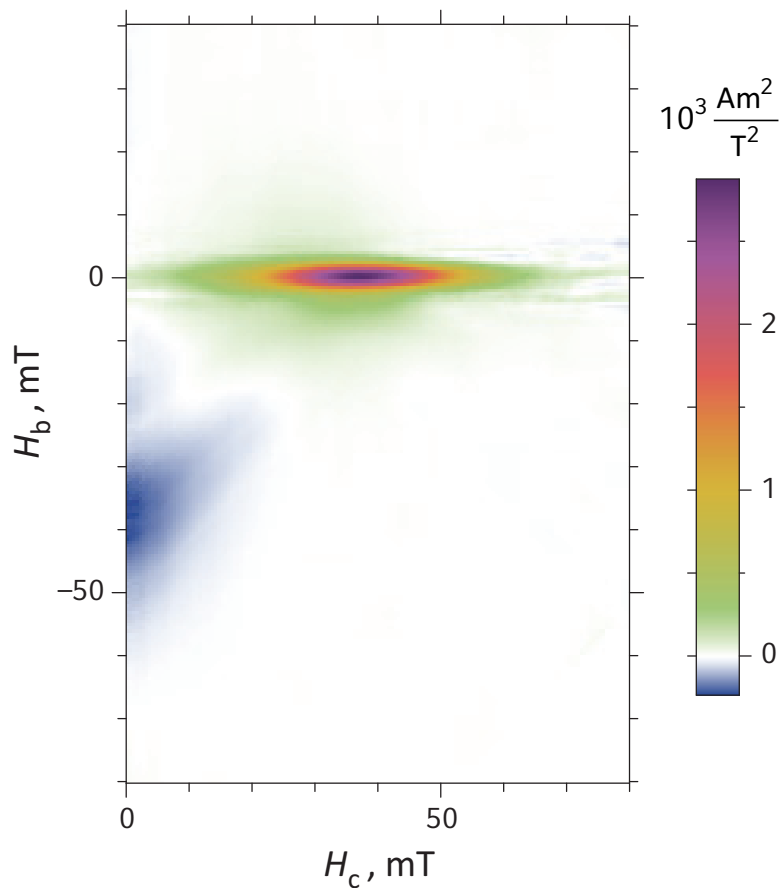


## VARIFORC User Manual

### Chapter 4:

## Calculate FORC diagrams





## Table of contents

|                                                                                                  |              |
|--------------------------------------------------------------------------------------------------|--------------|
| <b>4.1 CalculateFORC highlights .....</b>                                                        | <b>4-4</b>   |
| <b>4.2 Using CalculateFORC .....</b>                                                             | <b>4-6</b>   |
| <b>4.3 CalculateFORC file management .....</b>                                                   | <b>4-10</b>  |
| <b>4.4 Editing CalculateFORC options .....</b>                                                   | <b>4-15</b>  |
| <b>4.5 Full references to CalculateFORC options .....</b>                                        | <b>4-17</b>  |
| INPUT 01. Source data .....                                                                      | 4-18         |
| INPUT 02. Output function (updated) .....                                                        | 4-21         |
| INPUT 03-04. FORC output range (updated) .....                                                   | 4-23         |
| INPUT 05. Diagonal trim factor .....                                                             | 4-27         |
| INPUT 06. Output mesh size .....                                                                 | 4-29         |
| INPUT 07. Output grid origin .....                                                               | 4-32         |
| INPUT 08. Regularize field measurements (updated) .....                                          | 4-34         |
| INPUT 09. Weighted margin of polynomial regression rectangles (updated) .....                    | 4-37         |
| INPUT 10-11. Horizontal and vertical smoothing specifications (updated) .....                    | 4-41         |
| INPUT 12-13. Horizontal and vertical smoothing factor limits at given $H_c$ and $H_b$ (new) .... | 4-48         |
| INPUT 14. Diagonal smoothing factor limit near coercive fields (new) .....                       | 4-56         |
| INPUT 15-16. Diagonal smoothing factor limits at given $H$ and $H_r$ (updated) .....             | 4-62         |
| INPUT 17. Mean field correction parameters (new) .....                                           | 4-66         |
| INPUT 18. Error plots and significance threshold (updated) .....                                 | 4-75         |
| INPUT 19. Error matrix size limit .....                                                          | 4-80         |
| INPUT 20. Outlier detection threshold .....                                                      | 4-81         |
| INPUT 21. Clip negative coercivity distribution values .....                                     | 4-82         |
| INPUT 22. Confidence interval of coercivity distributions .....                                  | 4-84         |
| INPUT 23. FORC diagram ticks specifications .....                                                | 4-85         |
| INPUT 24. FORC diagram color saturation .....                                                    | 4-87         |
| INPUT 25. FORC diagram color scale clipping .....                                                | 4-88         |
| <b>4.6 Data formats exported by CalculateFORC .....</b>                                          | <b>4-91</b>  |
| <b>4.7 Literature .....</b>                                                                      | <b>4-100</b> |

## 4.1 CalculateFORC highlights

CalculateFORC is the main module of the VARIFORC package. It calculates FORC diagrams and related coercivity distributions from FORC measurements previously imported, corrected, and cleaned with the VARIFORC module ImportFORC (see Chapter 3 of this manual). Like other VARIFORC modules, CalculateFORC is controlled by user-defined options stored in a special parameter file that can be used for batch processing. The CalculateFORC workflow (Fig. 4.1) is based on the following processing steps, with unique features highlighted in *cursive*.

- 1) Define FORC diagram ranges automatically or by explicit limits. Automatic settings include the rectangular FORC space foreseen by the FORC measurement protocol [Pike et al., 1999].  
*The FORC space can be extended to all FORC measurements, taking advantage of intrinsic features of the FORC function.*
- 2) Calculate FORC matrices over *user-defined output grids*, independently of FORC measurement details, and without using intermediate regridding steps. *Compatible grids enable direct combination of different FORC datasets, e.g. for calculating averages and magnetization differences [e.g. Ludwig et al., 2013] without further interpolation steps* (see Chapter 7).
- 3) Offer regular and *advanced* smoothing options for calculating FORC diagrams, *using the VARIFORC protocol of Egli [2013] for optimal noise suppression* (updated in version 2.0).
- 4) *Support the calculation of other functions in FORC space (e.g. single and double derivatives). This option is useful for diagnostic purposes.*
- 5) *Calculate two types of coercivity distributions associated with magnetization curves defined by particular FORC measurement subsets, i.e. (a) the backfield or DC demagnetization, and (b) the irreversible component of the upper hysteresis loop branch.*
- 6) *Perform mean field corrections and simulate mean field effects* (new in version 2.0).
- 7) *Calculates different types of magnetizations related to FORC measurements by integrating the FORC function over special regions of the FORC space. These magnetizations serve as basis for quantitative FORC analyses and for comparison with conventional magnetic parameters* (see Chapter 8).
- 8) Export FORC matrices and coercivity distribution data for further processing, such as central ridge extraction with CalculateCR.

Use this manual to learn about CalculateFORC, and see the quick VARIFORC guide for a short summary and option reference. Refer to the FORC tutorial included in this manual (Chapter 8) for topical examples obtained with CalculateFORC.

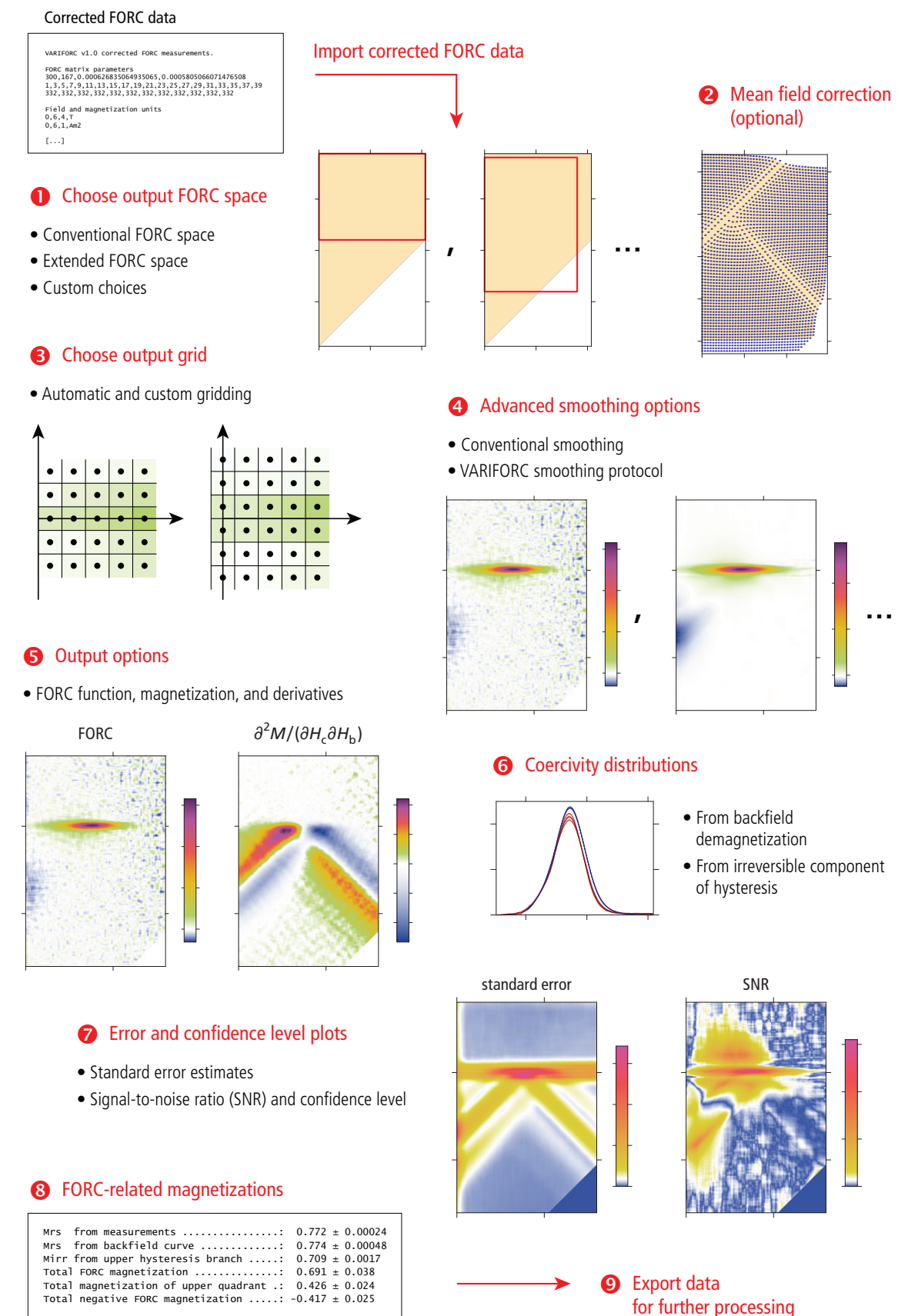


**Fig. 4.1:** Graphical representation of the typical CalculateFORC workflow.

## 4.2 Using CalculateFORC

Like all VARIFORC modules, CalculateFORC runs on a Wolfram Mathematica® Notebook. A starting copy of this notebook is provided with the VARIFORC installation package under:

```
VARIFORC_Install/Modules/ImportFORC/VARIFORC_calculateFORC.cdf
```

You can copy this file to a different folder for your convenience. The notebook stores all processing steps and graphical results; therefore, it is best renamed and saved with reference to the processed FORC data. The default notebook provided with the installation package is a .cdf file (computable document format) that works with both Wolfram Mathematica® and PlayerPro®. The content of a .cdf notebook cannot be modified with Player Pro®, but existing commands can be evaluated and results saved without restrictions. The .cdf notebook can be saved as a regular notebook (.nb) with Wolfram Mathematica®.

CalculateFORC notebooks begin with the following command line:

```
Get[FileNameJoin[{\$HomeDirectory, "VARIFORC", "VARIFORC_CalculateFORC_code.txt"}]]
```

which uploads CalculateFORC to the computation kernel. This line, as any other command in Mathematica® notebooks, is executed by placing the cursor on it and pressing the keys **SHIFT** and **ENTER** at the same time. A copyright message will appear below this line, confirming that CalculateFORC has been uploaded successfully.

CalculateFORC is then called by the command line

```
VARIFORC`CalculateFORC
```

to be executed by pressing the keys **SHIFT** and **ENTER** at the same time. At this point, CalculateFORC starts a system dialog for:

- 1) uploading a parameter file that contains user-defined processing options,
- 2) uploading corrected FORC measurements created by ImportFORC, and
- 3) choosing output files where results are stored.

The notebook appearance upon performing these steps is shown in [Fig. 4.2](#).

Files required by steps 1) and 2) should be ready before CalculateFORC is started. The parameter file is an unformatted text file containing all processing options to be used by CalculateFORC. You can find a template of this file with generically valid options in the VARIFORC installation package under:

```
VARIFORC_Install/Modules/CalculateFORC/Default_VARIFORC_CalculateFORC_Parameters.txt
```

You may copy this file to a directory hosting all VARIFORC processing files related to given FORC measurements. Parameters in this file can be modified with a text editor, according to your processing requirements (see [section 4.4](#) and the VARIFORC quick guide). File upload and output file naming are explained in [section 4.3](#).

**1** Upload source codes

```
In[1]:= Get[FileNameJoin[{$HomeDirectory, "VARIFORC", "VARIFORC_CalculateFORC_code.txt"}]]
Function VARIFORC`CalculateFORC for importing FORC measurements.
[VARIFORC package v1.0 for Wolfram Mathematica and Mathematica Player Pro.
© 2014 by Ramon Egli. All rights reserved.]
```

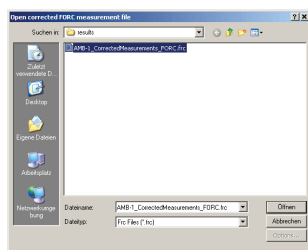
If used for scientific publications and presentations please cite as follows:  
Egli, R. (2013). VARIFORC: An optimized protocol for calculating non-regular first-order reversal curve (FORC) diagrams. *Global and Planetary Change* 110, 302-320.  
<http://dx.doi.org/10.1016/j.gloplacha.2013.08.003>

**2** Call CalculateFORC

```
In[2]:= VARIFORC`CalculateFORC
```

**3** Read auxiliary files

Initialization...

**4** Upload parameter file**5** Upload corrected measurement file**6** Define output file(s)**7** Begin processing

Read parameter file...

```
Input parameters from C:/.../Example/CalculateFORC_Parameters.txt:
INPUT 01. Source data type .....; FORC
INPUT 02. Output function .....; FORC
INPUT 03. Horizontal range of output FORC space .....; 0, 80
INPUT 04. Vertical range of output FORC space .....; -80, 40
INPUT 05. Diagonal trim factor .....; 0.5
INPUT 06. Output mesh size .....; 0.5
INPUT 07. Output grid origin .....; Automatic
INPUT 08. Use field measurements .....; Yes
INPUT 09. Weighted margin of polynomial regression rectangles ; 1
INPUT 10. Horizontal smoothing specifications .....; 10, 10, 0.06
INPUT 11. Vertical smoothing specifications .....; 10, 14, 0.06
INPUT 12. Central ridge specifications .....; 0.5, 0.8
INPUT 13. Smoothing factor limits along remanence diagonal ; None
INPUT 14. Plotted error parameter .....; SNR, 3
INPUT 15. Error matrix size limit .....; 2000
INPUT 16. Outlier detection threshold .....; 2.5
INPUT 17. Clip negative coercivity distribution values .....; Yes
INPUT 18. Confidence interval factor for distribution plots....; 2
INPUT 19. FORC plot ticks specifications .....; 0.05, 5
INPUT 20. Color scale saturation .....; 0.9
INPUT 21. Quantile for color scale clipping .....; 0.01
```

**Fig. 4.2:** Initialization of the CalculateFORC notebook (example with version 1.0).

After completing file upload and saving dialogs, CalculateFORC proceeds autonomously until the end, without requesting any further action by the user. The processing status is continuously updated by status messages, e.g.

Prepare output grid ...

warning messages, e.g.

WARNING. Upper H<sub>c</sub>-limit of the output grid is not entirely covered by measurement points.

error messages, e.g.

No CalculateFORC parameter file has been chosen. Program aborted.

summary tables, e.g.

**Summary of FORC magnetizations in Am<sup>2</sup>:**

|                                         |                                         |
|-----------------------------------------|-----------------------------------------|
| Mrs from measurements .....             | : 0.7721 ± 0.000240                     |
| Mrs from backfield curve .....          | : 0.7744 ± 0.000475, SNR>1 only: 0.7758 |
| Mirr from upper hysteresis loop .....   | : 0.7086 ± 0.001743, SNR>1 only: 0.7147 |
| Total FORC magnetization .....          | : 0.6908 ± 0.037778, SNR>1 only: 0.6908 |
| Total magnetization of upper quadrant : | 0.4261 ± 0.023772, SNR>1 only: 0.4261   |
| Total negative contributions .....      | -0.4175 ± 0.025184, SNR>1 only: -0.4175 |

and diagnostic plots as well as plots of final results. CalculateFORC ends with the following message containing the total computation time:

PROGRAM END. Total computation time 5m 6s.

You can save the notebook file with all messages and plots for your records and re-use it.

CalculateFORC error messages usually produce a program abort. If one of these messages appears, an error was encountered either in the parameter file, e.g.:

Unrecognized source data designation. Program aborted [INPUT 01].

or in the corrected measurements file, e.g.:

Error encountered in reading FORC data file (FORC protocol parameters).  
Valid files must be produced by ImportFORC! Program aborted.

or during evaluation:

Right H<sub>c</sub>-limit of the output grid is not sufficiently covered by measurement points!  
Program aborted.

Corrected measurement files produced by ImportFORC within the same VARIFORC release are fully compatible and do not generate reading errors unless accidentally modified. Newer CalculateFORC versions can read files produced by older ImportFORC versions, as well as older parameter file versions (full backward compatibility).

Error messages contain hints about the encountered problem. Errors generated by the parameter file arise from incorrect option specifications (see [section 4.5](#) for acceptable options), or by a corrupted file format. In the latter case, generate a new parameter file from the original copy

provided with the installation package. Evaluation errors are generated by improper parameter choices (e.g. overcorrection of negative mean fields yielding negative field steps).

- Large parts of the CalculateFORC code are dedicated to error handling in order to avoid unexpected crashes or incorrect results. Although VARIFORC functions have been extensively tested, the occurrence of unexpected errors cannot be completely excluded. Such errors might generate a cascade of other errors and/or a program crash.
- Unexpected errors likely cause Mathematica® notebooks to freeze. In this case, the Mathematica® Kernel should be forcefully terminated as described in Chapter 2.

- 💡 All information concerning CalculateFORC runs is stored in the Mathematica® notebook. You can save the notebook with its content for your records.
- 💡 Use only one Mathematica® notebook at the time.
- 💡 In order to avoid excessive memory usage, process a single dataset in each notebook.
- 💡 The time required for conventional FORC processing ( $SF = 5$ ) of high-resolution FORC data (~162'000 measurements) with a 2.9 GHz dual core processor is <3 minutes.
- 💡 Much longer times are required for processing high-resolution FORC data with variable smoothing protocols, due to the large smoothing factors (e.g.  $SF = 30$ ) used over parts of the FORC space. High-resolution FORC data (~162'000 measurements) are processed in ~50 min in case of variable smoothing parameters typical for magnetofossil-bearing sediments (Windows 8.1 with 2.9 GHz dual core processor and 8 GB RAM).

## 4.3 CalculateFORC file management

VARIFORC has a modular structure, so that each module performs a specific operation by reading data stored in measurement files or files containing processed data, and exporting results to one or more files that can be used by other VARIFORC modules. CalculateFORC deals with the core of FORC processing by reading:

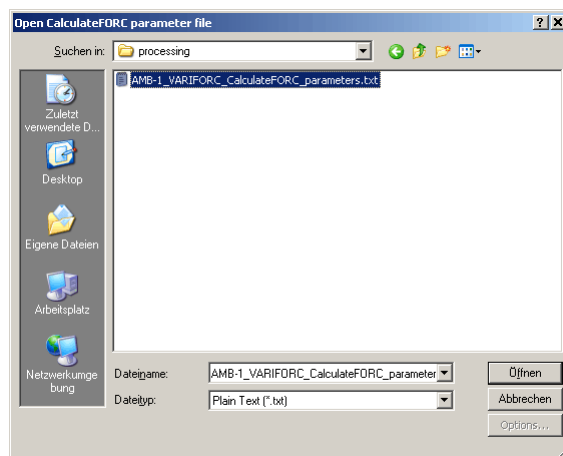
- 1) A text file containing user-defined processing parameters
- 2) Corrected FORC measurements created by ImportFORC as first processing step.

Results, in form of FORC matrices and coercivity distribution data, are exported to 2-6 files (depending on the chosen output type) with the same user-defined name root.

CalculateFORC calls the file dialog of your operating system in order to let you upload and export files, as described in the following.

### 4.3.1 Parameter file upload

The parameter file is uploaded through the following dialog window:



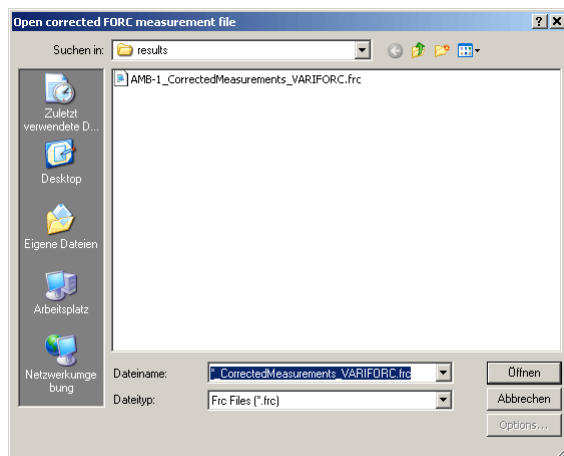
whose detailed appearance depends on your operating system. CalculateFORC automatically selects file names ending with VARIFORC\_CalculateFORC\_parameters.txt, which is default for all CalculateFORC parameter files. It is strongly recommended to keep this file name ending, so to avoid confusion with parameter files of other VARIFORC modules. The first part of the file name can be related to the sample being processed, e.g.:

```
/.../Sample01_VARIFORC_CalculateFORC_parameters.txt
```

If you do not find the parameter file in the expected directory, remove file name and file type filters, so that all files will be displayed.

### 4.3.2 Corrected measurement file upload

Corrected measurements files (created by the VARIFORC module ImportFORC as first processing step) are uploaded through the following dialog window:

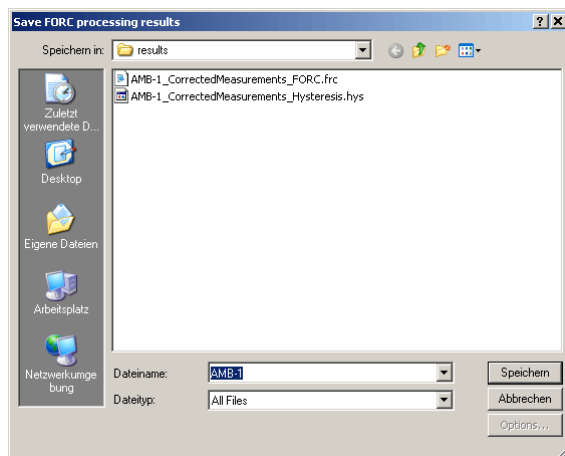


whose detailed appearance depends on your operating system. Be careful to choose a single corrected measurement file. Only file names ending with `CorrectedMeasurements_VARIFORC.frc` or `CorrectedMeasurementsDifferences_VARIFORC.frc` are displayed, according to the format type (corrected measurement or corrected measurement differences) specified in the parameter file (see [section 4.5](#)).

- CalculateFORC does not import raw measurements files. It only accepts corrected measurement files created by ImportFORC. Therefore, measurements must be imported with ImportFORC at first instance, before proceeding with CalculateFORC.
- ImportFORC preprocessing allows you to perform several corrections and define the unit system to be used for the calculation of FORC diagrams, coercivity distributions and related parameters.

### 4.3.3 Output file naming

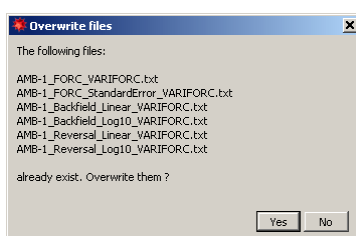
A root name for all output files created by CalculateFORC is entered through the following file saving dialog:



whose detailed appearance depends on your operating system. A name taken from the chosen corrected measurement file is proposed by default. Adopt this name or type a different name, without extension. The chosen name will be used as a common root for defining output file names by appending appropriated extensions.

- Default output file names suggested by CalculateFORC do not contain any reference to the chosen processing parameters (which, however, are stored in output files containing the FORC matrix).
- If you want to process the same FORC measurements with different parameter sets, extend the suggested file root name with hints to the chosen options (e.g. smoothing parameters), so that files produced by successive CalculateFORC runs will not be overwritten. If chosen file names already exist, CalculateFORC will open an overwrite file dialog (see below).

If output files with the same name (produced for instance by previous runs) are encountered, CalculateFORC opens the following overwrite file dialog:



If you choose to overwrite existing files, CalculateFORC will continue processing without further

input requests. Otherwise, the program is aborted and you should run it again with different output file names.

If "AMB-1" is the file name root entered with the file saving dialog, as in the above example, the following output files will be generated:

- 1) `/.../AMB-1_Backfield_Linear_VARIFORC.txt` for the coercivity distribution (on a linear field scale) derived from backfield demagnetization data contained in FORC measurements.
- 2) `/.../AMB-1_Backfield_Log10_VARIFORC.txt` for the coercivity distribution (on a logarithmic field scale) derived from backfield demagnetization data contained in FORC measurements.
- 3) `/.../AMB-1_Reversal_Linear_VARIFORC.txt` for the coercivity distribution (on a linear field scale) derived from irreversible magnetization changes occurring at reversal fields (i.e. along the upper branch of the hysteresis loop).
- 4) `/.../AMB-1_Reversal_Log10_VARIFORC.txt` for the coercivity distribution (on a linear field scale) derived from irreversible magnetization changes occurring at reversal fields (i.e. along the upper branch of the hysteresis loop).
- 5) `/.../AMB-1_FORC_VARIFORC.txt` for the output FORC matrix over the chosen FORC space.
- 6) `/.../AMB-1_FORC_StandardError_VARIFORC.txt` for the standard error of the output FORC matrix.

If a parameter other than the FORC function has been chosen as output of CalculateFORC, files 1-4 will not be created, and the term `FORC` in file names 5-6 will be replaced by the name of the parameter being calculated (e.g. `Hc2` for the second derivative of FORC magnetization with respect to  $H_c$ ).

#### 4.3.4 Folder organization

Because of the relatively large number of files produced by VARIFORC modules, VARIFORC input and output files are best organized in folders, depending on the purpose of FORC processing. If FORC measurements are used to characterize individual samples, each with different FORC protocols and processing requirements, you might create a folder system for each sample. For example, possible folders related to a sample named spec01 are:

/.../spec01/measurements/

for storing one or more measurements,

/.../spec01/processing/

for storing the CalculateFORC notebook (e.g. Spec01\_CalculateFORC.nb) and the corresponding parameter file (e.g. Spec01\_VARIFORC\_CalculateFORC\_parameters.txt), and

/.../spec01/results/

for storing processing results (e.g. Spec01\_CorrectedMeasurements\_VARIFORC.frc), along with those created by ImportFORC.

CalculateFORC will remember these directories, which are automatically opened during the next run. If you use CalculateFORC for the first time, or VARIFORC system files have been damaged, the following message appears

```
directory log file C:\...\VARIFORC_CalculateFORC_Directories.txt is incomplete!
VARIFORC_CalculateFORC continues with default directories and creates a new log file.
```

and default directories will be chosen.

If systematic measurements of several samples are performed with the same FORC protocol, you might keep the folder structure discussed above and use just one parameter file for all samples (e.g. MyProtocol\_VARIFORC\_CalculateFORC\_parameters.txt).

#### 4.4 Editing CalculateFORC options

Version 2.0 of CalculateFORC is controlled by 25 parameters (21 in version 1.0) that are uploaded from a parameter file ending with `_VARIFORC_CalculateFORC_Parameters.txt`. This is an editable text file with a template provided with the installation package (see [section 4.2](#)). This template contains universal parameters that can be used with practically any type of FORC measurements. You can copy this file to any folder, e.g. the same folder containing the FORC data and/or the CalculateFORC Mathematica® notebook, and use it as is. Nevertheless, in order to exploit all CalculateFORC capabilities and obtain optimized results, you should adapt these parameters to your requirements. For this purpose, open the CalculateFORC parameter file with a text editor. You will see a table similar to the following example:

```
Input parameters for package VARIFORC_CalculateFORC; (version 2.04).  
  
INPUT 01. Source data type ..... ; FORC  
INPUT 02. Output function ..... ; FORC  
INPUT 03. Horizontal range of output FORC space ..... ; All  
INPUT 04. Vertical range of output FORC space ..... ; All  
INPUT 05. Trim factor along lower diagonal limit ..... ; 0.5  
INPUT 06. Output mesh size ..... ; Normal  
INPUT 07. Output grid origin ..... ; Automatic  
INPUT 08. Regularize field measurements ..... ; No  
INPUT 09. Weighted margin of polynomial regression rectangles ..... ; 2  
INPUT 10. Horizontal smoothing specifications ..... ; 5,0.07  
INPUT 11. Vertical smoothing specifications ..... ; 5,0.07  
INPUT 12. Horizontal smoothing factor limit at given Hc ( | ) ..... ; None  
INPUT 13. Vertical smoothing factor limit at given Hb ( - ) ..... ; None  
INPUT 14. Diagonal smoothing factor limit near coercive fields ( / \ ) .. ; None  
INPUT 15. Diagonal smoothing factor limit at given H ( \ ) ..... ; None  
INPUT 16. Diagonal smoothing factor limit at given Hr ( / ) ..... ; None  
INPUT 17. Mean field correction parameters ..... ; None  
INPUT 18. Significance threshold of signal-to-noise ratio ..... ; 3  
INPUT 19. Error matrix size limit ..... ; 2000  
INPUT 20. Outlier detection threshold ..... ; 5  
INPUT 21. Clip negative coercivity distribution values ..... ; Yes  
INPUT 22. Confidence interval of coercivity distribution plots ..... ; 2  
INPUT 23. FORC diagram ticks specification ..... ; Automatic  
INPUT 24. FORC diagram color saturation ..... ; 0.95  
INPUT 25. Fraction of FORC diagram pixels with clipped colors ..... ; 0.01
```

Each line of this table (except for the first one) consists of a parameter option description (e.g. INPUT 01. Source data type) followed by the corresponding parameter value or option specification (e.g. FORC). Parameters and option specifications are separated from their descriptions by a semicolon (;). Multiple parameters in the same row (e.g. smoothing specifications) are always separated by a colon (:) and spaces have no meaning. You can change these parameters according to the guidelines given in [section 4.5](#) and save the parameter file with an appropriated name related to its usage context.

**Example 1:** If you routinely perform high-resolution FORC measurements of sediment samples using the same protocol, you can process them with a consistent set of options recalled by CalculateFORC from a parameter file named `Sediment_highres_VARIFORC_CalculateFORC_Parameters.txt`.

**Example 2:** Processing parameters to be used only for corrected FORC measurements from `File_1_CorrectedMeasurements_VARIFORC.frc`, are conveniently stored in a parameter file called `File_1_VARIFORC_CalculateFORC_Parameters.txt`.

- Always save processing parameters as unformatted text files. If you use a text processor such as Microsoft Word, do not forget to save as text (.txt) only. Formatted texts are not recognized by CalculateFORC.
- Do not change the table structure; in particular, do not add new lines. Multiple parameters representing the same input (e.g. INPUT 10 Horizontal smoothing specifications) must be entered as a single line.
- Acceptable parameter formats are explained in detail in section 4.5. Incorrect or unrecognized formats generate error messages with reference to the corresponding input line (e.g. INPUT 01).

The following suggestions help you with an efficient management of CalculateFORC processing options:

- 💡 Several input parameters can be set to automatic options, letting CalculateFORC choose optimal values. Use automatic options if possible, unless you have specific processing requirements. For your convenience, the parameter file provided with the installation package is already based on automatic options whenever possible.
- 💡 Use consistent FORC protocols for your measurements, so that only few sets of processing parameters are required. For example, all magnetofossil-bearing sediments can be measured with the same protocol and processed with the same parameters.
- 💡 If you have generated an invalid parameter file and you do not know how to restore the proper format, create a new file starting from the template provided with the installation package. For this reason, never overwrite templates in the installation package.

## 4.5 Full references to CalculateFORC options

All CalculateFORC parameter options are described in this section. You can refer to the VARIFORC quick guide for a compact summary.

Table of contents:

|                                                                                                  |      |
|--------------------------------------------------------------------------------------------------|------|
| INPUT 01. Source data .....                                                                      | 4-18 |
| INPUT 02. Output function (updated) .....                                                        | 4-21 |
| INPUT 03-04. FORC output range (updated) .....                                                   | 4-23 |
| INPUT 05. Diagonal trim factor .....                                                             | 4-27 |
| INPUT 06. Output mesh size .....                                                                 | 4-29 |
| INPUT 07. Output grid origin .....                                                               | 4-32 |
| INPUT 08. Regularize field measurements (updated) .....                                          | 4-34 |
| INPUT 09. Weighted margin of polynomial regression rectangles (updated) .....                    | 4-37 |
| INPUT 10-11. Horizontal and vertical smoothing specifications (updated) .....                    | 4-41 |
| INPUT 12-13. Horizontal and vertical smoothing factor limits at given $H_c$ and $H_b$ (new) .... | 4-48 |
| INPUT 14. Diagonal smoothing factor limit near coercive fields (new) .....                       | 4-56 |
| INPUT 15-16. Diagonal smoothing factor limits at given $H$ and $H_r$ (updated) .....             | 4-62 |
| INPUT 17. Mean field correction parameters (new) .....                                           | 4-66 |
| INPUT 18. Error plots and significance threshold (updated) .....                                 | 4-75 |
| INPUT 19. Error matrix size limit .....                                                          | 4-80 |
| INPUT 20. Outlier detection threshold .....                                                      | 4-81 |
| INPUT 21. Clip negative coercivity distribution values .....                                     | 4-82 |
| INPUT 22. Confidence interval of coercivity distributions .....                                  | 4-84 |
| INPUT 23. FORC diagram ticks specifications .....                                                | 4-85 |
| INPUT 24. FORC diagram color saturation .....                                                    | 4-87 |
| INPUT 25. FORC diagram color scale clipping .....                                                | 4-91 |

### INPUT 01. Source data

CalculateFORC uses corrected FORC measurements exported by ImportFORC as data source for the calculation of FORC diagrams and coercivity distributions. ImportFORC produces two types of corrected FORC datasets that can be selected with INPUT 01. The default choice is

```
INPUT 01. Source data type ....; FORC
```

for uploading FORC measurements that have been corrected for drift, outliers, and (optionally) for paramagnetic/diamagnetic contributions ([Fig. 4.3a](#)). In special cases, much better results are obtained with FORC measurements after subtraction of the lower branch of the hysteresis loop ([Fig. 4.3c](#)). In this case, the source data consist of differences between measured curves and hysteresis, as calculated by ImportFORC, and are selected with

```
INPUT 01. Source data type ....; DFORC
```

When calling the file opening dialog, CalculateFORC automatically filters file names with appropriated endings according to INPUT 01 (i.e. `_CorrectedMeasurements_VARIFORC.frc` if INPUT 01 has been set to FORC, and `_CorrectedMeasurementDifferences_VARIFORC.frc` if INPUT 01 has been set to DFORC).

The reason for preferring FORC measurements with subtracted hysteresis is related to FORC processing difficulties encountered in case of discontinuous magnetization derivatives. This is for instance the case of [Fig. 4.3a](#), where all FORCs are characterized by a sharp slope increase at  $H=0$ , which is produced by single-domain magnetic particles with vanishing coercivity. Another common case is that of samples containing superparamagnetic particles with very small saturation fields.

Derivative discontinuities are not correctly fitted with polynomials and generate FORC diagrams that might contain significant artifacts. For example, the sharp slope increase at  $H=0$  in [Fig. 4.3a](#) generates artifacts along the so-called remanence diagonal (i.e.  $H_b = -H_c$ ) of FORC diagrams, especially if advanced processing options involving different smoothing factors along  $H_c$  and  $H_b$  are used ([Fig. 4.3b](#)). In most cases, similar derivative discontinuities occurring at the same applied fields in all measurements can be removed by subtracting a curve with same characteristics – such as the major hysteresis branch – from all measurements ([Fig. 4.3c](#)). Because subtraction of the same curve from all FORCs does not affect FORC calculations, processing artifacts related to derivative discontinuities are efficiently eliminated without alteration of the original FORC signal ([Fig. 4.3d](#)).

Inspection of the graphical results generated by ImportFORC upon importing raw FORC measurements is recommended before setting INPUT 01. The DFORC option should be used whenever abrupt slope changes can be recognized in the measured curves, or when suspect artifacts associated with large error estimates appear in FORC diagrams generated by CalculateFORC (e.g. [Fig. 4.3b](#)).

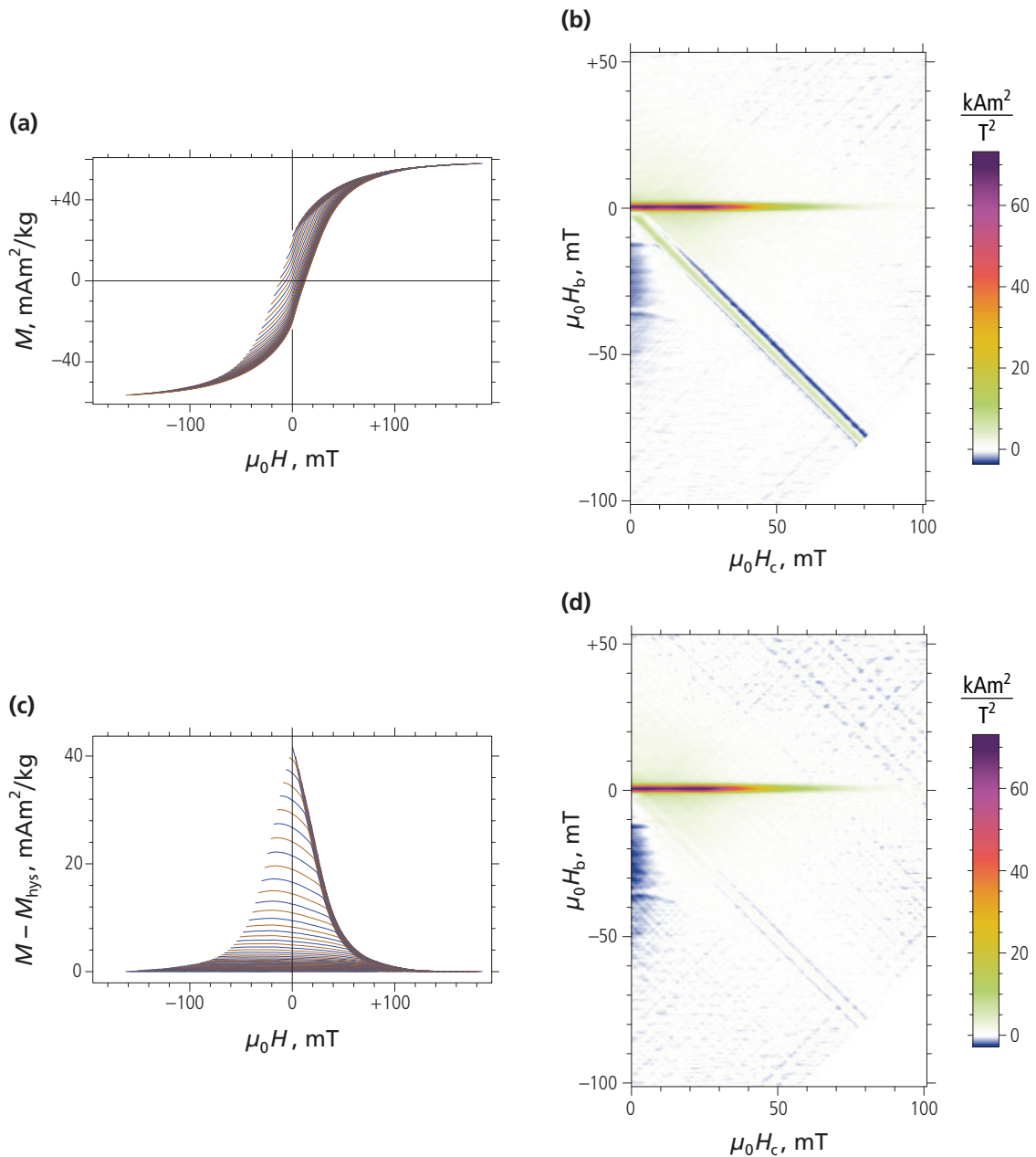


**Fig. 4.3:** Example of FORC measurements (left) and corresponding FORC diagrams (right) obtained with CalculateFORC from measurements of a sediment sample from the Indian Ocean. FORC diagrams have been calculated with constant smoothing factors of 8 and 4 along  $H_c$  and  $H_b$ , respectively: this choice is far from being optimal, and is used here only for demonstration purposes. **(a)** Corrected FORC measurements processed with ImportFORC. **(b)** FORC calculated from the measurements in (a). Strong processing artifacts occur along the remanence diagonal  $H_b = -H_c$ , as a consequence of the slope discontinuities near  $H = 0$  clearly seen in (a). **(c)** Modified FORC measurements obtained with ImportFORC upon subtraction of the lower hysteresis branch from all measurements. The resulting curves have regular derivatives near  $H = 0$ , which are correctly reproduced by polynomial regression. **(d)** FORC diagram obtained from the modified magnetization curves plotted in (c) upon setting INPUT 01 to DFORC. Processing artifacts along the remanence diagonal have disappeared. On the other hand, the noise level increased slightly with respect to the diagram obtained from regular measurements (a), as seen by negative diagonal stripes.

Generally, there are two main limitations to the systematic use of modified FORC measurements. First, clean subtraction of the lower hysteresis branch is only possible if FORC measurements are sufficiently extended, i.e. if the range of measured fields is such, that the last FORC starts at negative saturation, effectively coinciding with the lower branch of the major hysteresis loop (see Chapter 3). Second, the lower hysteresis branch reconstructed from FORC measurements contains noise that adds to the existing measurement errors. The increased noise level is clearly visible in Fig. 4.3d. In most cases, however, increased noise levels are compensated by the elimination FORC processing artifacts.

- The lower hysteresis branch is calculated by taking the envelope of FORC measurements as an approximation of the major hysteresis loop. Differences between this approximation and the real hysteresis loop are irrelevant for FORC processing purposes, as long as FORC measurements come sufficiently close to the saturation range. Otherwise, the reconstructed loop might contain artificial derivative discontinuities that are transferred to the modified FORC measurements.

- 💡 As a rule of thumb, regular FORC measurements should be used (i.e. INPUT 01 set to FORC) if these measurements appear as smooth curves without sharp slope discontinuities in plots generated by ImportFORC. Otherwise, FORC measurements with subtracted lower hysteresis branch (i.e. INPUT 01 is set to DFORC) should be used instead of regular ones.
- 💡 In some cases, real magnetization processes produce FORC features resembling derivative discontinuity artifacts [e.g. Acton *et al.*, 2007]. If such features are unaffected by the type of FORC data used (i.e. modified vs. unmodified FORC measurements), artifacts can be safely excluded.

## INPUT 02. Output function (updated)

INPUT 02 defines the function that should be calculated from FORC measurements and represented in FORC space. The standard choice is

```
INPUT 02. Output function ....; FORC
```

for obtaining the FORC function defined as:

$$\rho = -\frac{1}{2} \frac{\partial^2 M}{\partial H_r \partial H} = \frac{1}{8} \left[ \frac{\partial^2 M}{\partial H_c^2} - \frac{\partial^2 M}{\partial H_b^2} \right]$$

[Pike, 2003]. Other types of first and second derivatives with respect to the fields  $H_r$ ,  $H$ ,  $H_c$ , and  $H_b$  (e.g.  $\partial^2 M / (\partial H_c \partial H_b)$ ,  $\partial M / \partial H$ , etc.), as well as the measured magnetization itself, can be selected as output of CalculateFORC (Fig. 4.4). For example,

```
INPUT 02. Output function ....; H2
```

calculates the second derivative of FORCs with respect to the measurement field  $H$ . Such derivatives can serve as diagnostic tools for identifying the origin of unexplained FORC features or noise artifacts. An example of such applications is given in Egli [2013]. A full list of parameters that can be chosen as output function of CalculateFORC is given in Table 4.1.

**Table 4.1:** List of CalculateFORC output functions that can be obtained from FORC measurements  $M(H_r, H)$ . The fields  $H_c = (H - H_r)/2$  and  $H_b = (H + H_r)/2$  are the Cartesian coordinates of FORC space.

| INPUT 02 option | Output function                                                                   |
|-----------------|-----------------------------------------------------------------------------------|
| FORC            | $\rho = -\partial^2 M / (2 \partial H_r \partial H)$ (FORC function, Pike [2003]) |
| H2              | $\partial^2 M / \partial H^2$                                                     |
| Hr2             | $\partial^2 M / \partial H_r^2$                                                   |
| Hc2             | $\partial^2 M / \partial H_c^2$                                                   |
| Hb2             | $\partial^2 M / \partial H_b^2$                                                   |
| HcHb            | $\partial^2 M / (\partial H_c \partial H_b)$                                      |
| Hr              | $\partial M / \partial H_r$                                                       |
| H               | $\partial M / \partial H$                                                         |
| M               | $M$                                                                               |
| D               | $\partial M / \partial H_r + \partial M / \partial H$                             |

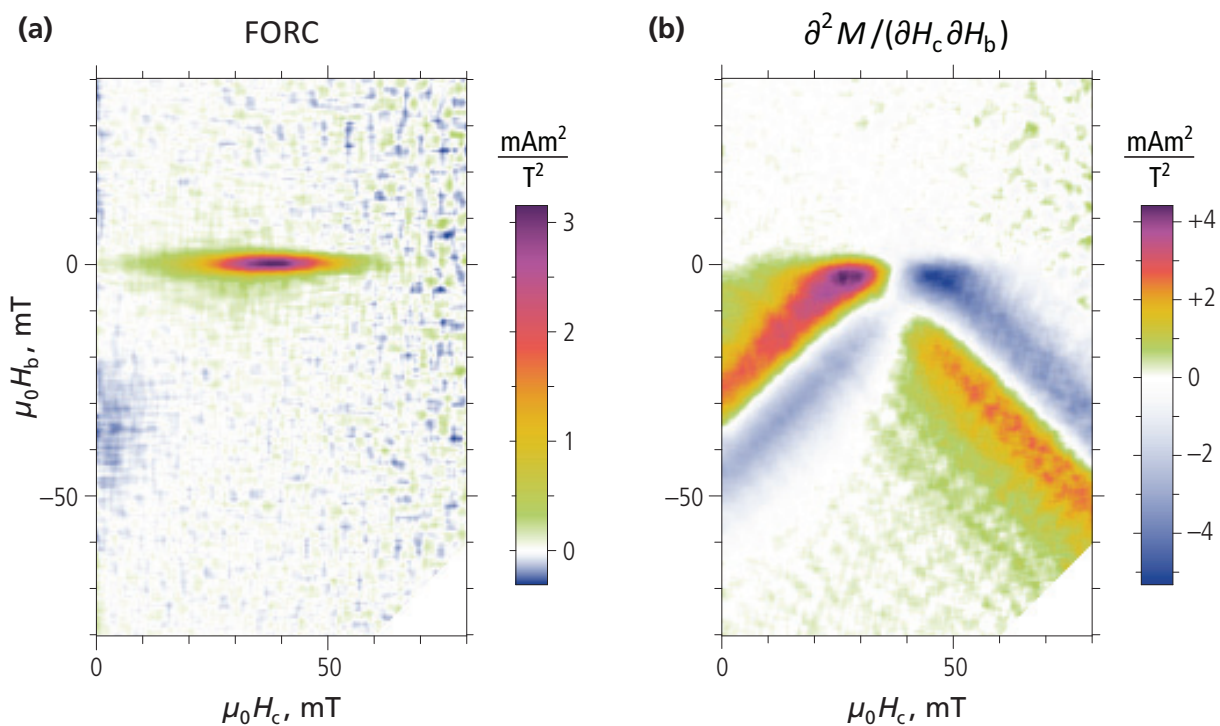


**Fig. 4.4:** CalculateFORC output function examples for measurements of cultured magnetotactic bacteria (see the downloadable example “Magnetospirillum 2”). **(a)** FORC diagram obtained with INPUT 02 set to FORC and conventional smoothing (SF = 5). **(b)** Mixed derivative  $\partial^2 M / (\partial H_c \partial H_b)$  obtained with INPUT 02 set to HcHb and conventional smoothing (SF = 5). Large amplitudes along diagonals coincide with steep regions of the hysteresis loop and are associated with maximum FORC diagram errors.



The color scale used by CalculateFORC for plotting functions in FORC space is optimized for best representation of the FORC function, which is characterized by large positive and small or completely absent negative amplitudes.

#### Updates from version 1.0:

- First derivatives with respect to  $H_r$  and  $H$ , as well as the measured magnetization itself, have been added.

### INPUT 03-04. FORC output range (updated)

The widespread FORC protocol of *Pike et al.* [1999] generates measurements that cover a trapezoidal region of Preisach coordinates (Fig. 4.5). On the other hand, FORC diagrams are conventionally plotted over the largest rectangular domain that is fully covered by measurements, thereby loosing information carried by some measurements. CalculateFORC offers several options for defining a rectangular output range over which the FORC matrix is calculated. Contrary to conventional processing, this range can be extended to all measurements, more closely approaching the maximum theoretical extension of the FORC function (Fig. 4.5b). The FORC output range is expressed in Preisach coordinates by the so-called *coercive field*  $H_c = (H - H_r)/2$  along the horizontal axis, and the *bias field*  $H_b = (H + H_r)/2$  along the vertical axis. The  $H_c$ - and  $H_b$ -ranges covered by the output FORC matrix are controlled by INPUT 03 and INPUT 04, respectively.

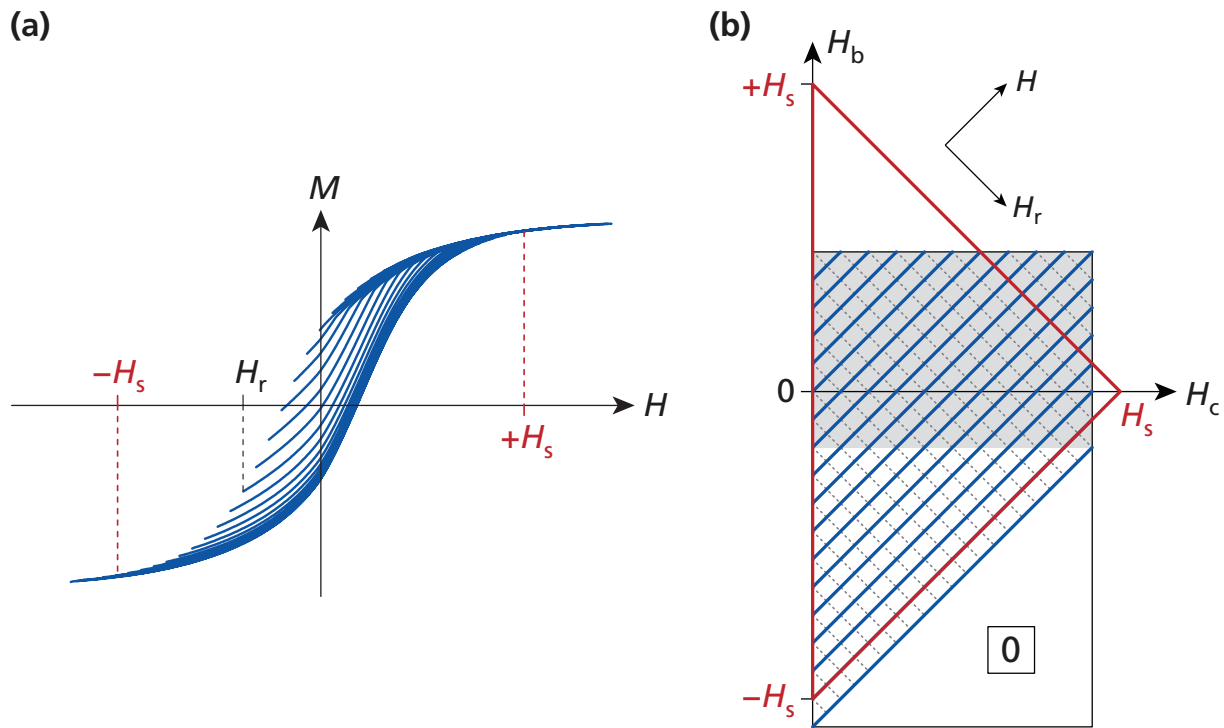


**Fig. 4.5:** Relation between ferrimagnetic hysteresis and FORC diagram range. (a) FORC measurements  $M(H_r, H)$  (blue lines) of a ferrimagnetic material with saturation field  $H_s$ , defined as the largest field amplitude in which magnetic irreversibility can occur. Up to exceptional cases explained in Chapter 8,  $H_s$  is the field where the two branches of the major hysteresis loop merge. (b) FORC diagram space spanned by the Preisach coordinates  $H_c = (H - H_r)/2$  and  $H_b = (H + H_r)/2$ . FORC trajectories (blue diagonal lines starting at  $H_c = 0$ ) cover a trapezoidal region that includes the rectangular area (gray) defined by the measurement protocol (i.e.  $[H_{c,\min}, H_{c,\max}]$  and  $[H_{b,\min}, H_{b,\max}]$ ). Non-zero FORC diagram amplitudes can be expected within the triangular region (red) with vertices  $(0, \pm H_s)$  and  $(H_s, 0)$ . Portions of the FORC diagram lying outside of the red triangle can be set to zero. FORC measurements cover all non-zero amplitudes if the measurement protocol coincides with  $[H_{c,\min}, H_{c,\max}] = [0, H_s]$  and  $[H_{b,\min}, H_{b,\max}] = [0, H_s]$ . CalculateFORC extrapolates the FORC function with zero values outside regions covered by measurements.

All measurements are comprised in the output FORC space if both INPUT 03 and INPUT 04 are set to All, i.e.:

```
INPUT 03. Horizontal range of output FORC space ....; All  
INPUT 04. Vertical range of output FORC space .....; All
```

In this case, the entire FORC region covered by measurements is included in the rectangular output range, compatibly with polynomial regression requirements (Fig. 4.6a). The output function is set automatically to zero over the lower right part of the output range, which is not covered by measurements. This option is recommended for preliminary low-resolution processing (i.e., INPUT 06 set to Fast) aimed at choosing the most suited output range.

Conventional FORC processing programs identify the FORC output range with the largest rectangular region that fits into the area covered by measurements (Fig. 4.6b). This area nearly coincides with the FORC ranges  $[H_c_{\min}, H_c_{\max}]$  and  $[H_b_{\min}, H_b_{\max}]$  used to define the measurement protocol. The conventional output range is chosen by setting INPUT 03 and INPUT 04 to All and Rectangle, respectively, i.e.:

```
INPUT 03. Horizontal range of output FORC space ....; All  
INPUT 04. Vertical range of output FORC space .....; Rectangle
```

This option sacrifices part of the information contained in FORC measurements, and should be chosen only if measurements outside the chosen rectangular range are uninteresting.

Finally the output range can be specified explicitly by entering the desired minimum and maximum  $H_c$ -fields (INPUT 03) and  $H_b$ -fields (INPUT 04), separated by a comma, i.e.:

```
INPUT 03. Horizontal range of output FORC space ....; 0, 90  
INPUT 04. Vertical range of output FORC space .....; -90, 40
```

(Fig. 4.6c). Explicit specification of the output range is useful for minimizing the processing time, because calculations can be limited to the range of fields where the FORC diagram contains significant information. Because this range is usually not known in advance, a preliminary Calculate FORC run should be performed at low resolution (INPUT 06 set to Fast) over the entire measurement range by setting INPUT 03 and INPUT 04 to All.

CalculateFORC plots the FORC spaces spanned by measurements and by the chosen output range, respectively. The output range is plotted by taking additional limits imposed by polynomial regression into account. These limits impose that all regression rectangles along the output range boundaries are occupied to at least 50% by measurement points. Additional limits along the diagonal limit of the measurement space, as specified with INPUT 05, are also taken into consideration. CalculateFORC verifies the compatibility of the chosen output range, producing an error message if it is not adequately covered by measurements. For example, the following message

```
Right Hc-limit of the output grid is not sufficiently covered by measurement points!  
Program aborted.
```

is produced for the case shown in Fig. 4.6d, and the program is interrupted. Warning messages, e.g.

```
WARNING! Right Hc-limit of the output grid is not entirely covered by measurement points.
```

are produced if polynomial regression along the edges of the output FORC space is based on partially filled rectangular arrays of measurement points. The calculation of a FORC diagram is still possible in those cases, but regression artifacts might appear at the edges of the chosen FORC space.

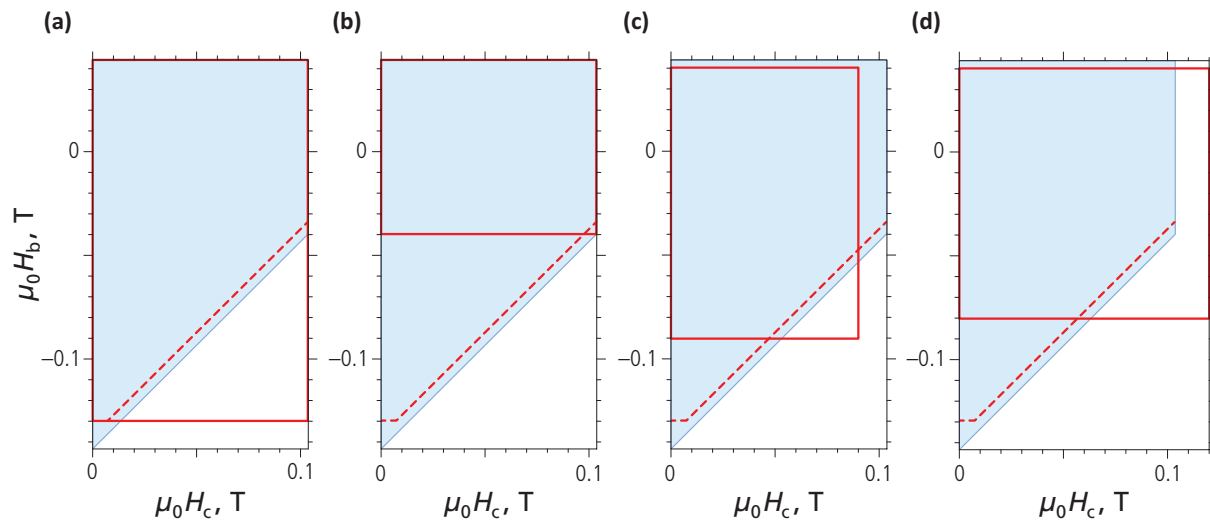


**Fig. 4.6:** Output range examples corresponding to different choices of INPUT 03 and INPUT 04, as plotted by CalculateFORC during processing. From version 2.0 on, polynomial regression rectangles are plotted over the output range. The region covered by FORC measurements is shaded in light blue, while the output range defined by INPUT 03 and INPUT 04, and by polynomial regression constraints, is plotted as a red rectangle. The dashed red line represents an additional limit imposed by INPUT 05, which excludes points of the output range located near the diagonal limit of the measurement space. The output function is set by default to zero below this limit. **(a)** Maximum possible output range obtained by setting INPUT 03 and INPUT 04 to All. The region with  $H_b < -0.13 \text{ T}$  is excluded from the output range because regression rectangles corresponding to the chosen smoothing factor (i.e. SF = 5) are not sufficiently covered by measurements. **(b)** The largest rectangular output range that is completely covered by measurements is obtained by setting INPUT 03 to All and INPUT 04 to Rectangle. This choice coincides with that of conventional FORC processing software. **(c)** Manual choice of the output range, obtained with explicit specification of the  $H_c$ -range (INPUT 03 set to 0, 0.09) and  $H_b$ -range (INPUT 04 set to -0.09, 0.04). As with (a), the FORC function is set to zero over the lower right corner that is not covered by measurements. **(d)** Invalid output ranges exceeding the maximum rectangular area defined by the measurements (in this example,  $H_c < 0.13 \text{ T}$ ) are not processed.

- FORC measurements start by definition at  $H=H_r$ , which means that the measured FORC space begins always at  $H_c=0$ . In most cases, this is also the left limit conveniently chosen for the output range.
- Unlike some older processing software, CalculateFORC can correctly handle FORC signatures of magnetization processes occurring at  $H_c=0$ , such as the vertical ridge produced by magnetic viscosity. Therefore,  $H_c=0$  does not need to be excluded from the output range.

- 💡 The output range options of CalculateFORC, combined with an appropriate choice of the FORC measurement protocol, minimize the number of measurements required for covering all magnetization processes up to the saturation field  $H_s$  (Fig. 4.5). In particular, the FORC range specified with the measurement protocol does not need to include large negative values of  $H_b$ , because measurements over  $H_b < H_{b,min}$ , where  $H_{b,min}$  is the lower  $H_b$ -limit set with the measurement protocol, can be included in the FORC diagram if INPUT 04 is All.
- 💡 The MicroMag™ control software automatically extends the chosen measurement range by adding a certain number of measurement points in order to compensate for the range loss produced by data processing with a given smoothing factor SF. For example, if SF = 5 is entered in the FORC measurement protocol, the measurement range is extended by 5 points in each direction, except at  $H=H_r$  (i.e.  $H_c=0$ ).
- 💡 CalculateFORC verifies that calculation of the output function is adequately supported by FORC measurements. For this purpose, each regression rectangle must be occupied to at least 50% by measurement points. More conservative choices leading to 100% filled regression rectangles, can be obtained by reducing the output range. The upper and right limits are controlled by INPUT 04 and INPUT 03, respectively. The diagonal limit defined by the measurement range, on the other hand, is controlled by INPUT 05. Finally, the left limit should be  $H_c=0$ , unless the FORC diagram is focusing on high-coercivity contributions. Unlike all other limits, regression rectangles along  $H_c=0$  are always half-filled, because measurements cannot extend over  $H_c < 0$ .

#### Updates from version 1.0:

- The chosen output FORC space is now plotted together with a schematic representation of regression rectangles generated according to the chosen smoothing options.

### INPUT 05. Diagonal trim factor

Polynomial regression artifacts might appear if large smoothing factors are used to process data near the lower diagonal limit of the measured FORC space (Fig. 4.7). Artifacts of this type are caused by polynomial regression over partially filled rectangular arrays of measurement points. They can be eliminated by adding an extra margin along the lower diagonal limit, below which the output function is set to zero. Regression rectangles above this limit, on the other hand, are more completely filled. The width of the extra margin to be added along the diagonal limit of the measurement range is controlled by INPUT 05, and it is expressed as fraction of the extra margin required to ensure polynomial regression with completely filled arrays of measurement points. For example, setting INPUT 05 to 0.6 means that the extra margin corresponds to 60% of the margin necessary to fill all regression rectangles along the lower limit of the measurement range. In the example of Fig. 4.7, this choice eliminates all visible artifacts.

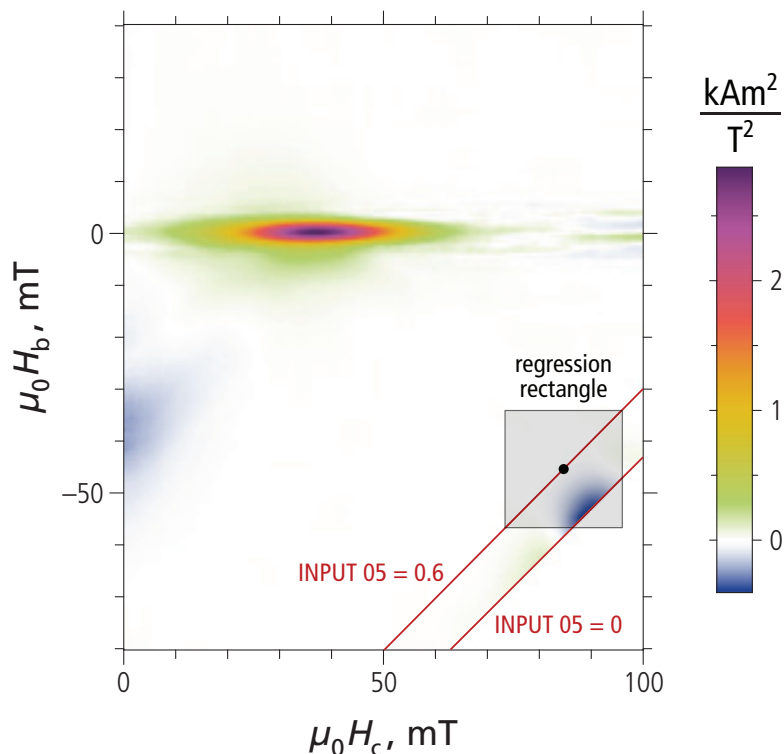


**Fig. 4.7:** FORC diagram of magnetotactic bacteria (see the downloadable example “Magnetospirillum 2”), obtained with CalculateFORC using advanced smoothing options. The negative anomaly near the lower right limit of the measured FORC space (red line labeled as INPUT 05 = 0), is a polynomial regression artifact produced by poorly fitted parts of the measured curves, where  $M/H$  is particularly large. The size of rectangular arrays used for polynomial regression in this region of the FORC diagram is shown for one point marked with a black dot (shaded area). INPUT 05 = 0.6 introduces an extra margin along the lower diagonal limit of the measured FORC space, so that regression rectangles are covered to 87% by measurement points. This margin is sufficient for eliminating the artifacts seen with INPUT 05 = 0.

Accordingly, INPUT 05 is a number comprised between 0 and 1, where

```
INPUT 05. Diagonal trim factor ....; 0
```

means that the diagonal limit of the measured FORC space is left unchanged and coincides with the measurement range ([Fig. 4.7](#)). On the other hand,

```
INPUT 05. Diagonal trim factor ....; 1
```

eliminates all polynomial regressions over partially filled arrays of measurement points along the diagonal limit. With this option, regression artifacts are eliminated at cost of a smaller output range. A compromise is obtained with intermediate values of INPUT 05. For example,

```
INPUT 05. Diagonal trim factor ....; 0.6
```

is sufficient to remove visible regression artifacts in the example of [Fig. 4.7](#).

Because the presence of regression artifacts along the lower diagonal limit of the measured FORC space is hardly predictable, it is recommended to perform a preliminary CalculateFORC run with low resolution (with INPUT 06 set on Fast) and INPUT 05 set to zero, in order to assess possible problems that can be solved by increasing INPUT 05.

- 💡 Polynomial regression artifacts along the diagonal limit of the measured FORC range are always solved by setting INPUT 05 to 1. In most cases, setting INPUT 05 to 0.6, as in the example of [Fig. 4.7](#), is already sufficient to eliminate these artifacts.
- 💡 Regression artifacts are typically caused by excessive smoothing over some regions of the FORC diagram, where the fitted second-order polynomial cannot reproduce the correct shape of measured curves. Particularly critical places are those where the magnetization changes rapidly, yielding large first derivatives (i.e.  $\partial M / \partial H$  and  $\partial M / \partial H_r$ ). Version 2.0 of CalculateFORC provides new options (i.e. INPUT 14-16) for limiting the size of regression rectangles over such regions. The use of such option greatly reduces the occurrence of regression artifacts along the lower diagonal limit of the measured FORC range.

### INPUT 06. Output mesh size

The output function (typically a FORC diagram) is calculated over a regular array of points that covers the output range defined by INPUT 03 and INPUT 04. The mesh size  $\Delta H$  of this array is the same along  $H_c$  and  $H_b$ , and is defined by INPUT 06. The array builds a Cartesian grid in  $(H_c, H_b)$ -coordinates, which is rotated by 45° with respect to the grid of measurement points, whose mesh size  $\delta H$  coincides with the field step size of measurements (Fig. 4.8). Therefore, the two grids do not overlap. In order to preserve the original measurement resolution, the mesh size  $\Delta H$  of the output grid should be at least as small as the field steps  $\delta H$  used for FORC measurements. On the other hand, the time required to calculate a FORC diagram is inversely proportional to  $(\Delta H)^2(\delta H)^2$ , reaching several hours in case of high-resolution measurements (i.e.  $\delta H \leq 0.5$  mT). CalculateFORC offers several possibilities for choosing the best output mesh size, depending on processing speed and resolution requirements.

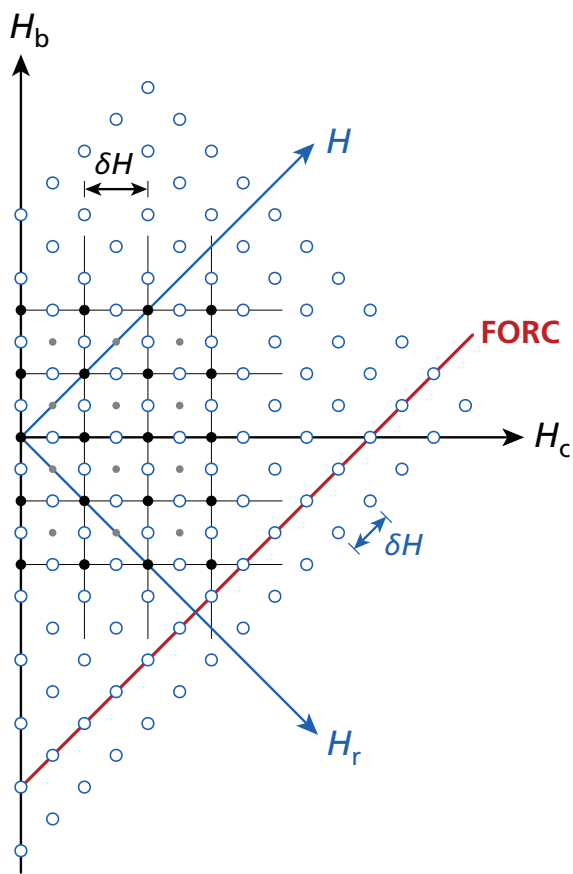


**Fig. 4.8:** Grid of FORC measurement points (blue circles) with field step size  $\delta H$  (as determined by the measurement protocol) and output grid with mesh size  $\Delta H = \delta H$  (black dots), obtained by setting INPUT 06 to Normal. The trajectory of a single measurement curve  $M(H_r, H)$  is highlighted in red. An output grid with double resolution (i.e.  $\Delta H = \delta H/2$ ) is obtained with INPUT 06 set to Fine (additional gray dots). Because of unavoidable irregularities of the measurement grid, output grid points never coincide exactly with measurement points, contrary to what is shown in this idealized example.

In many cases, a quick preliminary run of CalculateFORC is needed for tuning processing parameters, such as smoothing factors. Processing speed is more important than resolution in preliminary runs, while the opposite is true in case of publishing-quality diagrams containing low-dimensional FORC signatures such as the central ridge. Mesh sizes suitable for preliminary processing are automatically set with

```
INPUT 06. Output mesh size ....; Fast
```

or

```
INPUT 06. Output mesh size ....; Coarse
```

In this case the output mesh size  $\Delta H$  is chosen so, that the FORC matrix does not exceed 50 (Fast) or 100 (Coarse) points along each dimension. These options provide sufficient resolution for the identification of main FORC diagram features (Fig. 4.9a); however, they should never be used for definitive FORC processing, because of unavoidable resolution loss.

The original measurement resolution is preserved if  $\Delta H \leq \delta H$ . Two options are offered in order to fulfill this condition, namely  $\Delta H = \delta H$ , obtained with

```
INPUT 06. Output mesh size ....; Normal
```

(Fig. 4.8), and  $\Delta H = \delta H/2$ , obtained with

```
INPUT 06. Output mesh size ....; Fine
```

The latter option provides the highest meaningful resolution to be used when further processing of special FORC features with other VARIFORC modules is planned (e.g. central ridge analysis with IsolateCR).

The output mesh size can also be entered explicitly. For example

```
INPUT 06. Output mesh size ....; 0.5
```

is used for obtaining meshes with  $\Delta H = 0.5$  mT, regardless of measurement points spacing (Fig. 4.9b). In this case,  $\Delta H$  must be expressed with the same field unit of the imported FORC measurements (i.e.  $\Delta H = 0.5$  if measurement fields are expressed in mT, and  $\Delta H = 5$  if measurement fields are expressed in Oe). The field unit is specified in the file header of FORC data files produced by Import FORC. Explicit specifications of the output mesh size are used to calculate FORC diagrams over exactly determined grids that are independent of measurement fields. Such grids support quantitative FORC analyses based on the combination of measurements obtained from different samples [Ludwig et al., 2013].

- Identical output grids can be generated by explicit mesh size and grid origin specifications with INPUT 06 and INPUT 07, respectively.

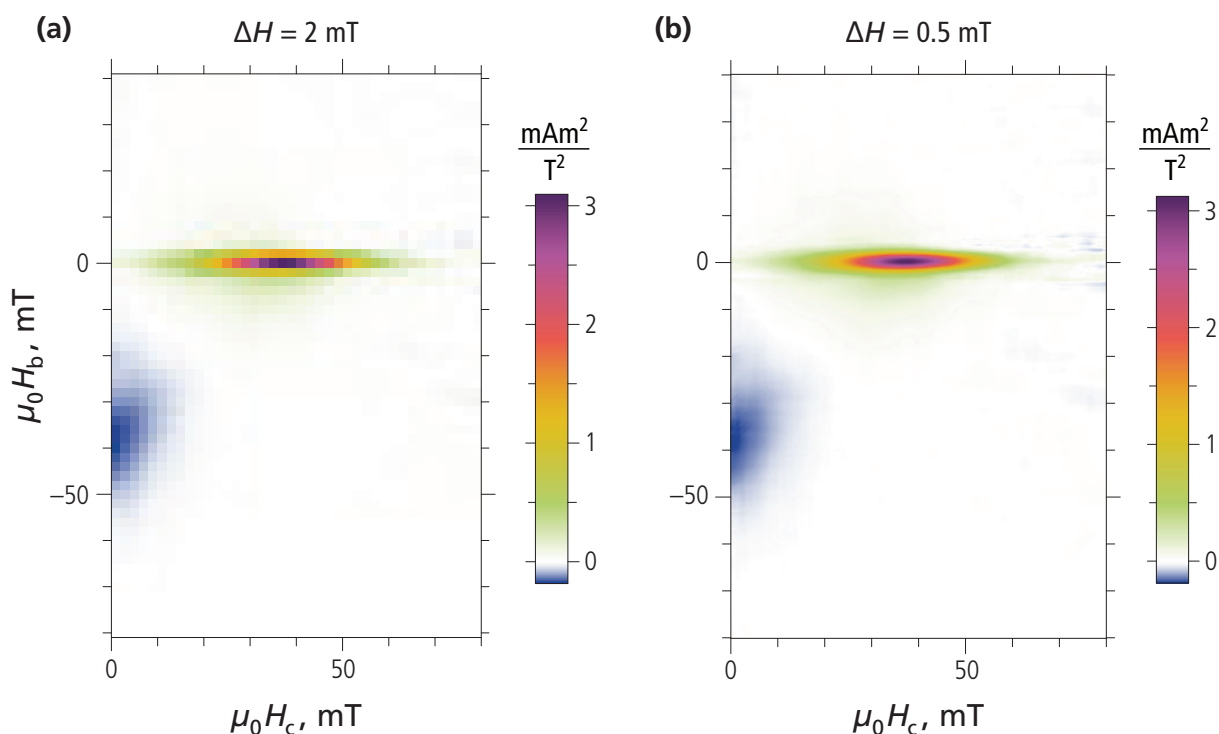


**Fig. 4.9:** FORC diagrams of magnetotactic bacteria (see the downloadable example “Magnetospirillum 2”), obtained with CalculateFORC from the same set of measurements and different output grid mesh sizes  $\Delta H$  defined by INPUT 06. The field step size of measurements was  $\delta H = 0.627 \text{ mT}$ . **(a)**  $\Delta H = 2 \text{ mT}$ , obtained by setting INPUT 06 to Fast. **(b)**  $\Delta H = 0.5 \text{ mT}$ , obtained by setting INPUT 06 to 0.5. The token field unit is mT, as in the source file of corrected measurements. A similar FORC diagram with  $\Delta H = \delta H = 0.627 \text{ mT}$  would be obtained with INPUT 06 set to Normal. The total processing time for (a) and (b) on a PC equipped with a 2.9 GHz Pentium dual core processor was 53'' and 55', respectively (Mathematica® 9).

- 💡 In case of definitive FORC diagram calculations, the output mesh size should be at least as small as the measurement steps in order to avoid resolution loss (i.e. INPUT 06 set to Normal, Fine, or explicitly specified by  $\Delta H \leq \delta H$ ).
- 💡 Further processing of special FORC signatures such as the central ridge, works best with CalculateFORC results based on  $\Delta H \approx \delta H/2$  (i.e. INPUT 06 set to Fine, or explicitly specified by  $\Delta H \leq \delta H/2$ ).
- 💡 If results obtained with CalculateFORC are used for further analyses (e.g. averaging of several FORC diagrams and background subtraction), the same output mesh size (explicitly entered with INPUT 06) and grid origin (see INPUT 07) should be chosen for all FORC diagrams in order to generate compatible FORC matrices.
- 💡 Standardized mesh sizes should be used whenever possible (e.g.  $\Delta H = 0.1, 0.2, 0.5 \text{ mT}$ ).

### INPUT 07. Output grid origin

INPUT 07 specifies the exact position of output grid points, once the mesh size has been set with INPUT 06. The recommended default setting

```
INPUT 07. Output grid origin ....; Automatic
```

creates an output grid with mesh size  $\Delta H$  by taking the point with FORC coordinate  $(\Delta H/2, 0)$  as the grid origin (Fig. 4.10a). Output grid coordinates are then given by  $(\Delta H/2 + k\Delta H, j\Delta H)$  with integers  $k$  and  $j$ . This choice is motivated by the fact that each point of the output grid represents the center of a square pixel and that the pixel coverage coincides exactly with the output range defined by INPUT 03 and INPUT 04, after adjusting it to contain an integer number of pixels. This means that if  $H_c = 0$  is the left limit of the output range, leftmost pixels must be centered at  $H_c = \Delta H/2$ . With this convention, the integral of the FORC function over any region of the FORC diagram coincides with the sum of pixel values contained in this region. Furthermore, the ideal location of the central ridge along  $H_b = 0$  coincides exactly with a pixel row. The Automatic choice of INPUT 07 is therefore strongly recommended. Different grid origins can be set by entering their coordinates explicitly. For example:

```
INPUT 07. Output grid origin ....; 0, 0.25
```

places the grid origin at  $(0, 0.25 \text{ mT})$ , so that leftmost pixels of a grid with mesh size  $\Delta H = 0.5 \text{ mT}$  are centered at  $H_c = 0$  (Fig. 4.10b).

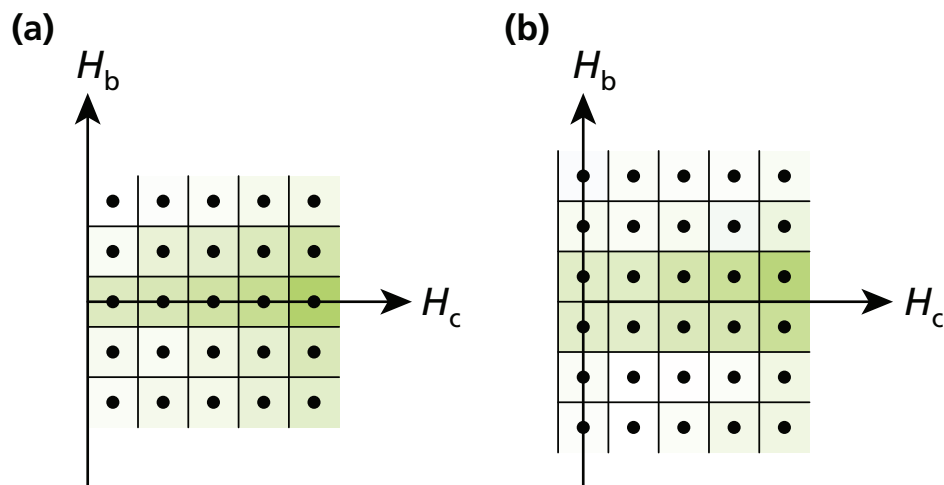


**Fig. 4.10:** Strongly zoomed excerpts of FORC diagrams obtained from measurements of cultured magnetotactic bacteria (see the downloadable example “Magnetospirillum 2”). Both diagrams were generated with CalculateFORC from the same set of measurements, same mesh size  $\Delta H = 2 \text{ mT}$ , and different output grid origins defined by INPUT 07. The field step size of measurements was  $\delta H = 0.627 \text{ mT}$ . Dots are output grid coordinates and shaded areas are the corresponding pixels colored according to the FORC function value. (a) Default grid origin  $(\Delta H/2, 0)$  obtained by setting INPUT 07 to Automatic. (b) Grid origin  $(0, \Delta H/2)$  obtained by setting INPUT 07 to  $0, 0.3135$ .

- The output range set by INPUT 03 and INPUT 04 is trimmed in order to make it coincide with pixel edges. This operation is not performed with left limit of the output range if this limit is comprised between  $H_c=0$  and  $H_c=\Delta H/2$ . In this case, the first pixel column extends over negative  $H_c$ -values and it is therefore truncated to  $H_c=0$  when FORC integrals are calculated.

- 💡 The output grid origin can be chosen so, that a certain pixel row or column is centered on a particular FORC diagram feature. For example, the central ridges of magnetofossil-bearing sediments is slightly shifted because of thermal activation effects. The mean vertical position  $H_b \approx +0.5$  mT can be matched by choosing  $(\Delta H/2, 0.5$  mT) as output grid origin.
- 💡 The output grid origin can be placed anywhere in FORC space: all coordinates with same remainder from division by  $\Delta H$  produce the same output grid.

### INPUT 08. Regularize field measurements (updated)

Common FORC measurement protocols, including those accepted by VARIFORC, produce measurements that form a regular grid in FORC space. Real measurement grids are slightly irregular due to limitations in field control and measurement precision. Especially first and last measurement points of magnetization curves measured in continuous mode can be systematically offset (Fig. 4.11), due to changes of the field sweep rate. INPUT 08 is an option for choosing whether measurement point coordinates are obtained from measured fields or replaced with values corresponding to a best-fit regular grid. The latter option is best suited to cases where field measurement errors are not negligible in comparison to the field steps used for measurements. In practice, the performance of a given magnetometer in terms of field control precision is best evaluated by comparing high-resolution FORC diagrams obtained with both options.

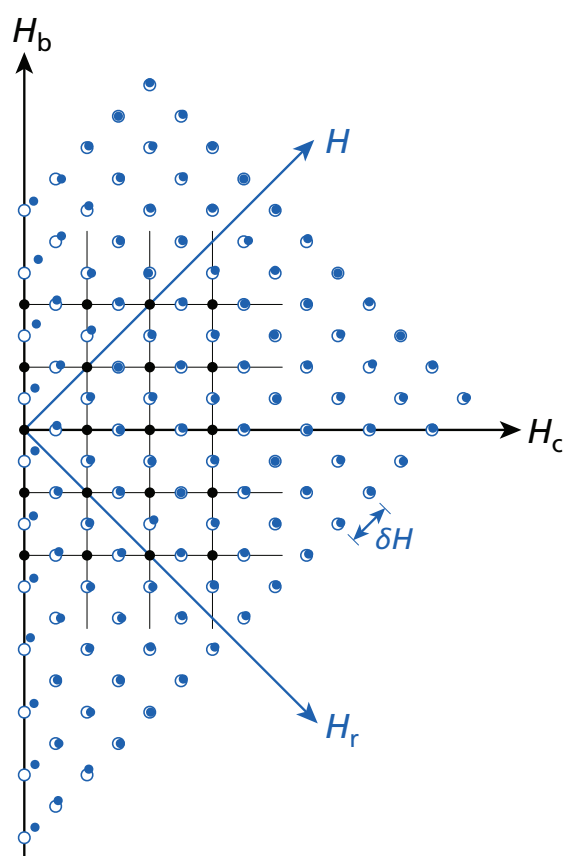


**Fig. 4.11:** Grid of FORC measurement points (blue) corresponding to a constant field step size  $\delta H$ , and output grid (black dots) with mesh size  $\Delta H = \delta H$ . Measurement coordinates (blue dots) differ from the ideal measurement grid because of (small) field control and/or field measurement errors. If deviations from the ideal measurement grid are real, i.e. due to field control limitations, measured coordinates (dots) should be taken for polynomial regression. On the other hand, if deviations from the ideal measurement grid are due to field measurement errors, polynomial regression is best based on the ideal grid (circles).

Measurement point coordinates are calculated from measured fields if

INPUT 08. Regularize field measurements ....; No

while an idealized, best-fit grid is used if

INPUT 08. Regularize field measurements ....; Yes

The two options produce nearly identical results when applied to high-resolution FORC measurements obtained with MicroMag™ magnetometers (Fig. 4.12). This means that the magnetic field is controlled and measured with a precision that largely exceeds the smallest field step sizes typically used with FORC measurements. For this reason, INPUT 08 set to No is the recommended option for processing all MicroMag™ FORC measurements.

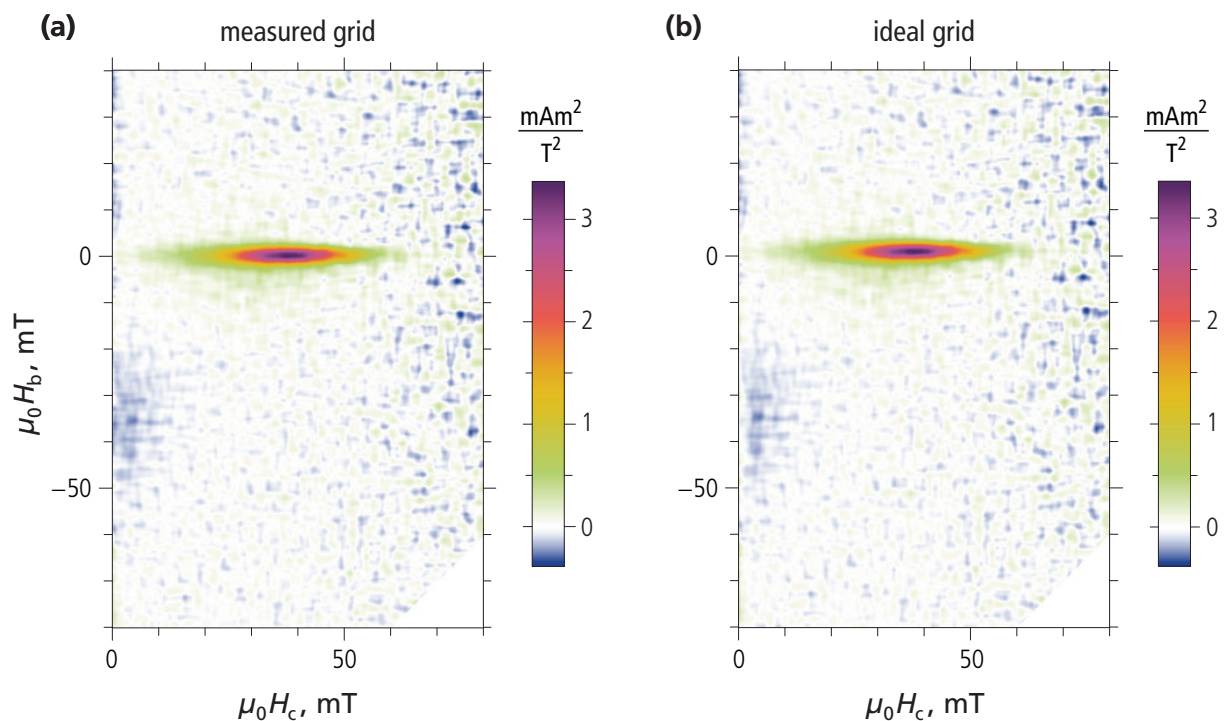


**Fig. 4.12:** FORC diagrams of cultured magnetotactic bacteria (see the downloadable example “Magneto-spirillum 2”), obtained with CalculateFORC from the same set of measurements and different assumptions about measurement point coordinates. In both cases, conventional processing with SF = 5 has been used to calculate the FORC function over the same grid of output points. **(a)** Measurement point coordinates used for polynomial regression coincide with field measurements (i.e. INPUT 08 set to No). **(b)** Measurement point coordinates used for polynomial regression have been replaced by a regular best-fit grid. Measured coordinates deviate from the best-fit grid by <0.04 mT, which is only 6% of the mean field step ( $\delta H = 0.627$  mT). The two FORC diagrams are practically undistinguishable, even with respect to noise features. This means that measurement field errors are negligible in this example.

- If INPUT 08 is set to Yes, a best-fit regular grid is obtained by fitting the measured coordinates with a second-order polynomial. Additional offsets produced by first and last points in each FORC are taken into consideration by assuming a constant offset of those points from the best-fit grid.
- Regardless of INPUT 08, a best-fit regular grid is used for fast location of measurement points needed for polynomial regression.

**Updates from version 1.0:**

- The description of INPUT 08 has been changed from “Use field measurements” to “Regularize field measurements”, so that the meaning of Yes and No options is exchanged. However, parameter files produced for version 1.0 of CalculateFORC are correctly interpreted by version 2.0 according to the old definition.

### INPUT 09. Weighted margin of polynomial regression rectangles (updated)

FORC diagram calculation is based on polynomial regression over measurement point subsets located within a certain range from each point of the output grid. Measurement point selection is formally equivalent to the application of a weight function to all measurements. For the simplest case of rectangular selections [Pike *et al.*, 1999], the weight function is equal to 1 within the chosen rectangular domain, and zero outside (Fig. 4.13a). This is the simplest and fastest processing option, because it minimizes the amount of measurement points used for each calculation. The disadvantage of this procedure, however, is that, as the regression rectangle is moved over different points of the FORC space, discontinuities arise from the sudden inclusion/exclusion of measurements. These discontinuities are usually masked by measurement noise and are mostly unnoticeable. As far as the output function continuity is concerned, best weight functions should be infinitely derivable, forcefully including more measurement points and increasing computation time. For example, the LOESS smoothing algorithm implemented by Harrison and Feinberg [2008] uses a “tricube” weight function based on the Euclidean distance between measurement and output grid points within a given maximum distance.

A good compromise between the efficiency of unweighted polynomial regression over rectangular arrays of measurement points on one hand, and infinitely derivable weight functions on the other hand, is represented by weighted regression within rectangular point arrays, as implemented in CalculateFORC. The rectangular weight function provides a smooth transition from zero weight at the edge of the selected range of measurement points to unit weight within 1 (Fig. 4.13b) or 2 (Fig. 4.13c) times the field step size  $\delta H$  of FORC measurements. The smooth transition is supported by second-order polynomials and has continuous first derivatives.

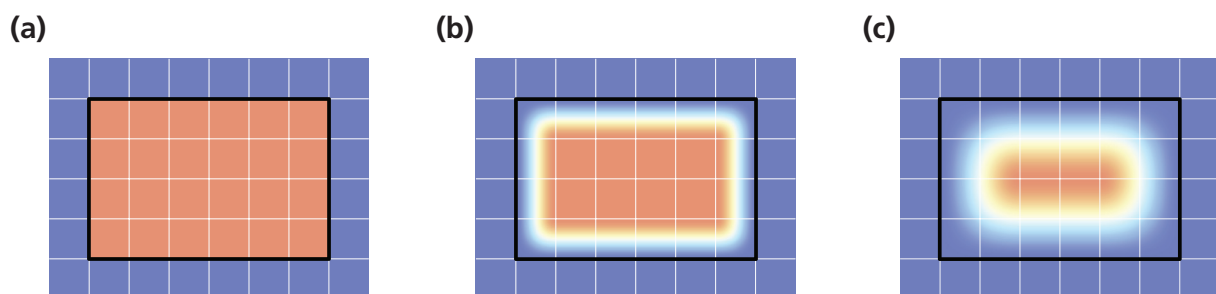


**Fig. 4.13:** Three weight functions used by CalculateFORC, shown for the example of a regression rectangle extending over  $6 \times 4$  mesh units  $\delta H$ , where  $\delta H$  is the field step size of FORC measurements. The color scale ranges from 0 (blue) to 1 (red). **(a)** Unit weight function obtained with INPUT 09 set to 0. **(b)** Weight function with a continuous transition over one mesh unit (INPUT 09 set to 1). **(c)** Weight function with a continuous transition over two mesh units (INPUT 09 set to 2). The smoothing factors corresponding to the definition given in Pike *et al.* [1999], are  $3 \times 2$  in (a),  $2.5 \times 1.5$  in (b), and  $2 \times 1$  in (c). Larger regression rectangles containing more measurement points are needed for obtaining the same smoothing effect with smoother weight functions, at the cost of computation time.

Weighted regression over rectangular selections of measurement points improve the FORC function continuity without adding excessive computational costs in terms of additional points needed to attain a given smoothing degree. The weight function used for polynomial regression is chosen through INPUT 09 among the three options illustrated in Fig. 4.13. A compromise between processing speed and result quality is obtained with

`INPUT 09. weighted margin of polynomial regression rectangles ...; 1`

(Fig. 4.13b). In this case, the weight function increases from 0 at the edge of the rectangular selection to 1 within a distance  $\delta H$  corresponding to the measurement field step [Egli, 2013]. This distance is doubled by entering

`INPUT 09. weighted margin of polynomial regression rectangles ...; 2`

for best quality results (Fig. 4.13c), while all points are given a unit weight with

`INPUT 09. weighted margin of polynomial regression rectangles ...; 0`

for faster computation (Fig. 4.13a).

In most cases, and especially with high-resolution measurements, the choice of INPUT 09 is irrelevant. The role of weight functions becomes evident only when processing noise-free measurements, and if the output grid mesh is finer than measurement field steps (Fig. 4.14). In this case, FORC diagram quality increases in terms of continuity as the transition margin of the weight function is thickened.

The FORC resolution associated with polynomial regression within a given rectangular array of measurement points depends on the weight function, because its continuous transition from 0 to 1 reduces the effective amount of measurements considered for regression and increases resolution correspondingly. This effect is taken into account by version 2.0 of CalculateFORC, which means that the size of regression rectangles is chosen so, that the effective smoothing effect coincides with that of unweighted regression with the smoothing factors specified with INPUT 10 and INPUT 11. With other words, the horizontal and vertical resolution of the FORC diagram is identical to that of conventional FORC processing (as defined in Pike *et al.* [1999]) with same smoothing factors. The relationship between FORC diagram resolution and smoothing factor is specified in Table 4.2.

**Table 4.2:** Relationships between field step size  $\delta H$  of FORC measurements, smoothing factors  $s$  entered with INPUT 10-11, size of smoothing rectangles, and FORC diagram resolution  $\Delta H$ , expressed as full-width-to-half-maximum of processed impulse features (e.g. the central ridge).

|                                    | INPUT 09 = 0      | INPUT 09 = 1      | INPUT 09 = 2      |
|------------------------------------|-------------------|-------------------|-------------------|
| $\Delta H$ = resolution            | $(s+0.5)\delta H$ | $(s+0.5)\delta H$ | $(s+0.5)\delta H$ |
| $L$ = size of regression rectangle | $2s\delta H$      | $(2s+1)\delta H$  | $(2s+2)\delta H$  |

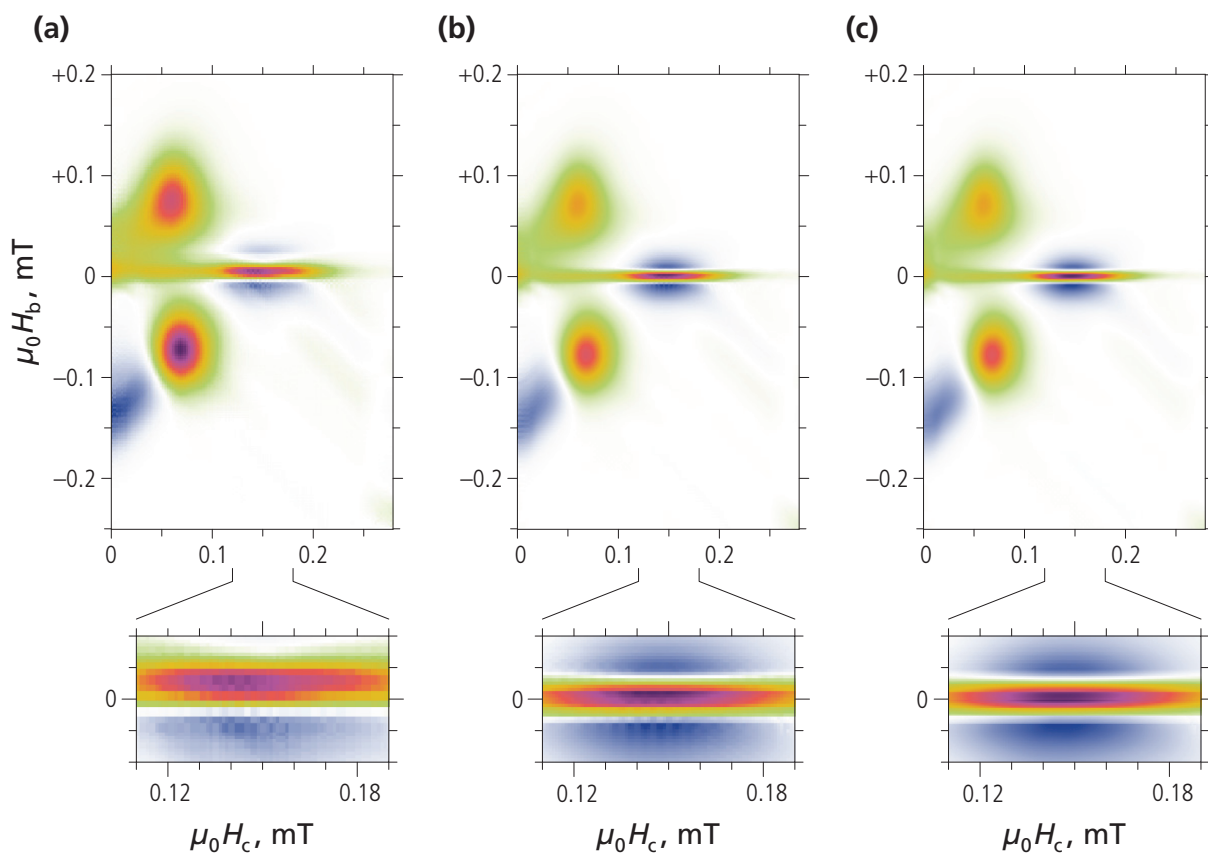


**Fig. 4.14:** FORC diagram of iron nanoparticles (see the downloadable example “Nanodots” and Winklhofer *et al.* [2008]), generated by CalculateFORC using different weight function options and identical regression rectangles. Other processing options are identical for the three diagrams. The output grid (mesh size: 1 mT) is much finer than the ~5 mT field steps of measurements. A zoomed detail of the central ridge peak is shown below each plot. **(a)** Unweighted polynomial regression (e.g. Fig. 4.13a) obtained with INPUT 09 set to 0. The FORC function is discontinuous, with apparent pixels corresponding to the field step size of measurements. **(b)** The FORC function becomes almost continuous if the weight function is characterized by a smooth transition from 0 to 1 over the distance between measurement points (e.g. Fig. 4.13b). This result was obtained by setting INPUT 09 to 1. **(c)** Same as (b), after doubling the transition width of the weight function (INPUT 09 set to 2, e.g. Fig. 4.13c). Residual discontinuities of the FORC function are completely removed in this example. Notice the increased resolution with respect to (a), due to the fact that less measurement points are effectively used for polynomial regression over identical smoothing rectangles.

- 💡 Setting INPUT 09 to 1 is recommended for most applications and can be used as default choice.
- 💡 A smoother weight function (i.e. INPUT 09 = 2) yields best-quality results. It should be used if measurement noise is very small and the output mesh size is smaller than the field step of FORC measurements (e.g. Fig. 4.14).

- The use of unweighted polynomial regression over rectangular selections of measurement points (i.e. INPUT 09 = 0) is prone to processing artifacts due to the sudden inclusion/exclusion of measurement points.
- The option INPUT 09 = 0 is provided only for completeness and is not recommended.

**Updates from version 1.0:**

- The influence of the weight function on the FORC diagram resolution is now compensated by an automatic adjustment of the size of smoothing rectangles. Unlike in version 1.0, the effective resolution is always equivalent to that of conventional processing with unit weight function and same smoothing factors.

### INPUT 10-11. Horizontal and vertical smoothing specifications (updated)

As with other FORC software, FORC diagram calculation is based on second-order polynomial regression of measurements points located within a certain distance from given FORC coordinates. The FORC diagram resolution is controlled by this distance and by the weight function applied to the measurement points. CalculateFORC performs a weighted polynomial regression with measurement points located within upright rectangles centered on output grid points (Fig. 4.15). The size of the rectangles is  $(2s_c + m)\delta H \times (2s_b + m)\delta H$ , where  $s_c$  and  $s_b$  are the horizontal and vertical smoothing factors, respectively  $\delta H$  is the field step size of measurements [Egli, 2013], and  $m$  is the transition margin of the weight function entered with INPUT 09. The smoothing factors  $s_c$  and  $s_b$  are numbers  $\geq 1$  that define the horizontal and vertical resolution of the FORC diagram. From version 2.0 on, regression rectangles can be cut along diagonals by optional smoothing factor limits entered with INPUT 12 - 16.

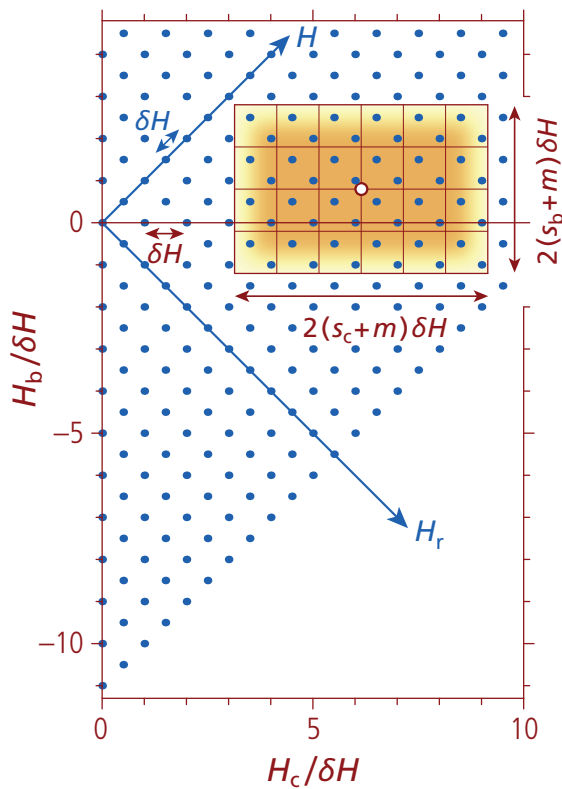


**Fig. 4.15:** Polynomial regression procedure used by CalculateFORC. Blue dots represent the grid of measurement points with field step  $\delta H$ . Calculation of the FORC function for given coordinates of the output grid (white circle), is based on polynomial regression of all measurement points located within a centered rectangle with dimensions  $(2s_c + m)\delta H \times (2s_b + m)\delta H$  (shaded), where  $s_c$  and  $s_b$  are the horizontal and vertical smoothing factors, respectively, and  $m$  is the transition margin of the weight function entered with INPUT 09. In this example,  $s_c = 3.5$ ,  $s_b = 2.5$ , and  $m = 1$ . The orange shading inside the rectangle represents the weight  $w$  given to measurements, ranging from  $w = 0$  (white) along the rectangle edge to  $w = 1$  for all points with distances  $> \delta H$  to the edge.

The smoothing factors  $s_c$  and  $s_b$  used by CalculateFORC are fully equivalent to the smoothing factor SF of conventional FORC processing, as defined by Pike *et al.* [1999], producing therefore the same effects as SF along horizontal ( $s_c$ ) and vertical ( $s_b$ ) directions, respectively. Different horizontal and vertical smoothing factors can be chosen (anisotropic smoothing), and both factors are functions of the FORC coordinates (variable smoothing). The additional flexibility gained with this approach is used to adapt polynomial regression to the intrinsic characteristics of the FORC function, obtaining the best compromise between the opposed needs of high resolution and measurement error suppression [Egli, 2013].

Horizontal and vertical smoothing factors are set with INPUT 10 and INPUT 11, respectively. In the simplest case of conventional FORC processing, a single, constant smoothing factor  $s_c = s_b = SF$  is used over the entire FORC space. For example, conventional FORC processing with SF = 5 is obtained with:

```
INPUT 10. Horizontal smoothing specifications ....; 5  
INPUT 11. Vertical smoothing specifications .....; 5
```

(Fig. 4.16a-c). Conventional FORC processing is recommended for preliminary runs of CalculateFORC, because of higher computation speed, especially if INPUT 06 is set to Fast. Any number factor  $\geq 1$ , including fractional ones (e.g. 2.5), can be entered as smoothing factor. Same values for horizontal and vertical smoothing are highly recommended.

The variable smoothing procedure (VARIFORC) introduced by Egli [2013] represents a generalization of conventional processing, where the horizontal and vertical smoothing factors are linear functions of the FORC coordinates  $H_c$  and  $H_b$ . In practice,  $s_c$  and  $s_b$  increase linearly when moving away from the FORC diagram origin, following the natural tendency of FORC functions to become smoother as  $H_c$  or  $|H_b|$  increase. An example of regression rectangles resulting from linearly increasing smoothing factors is shown in Fig. 4.16d. This smoothing procedure yields FORC diagrams with enhanced signal-to-noise ratios, widely expanding the range of significant contributions while preserving details near  $H_c = 0$  and  $H_b = 0$  (Fig. 4.16e).

**Fig. 4.16:** Examples of conventional FORC processing (top plots) and variable smoothing processing (bottom plots), obtained with the same measurements of a volcanic ash sample (see the downloadable example "Volcanic ash"). Graphics have been produced by CalculateFORC with small editorial modifications as part of the standard output. (a-c) Conventional processing with fixed smoothing factor SF = 4 (i.e. both INPUT 10 and INPUT 11 set to 4). (d-f) Variable smoothing (VARIFORC) with minimum smoothing factor SF = 4 and increase rate  $\lambda = 0.08$  in both vertical and horizontal directions (i.e. both INPUT 10 and INPUT 11 set to 4, 0, 0.08). (continues on front page)

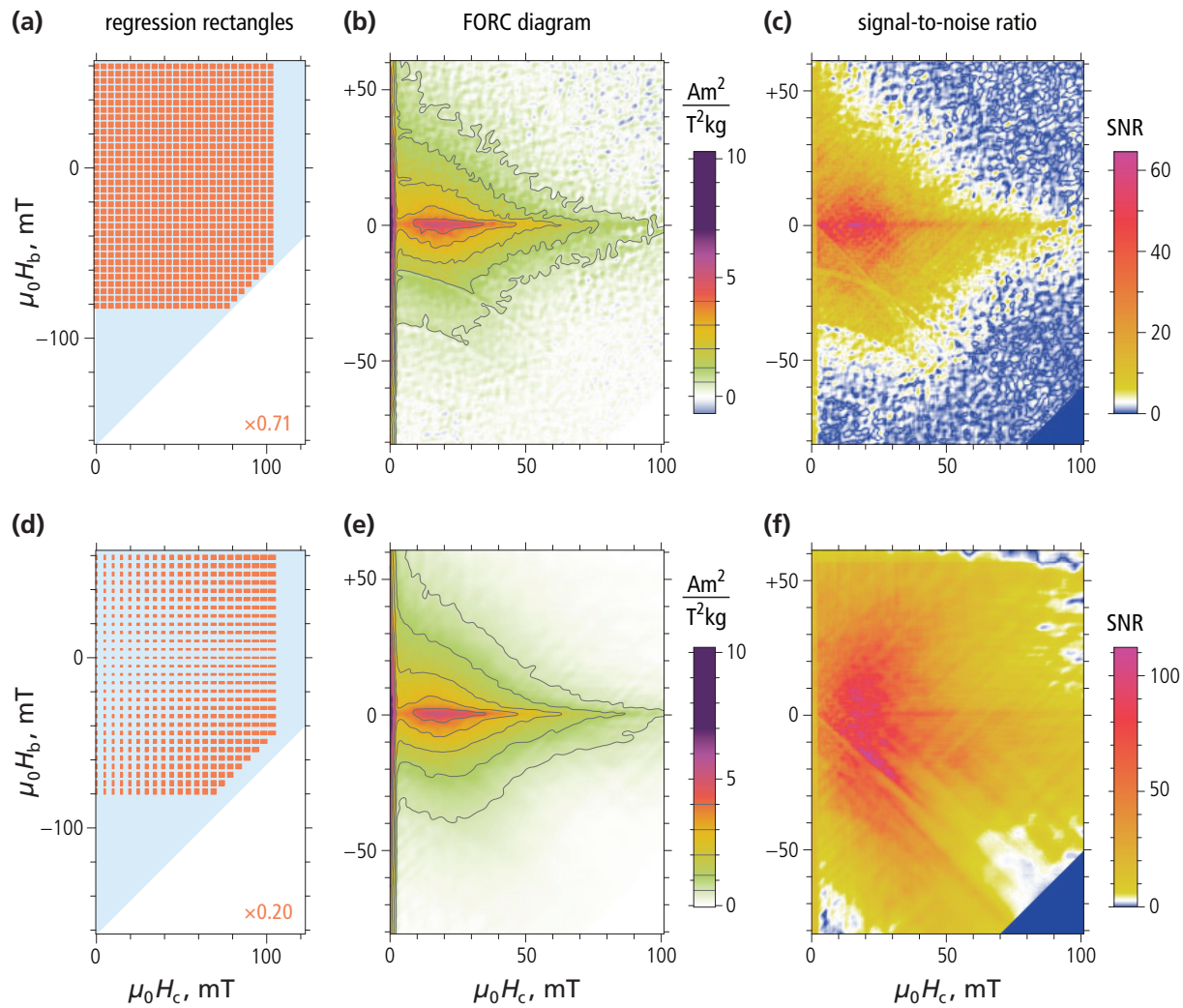


**Fig. 4.16 (continued):** (a,d) FORC space covered by measurements (shaded in blue), and schematic representation of regression rectangles (orange, not to scale) over the chosen output range of the FORC diagram. Regression rectangles are scaled by a factor shown at the lower left corner. The maximum horizontal and vertical smoothing factor corresponding to the regression rectangles in (d) is  $\sim 20$ . (b,e) FORC diagrams (contour lines added with the VARIFORC module PlotFORC). Measurement noise is clearly visible in (b). The diagrams contain two critical features superimposed to a continuous background typical for pseudo-single domain crystals: a vertical ridge along  $H_c = 0$ , due to magnetic viscosity, and a faint central ridge along  $H_b = 0$ . Both features require highest resolution along one direction in order to be correctly resolved: this condition is automatically met by the variable smoothing procedure, so that measurement noise in (e) is suppressed without losing important details. (c,f) Signal-to-noise ratios (SNR) of the FORC diagrams shown in (b,e), obtained by dividing the FORC function amplitude by the estimated standard error. The color scale is chosen so, that SNR values corresponding to significant values of the FORC function are plotted with warm colors (orange to red). White and blue regions of the plots, on the other hand, represent parts of the FORC diagram that do not differ significantly from zero. The significant region of the FORC diagram is clearly larger in (f).

Variable smoothing along each dimension is specified through INPUT 10 and INPUT 11 by number pairs, where the first number is the minimum smoothing factor,  $s_{c,0}$  or  $s_{b,0}$ , and the second

number is the increase rate,  $\lambda_c$  or  $\lambda_b$ , so that the horizontal and vertical smoothing factors are given by:

$$\begin{aligned}s_c &= s_{c,0} + \lambda_c \frac{H_c}{\delta H} \\s_b &= s_{b,0} + \lambda_b \frac{|H_b|}{\delta H}\end{aligned}\quad (1)$$

Same specifications for INPUT 10 and INPUT 11, i.e.  $s_{c,0} = s_{b,0}$  and  $\lambda_c = \lambda_b$ , are highly recommended. For example,

INPUT 10. Horizontal smoothing specifications ....; 4, 0.08  
INPUT 11. Vertical smoothing specifications .....; 4, 0.08

(i.e.  $s_{c,0} = s_{b,0} = 4$  and  $\lambda_c = \lambda_b = 0.08$ ) have been used to generate the FORC diagram of Fig. 4.16e.

Reasonable smoothing parameter choices are guided by the following criteria. The minimum smoothing factor should be just large enough to yield a decent representation of the FORC function near  $H_c = 0$  and  $H_b = 0$ . This is the same criterion used for conventional processing. The smoothing factor increase rate(s), on the other hand, are usually comprised between 0.06 and 0.12 [Egli, 2013]. Larger values, up to  $\sim 0.2$ , can be used at cost of computation speed, and with increased risk of producing smoothing artifacts due to excessively large regression rectangles (e.g. Fig. 4.17).

FORC measurements of samples with squared hysteresis loop are particularly prone to smoothing artifacts, because most changes of the magnetization curves are concentrated near the positive and negative coercive fields. In FORC space, these fields define two diagonals departing from the central maximum of the FORC function (dashed lines in Fig. 4.17c), where smoothing artifacts can be expected. This problem has been addressed with version 2.0 of CalculateFORC, which can automatically limit the size of regression rectangles where necessary (see INPUT 14).

**Fig. 4.17 (front page):** FORC processing examples based on FORC measurements of magnetotactic bacteria (see the downloadable example “Magnetospirillum 2”). **(a)** Conventional processing with constant smoothing factor SF = 4 (i.e. both INPUT 10 and INPUT 11 set to 4). A central ridge along  $H_b = 0$  is clearly distinguishable, while remaining parts of the FORC diagram are dominated by measurement noise. **(b)** Variable smoothing (VARIFORC) with minimum smoothing factor SF = 4 and increase rate  $\lambda = 0.07$  in both vertical and horizontal directions (i.e. both INPUT 10 and INPUT 11 set to 4, 0.07). Measurement noise has been reduced significantly in comparison to (a), but its effects are still visible on contour lines.

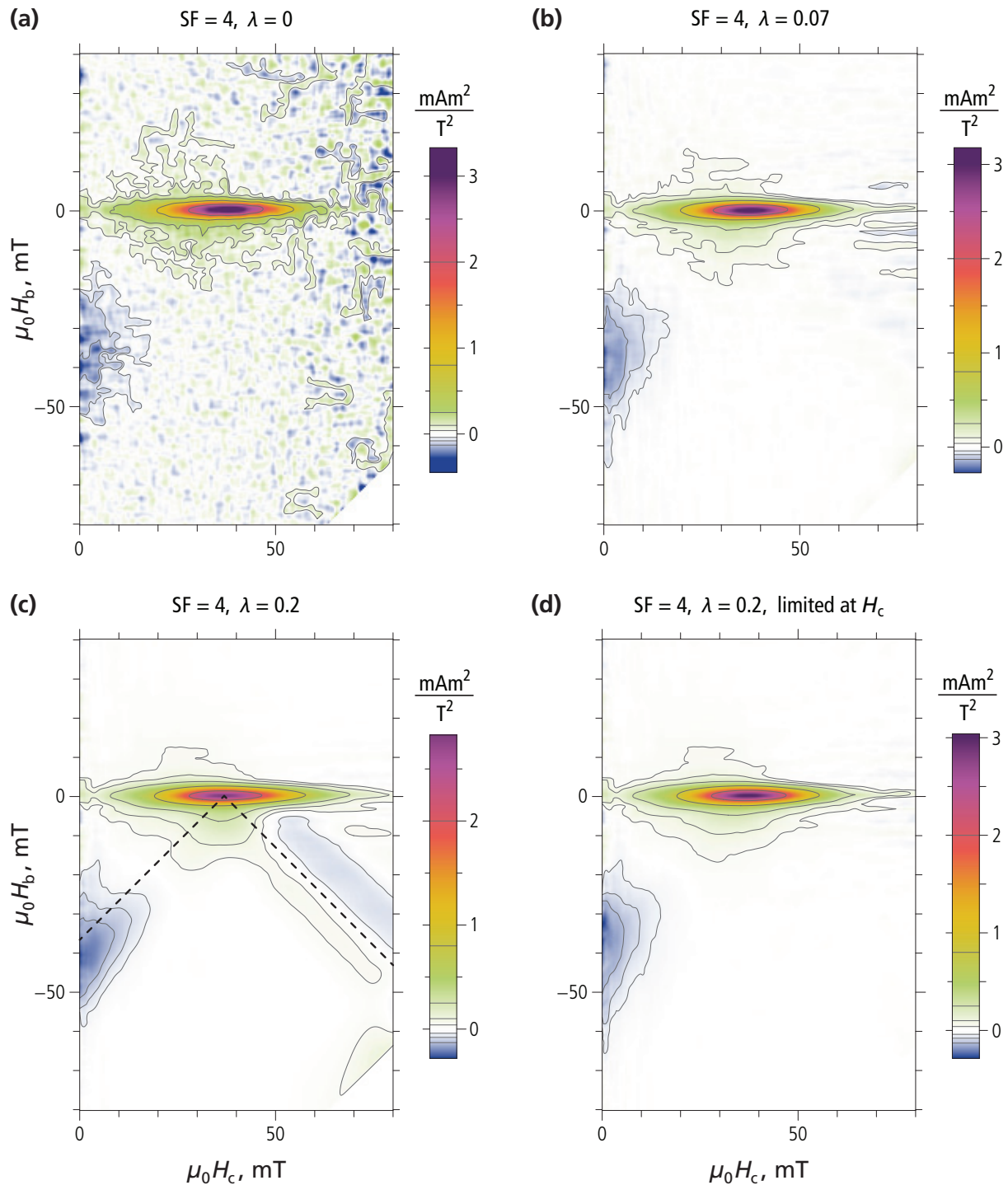


**Fig. 4.17 (continued):** (c) Same as (b), with a smoothing factor increase rate  $\lambda = 0.2$  (i.e. both INPUT 10 and INPUT 11 set to 4, 0.2). Measurement noise is almost completely suppressed, but smoothing artifacts appear along the dashed line, where derivatives of measured curves with respect to  $H_r$  and  $H$  are largest. Here, second-order polynomials cannot fit the shape of measured curves over the relatively large size of regression rectangles defined by INPUT 10 and INPUT 11. This problem is particularly evident for this sample, because of its squared hysteresis loop. (d) Same as (c), after limiting the size of regression rectangles with INPUT 14 set to Automatic. Polynomial regression artifacts are now suppressed, along with most measurement noise contributions.

As demonstrated by the example of Fig. 4.17, CalculateFORC offers many processing options that cannot be fully automatized. Nevertheless, the choice of smoothing parameters is guided by a relatively simple strategy (see Chapter 8). As far as INPUT 10 and INPUT 11 are concerned, this strategy can be summarized by the following steps:

- 1) Unless optimal processing parameters can be taken from previous analyses of similar measurements, FORC calculation should begin with a preliminary, low-resolution run (i.e. INPUT 06 is set to Fast) based on constant smoothing factors comprised between 3 and 5 (i.e. INPUT 10 and INPUT 11 are both set to 3, 4 or 5). This preliminary run (e.g. Fig. 4.9a) takes only 1-2 minutes even in case of most demanding high-resolution measurements and is usually sufficient for identifying the main FORC diagram features. Options for capturing high-resolution features, such as horizontal and vertical ridges, should be ignored at this stage.
- 2) The choice of INPUT 10 and INPUT 11 is guided by the overall signal-to-noise ratio (SNR) of the FORC function, which, since version 2.0, is always plotted along with the FORC diagram (e.g. Fig. 4.16c). Values  $\geq 15$  (orange to red in SNR plots) ensure a suitable representation of the FORC function with meaningful contour lines.  $\text{SNR} \geq 15$  is required around the central peak and over any other place with important contributions. If this condition is not met, a new preliminary run should be obtained after increasing the smoothing factors.
- 3) All FORC contributions visible on the preliminary FORC diagram should exceed the significance threshold (i.e.  $\text{SNR} > 3$ ), appearing as yellow, orange, and red regions in the SNR plot. Depending on the amount of measurement noise, this condition is met with conventional processing only within a limited distance from the central maximum of the FORC function. This situation can be improved with variable smoothing. The benefit of variable smoothing is tested with a new preliminary run after adding a proper increase rate  $\lambda$  to INPUT 10 and INPUT 11. The recommended initial value is  $\lambda = 0.07$ .
- 4) The quality of preliminary runs obtained with variable smoothing is checked again with SNR plots. The significant range of the FORC diagram should have increased significantly. If measurement noise reduction is not sufficient, larger values of  $\lambda$  can be chosen. Smoothing artifacts should be checked after every run, especially if  $\lambda > 0.1$ , and when processing FORC measurements associated with rectangular hysteresis loops. If artifacts similar to those of Fig. 4.17c appear, a dedicated smoothing factor limitation (INPUT 14) can be used to remove them (Fig. 4.17d). The color scale used by Calculate FORC facilitates the detection of undesired smoothing effects down to very small amplitudes.
- 5) Local smoothing factor limits can be added in order to resolve particular FORC diagram features, such as horizontal and vertical ridges (INPUT 12 and INPUT 13), once the global smoothing options have been set with INPUT 10 and INPUT 11.
- 6) Steps 1-5 should be repeated with low-resolution runs as long as satisfactory noise suppression is not reached. A feeling for variable smoothing optimization is gained after few trials with the

numerous downloadable examples available online. As a general rule-of-thumb, identical parameters should be chosen for INPUT 10 and INPUT 11.

Once optimal smoothing parameters for the overall FORC diagram have been chosen a definitive run is performed with the desired resolution.

- 💡 Unless optimized processing options can be retrieved from previous measurements of similar samples, low-resolution preliminary processing (i.e. INPUT 06 is set to Fast) should be used to evaluate the effectiveness of smoothing parameters chosen with INPUT 10 and INPUT 11.
- 💡 Several VARIFORC processing examples for common types of magnetic materials can be downloaded along with the installation package. The smoothing parameters chosen for these examples provide excellent starting points.
- 💡 In most cases, variable smoothing yields better results than conventional processing, because it exploits the common tendency of Preisach-type FORC functions to become progressively more “smeared” as the distance from  $H_c=0$  and  $H_b=0$  increases, enabling polynomial regression over larger selections of measurement points.

- The FORC processing time is proportional to (1) the number of measurement points, (2) the number of output grid points, and (3) the smoothing factors. Using a PC with Intel core i7 processor, the total runtime for the full-resolution examples of Fig. 4.17 (300 curves) is 4'44" with conventional processing ( $s_0 = 4$ ), 15' with  $\lambda = 0.07$ , and 44' with  $\lambda = 0.2$ .
- Error calculations associated with large smoothing factors are very memory demanding. If variable smoothing is used, the maximum size of error matrices should be limited with INPUT 19.

#### Updates from version 1.0:

- The variable smoothing procedure has been improved and related options are completely reorganized in version 2.0. Nevertheless, version 2.0 accepts parameter files written for version 1.0, with unavoidable functionality limitations.
- As far as INPUT 10 and INPUT 11 are concerned, these options are now used only for controlling global smoothing parameters (i.e. the minimum smoothing factor and its increase rate), with no reference to special FORC features such as vertical and horizontal ridges. Options for such features are now deferred to INPUT 12 - 16.

**INPUT 12-13. Horizontal and vertical smoothing factor limits at given  $H_c$  and  $H_b$  (new)**

General smoothing options valid for the whole FORC diagram are entered with INPUT 10 and INPUT 11. Additional limitations of the smoothing factors might be required at specific places in FORC space. For example, higher resolution is required across ridges of the FORC function. In case of horizontal and vertical ridges, the size of regression rectangles set by INPUT 10 - 11 is additionally limited with INPUT 12 - 13 at  $H_c$  - and  $H_b$  -coordinates where these ridges occur.

The working principle of INPUT 12 - 13 is best illustrated with a sample featuring a horizontal, so-called central ridge [Egli *et al.*, 2010] along  $H_b \approx 0$  (Fig. 4.18). This ridge is a characteristic signature of non-interacting single-domain particles, and – being essentially a 1D-feature of a 2D-diagram – it requires its own smoothing parameters for correct processing. For this reason, the smoothing strategy applied to whole FORC diagram is controlled by INPUT 10 - 11, while the extra vertical resolution required for processing the central ridge is obtained with INPUT 13. Even if the FORC diagram of Fig. 4.18 is dominated by the central ridge, the smoothing factors chosen with INPUT 10 - 11 should be large enough to remove measurement noise from the weak background contributions over the whole FORC space (Fig. 4.18e). Once appropriated values of INPUT 10 - 11 have been chosen, the height of regression rectangles over the central ridge needs to be limited with INPUT 13 (Fig. 4.18h), in order to increase the vertical resolution over this part of the FORC diagram. This step is particularly important for further quantitative processing of the resulting FORC diagram (e.g. with the VARIFORC module IsolateCR), in which case the central ridge needs to be isolated and should therefore overlap only minimally with other contribution.

**Fig. 4.18 (front page):** FORC processing examples based on FORC measurements of a magnetofossil-bearing pelagic carbonate sample (see the downloadable example “Pelagic carbonate”). **First row:** Regression rectangles (orange) corresponding to three different sets of processing parameters, and FORC measurement range (light blue). **Second row:** FORC diagrams obtained with the processing parameters shown in the first row. Contour lines have been added with PlotFORC. **Third row:** Signal-to-noise ratios (SNR) corresponding to the FORC diagrams shown above. Regions plotted with warm colors (yellow-orange-red) represent parts of the FORC diagrams that passed a significance test. **(a-c)** Conventional processing with fixed smoothing factor  $s_0 = 4$  (i.e. both INPUT 10 and INPUT 11 set to 4). A central ridge along  $H_b = 0$  is clearly distinguishable, while remaining parts of the FORC diagram are dominated by measurement noise. **(d-f)** Variable smoothing (VARIFORC) with minimum smoothing factor  $s_0 = 9$  and increase rate  $\lambda = 0.08$  in both vertical and horizontal directions (i.e. both INPUT 10 and INPUT 11 set to 9, 0.08). This choice of the smoothing parameter has been dictated by the observation that the FORC diagram in (b) is dominated by measurement noise even in proximity of the central ridge, which means that  $s_0$  needs to be increased. Measurement noise has been reduced significantly in comparison to (b), as seen by the smooth contour lines. Furthermore, almost the whole FORC diagram is now significant. On the other hand, increasing  $s_0$  produced excessive vertical smearing of the central ridge.

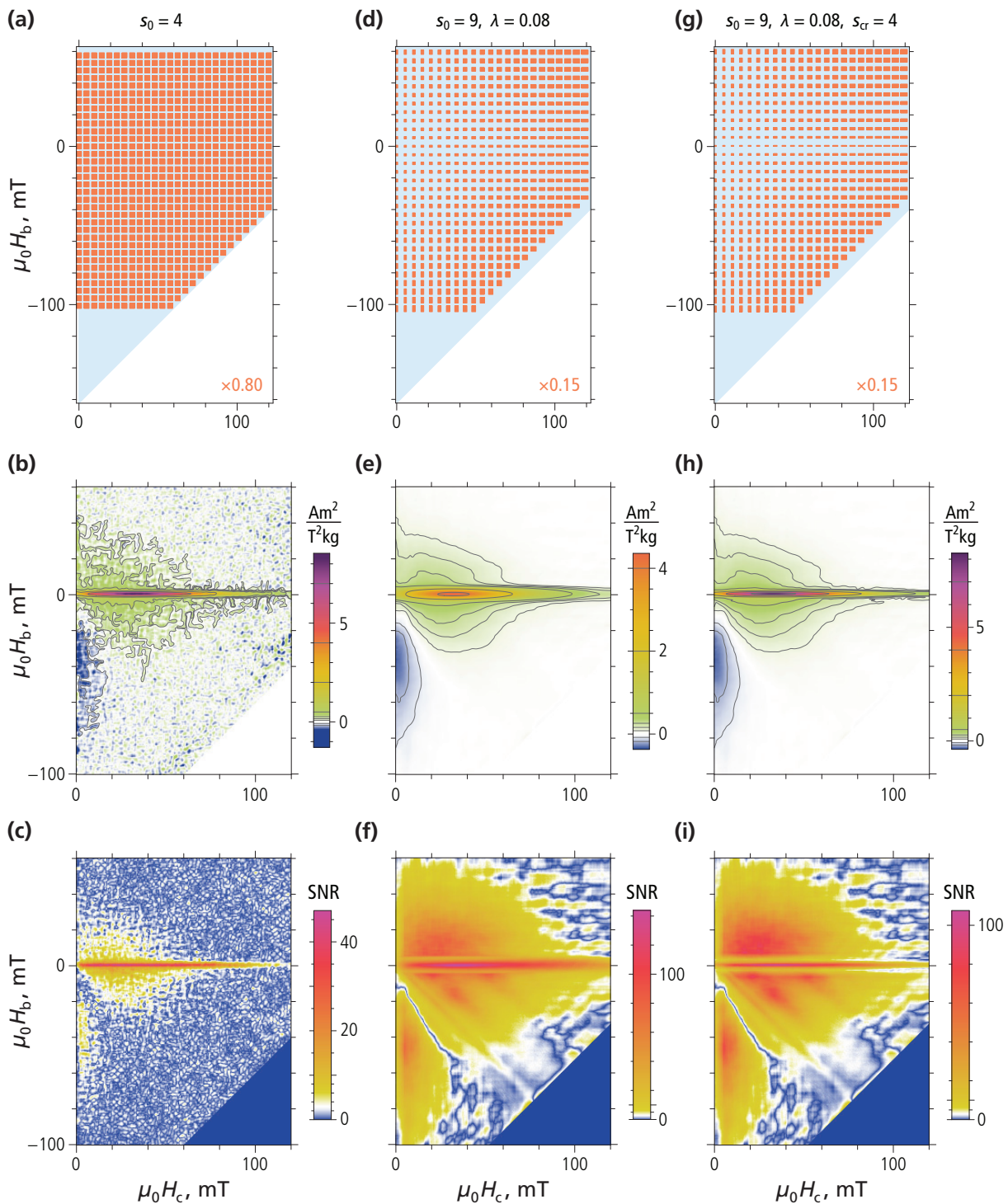


**Fig. 4.18 (continued):** (g-i) Same variable smoothing as in (a), after limiting the vertical smoothing factor to  $s_{cr} = 4$  over the central ridge (i.e. INPUT 13 set to  $0.4, 4, 0.5$ ). The central ridge has now the same sharpness as in (b), while measurement noise is adequately suppressed over the remaining FORC contributions. Conventional processing with a relatively small smoothing factor (left plots) gives an idea of the main FORC diagram signatures that need to be considered for the choice of optimized smoothing parameters, first over the whole diagram (middle plots), and finally over special high-resolution features requiring extra smoothing factor limitations (e.g. the central ridge, right plots).

The default settings for INPUT 12-13:

```
INPUT 12. Smoothing factor limit at given Hc ( | ) ....; None
INPUT 13. Smoothing factor limit at given Hb ( - ) ....; None
```

are used to process FORC diagrams that do not contain a horizontal or a vertical ridge. Extra smoothing factor limitations, required for instance to ensure elevated vertical resolutions across a horizontal ridge, are defined by three numbers, e.g.

```
INPUT 13. Smoothing factor limit at given Hb ( - ) ....; 0.4,4,0.5
```

as used for the example of Fig. 4.18g-i. The first number represents the position of the ridge in the FORC diagram, namely the  $H_c$ -value at which a vertical ridge occurs, or the  $H_b$ -value at which a horizontal ridge occurs (Fig. 4.19b). These coordinates need to be expressed with the same field units used for the FORC data, as reported in file headers. In all cases known so far, vertical and horizontal (central) ridges occur at or very close to  $H_c=0$  and  $H_b=0$ , respectively. Nevertheless, any position within the chosen output range of the FORC diagram can be specified. Central ridges of magneto-fossil-bearing sediment samples are characterized by a  $\sim 0.4$  mT vertical shift (i.e.  $H_b = +0.4$  mT, Fig. 4.20).

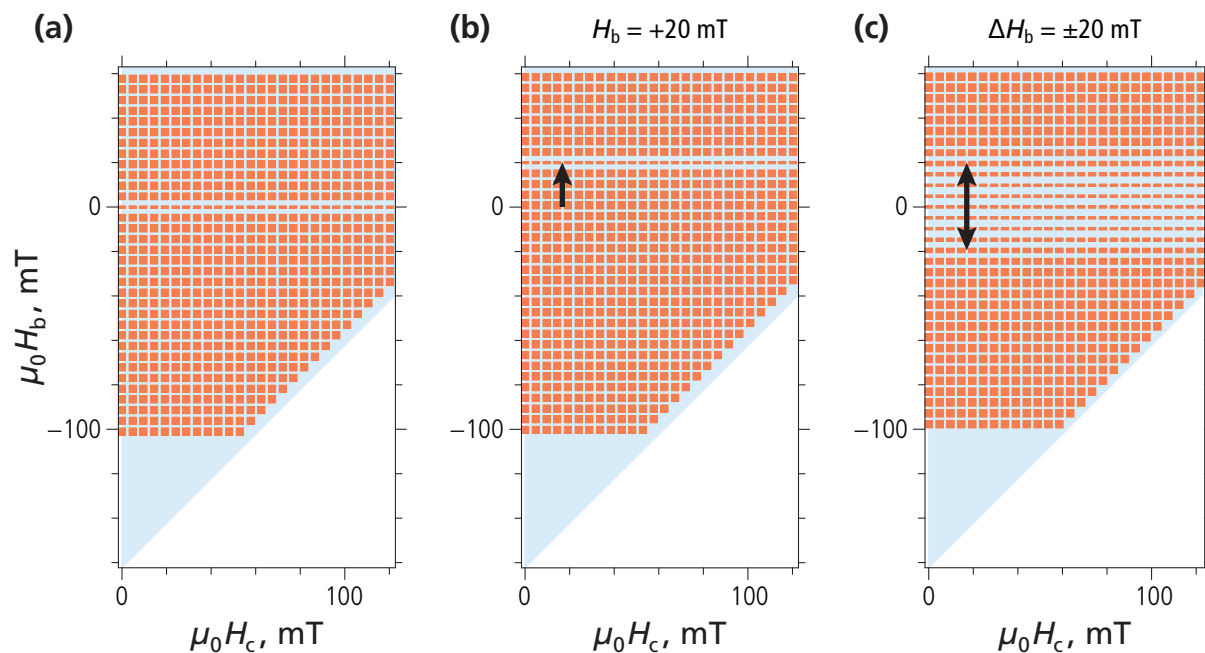


**Fig. 4.19:** Examples of regression rectangles (orange) resulting from constant smoothing factors (i.e.  $s_c = s_b = 9$ ) with an extra  $s_b$ -limit of 3 over a range of  $H_b$ -values set by INPUT 13. (a) Ideal central ridge ( $H_b = 0$ ) with zero intrinsic width (i.e. INPUT 13 set to  $0, 3, 0$ ). (b) Same as (a), for a ridge that is shifted upwards by +20 mT (arrow, INPUT 13 set to  $20, 3, 0$ ). (c) Same as (a), for a “ridge” with 20 mT intrinsic half-width (arrow, INPUT 13 set to  $0, 3, 20$ ). Examples (b-c) have exaggerated in order to show the effect of parameters chosen with INPUT 13.

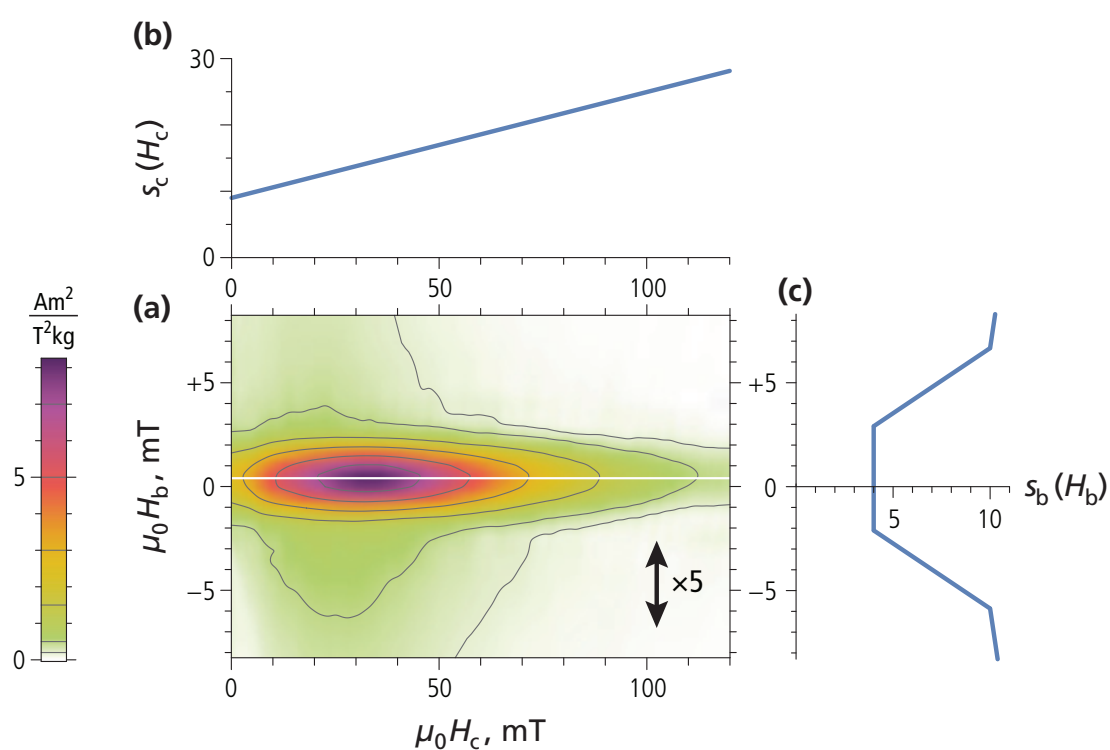


**Fig. 4.20:** (a) Detail of the pelagic carbonate FORC diagram shown in Fig. 4.18h, focusing on the region occupied by the central ridge. A 5-fold vertical exaggeration has been used to resolve details along  $H_b$ . A  $\sim 0.4$  mT upward shift of the central ridge is highlighted by the white line: it is a common feature of magnetofossil-rich sediments. The vertical ridge extension, on the other hand, coincides with the vertical resolution  $\Delta H_b = (s_b + 0.5)\delta H \approx 2.3$  mT of the diagram along  $H_b = 0$ , and is almost entirely due to smoothing. (b) The horizontal smoothing factor over the central ridge is a linear function of  $H_c$ , according to the INPUT 10 settings 9, 0, 0.08. (c) The vertical smoothing factor across the central ridge is limited to 4, according to the INPUT 13 settings 0, 4, 4, 0.5. The other parameters of INPUT 13 (i.e. vertical shift and intrinsic width) have been deduced from a detailed analysis of vertical central ridge profiles with the VARIFORC module IsolateCR.

The second number in INPUT 12-13 represents the smoothing factor limit to be used over the ridge. As with all smoothing factors used in CalculateFORC, it is an integer or fractional number  $\geq 1$ . The third number represent the intrinsic half-width of the ridge, i.e. without considering the widening due to smoothing. In principle, ridges are defined as 1D-objects with zero width; in practice, however, a finite width is generated by phenomena such as thermal activation effects and residual magnetostatic interactions [Egli, 2006]. Any positive number can be entered as intrinsic half-width: this number is assumed to have the same field unit of the imported FORC measurements. The effect of a finite half-width is to increase the range over which the smoothing factor limitation is applied (Fig. 4.19c). The intrinsic vertical half-width of central ridges produced by magnetofossil-rich sediments is of the order of 0.5 mT, i.e. less than the maximum currently attainable FORC diagram resolution. The transition from smoothing factors limited by INPUT 12-13 to regular

processing parameters is continuous (Fig. 4.20c), ensuring correct results according to the principles explained in Egli [2013].

The processing principles illustrated above for the central ridge apply in a similar manner to vertical ridges (INPUT 12), as shown in Fig. 4.21 for the case of a sample featuring both a horizontal and a vertical ridge. INPUT 12 and INPUT 13 can also be defined by fewer parameters. For example,

INPUT 13. Smoothing factor limit at given  $H_b$  ( - ) ....; 0.4,4

means that a horizontal ridge is expected at  $H_b = 0.4$  field units (e.g. mT) and that the vertical smoothing factor is limited to 4. A zero vertical half-width is assumed for the missing parameter. Finally,

INPUT 13. Smoothing factor limit at given  $H_b$  ( - ) ....; 0.4

means that no smoothing factor limitation is applied; however,  $H_b = 0.4$  field units (e.g. mT) is taken as the origin for the linear increase of vertical smoothing factors with the increase rate defined with INPUT 11. This option is useful for redefining variable smoothing “origins” that differ from the default  $H_c = H_b = 0$ , e.g. when processing Preisach-type functions with a vertical or horizontal shift.

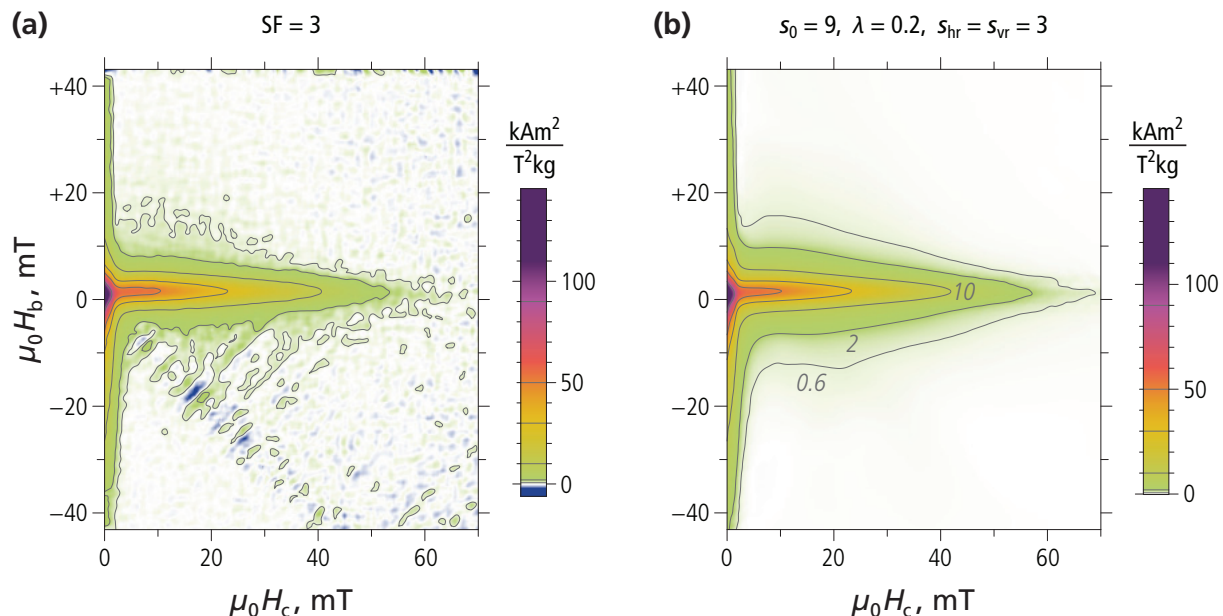


**Fig. 4.21:** FORC processing examples based on high-resolution measurements of an ash flow tuff containing acicular magnetite crystals [Schlanger *et al.*, 1991]. The vertical and horizontal ridges are typical signatures of magnetically viscous, non-interacting single-domain particles with uniaxial anisotropy [Newell, 2005; Egli *et al.*, 2010]. Unlike the case of sediment magnetofossils, the ridges feature a relatively large intrinsic width due to thermal activation effects [Egli, 2006]. **(a)** Conventional processing with a constant smoothing factor SF = 3. Measurement noise is visible outside of the ridges, especially along the remanence diagonal  $H_b = -H_c$ . **(b)** Advanced processing with variable smoothing (i.e. INPUT 10-11 set to 9, 0.2) and smoothing factor limitation over the vertical ridge (i.e. INPUT 12 set to 0, 3, 0.4) and over the central ridge (i.e. INPUT 13 set to 1.6, 3, 0.4). Residual measurement noise is <0.6  $\text{kAm}^2/\text{T}^2\text{kg}$ , i.e. 0.4% of the FORC function maximum near the origin. Color scales and contour levels are identical in the two diagrams.

The best definition of INPUT 12-13 parameters depends on the intrinsic properties of vertical and horizontal ridges. If these are not known a-priori, a preliminary run should be performed with default values (e.g.  $H_c=0$  or  $H_b=0$  and zero width). Shifts of the ridge positions from the expected positions are easily identified by inspecting the FORC diagram (e.g. Fig. 4.20 and Fig. 4.21). The intrinsic ridge width, on the other hand, is not directly deducible from the FORC diagram, because of unavoidable smoothing effects, and requires further processing, for instance with the VARIFORC module IsolateCR (Fig. 4.22). In any case, FORC processing does not rely critically on precise ridge width estimates, and default values can be entered for given sample categories (e.g. magnetofossil-rich sediment samples).

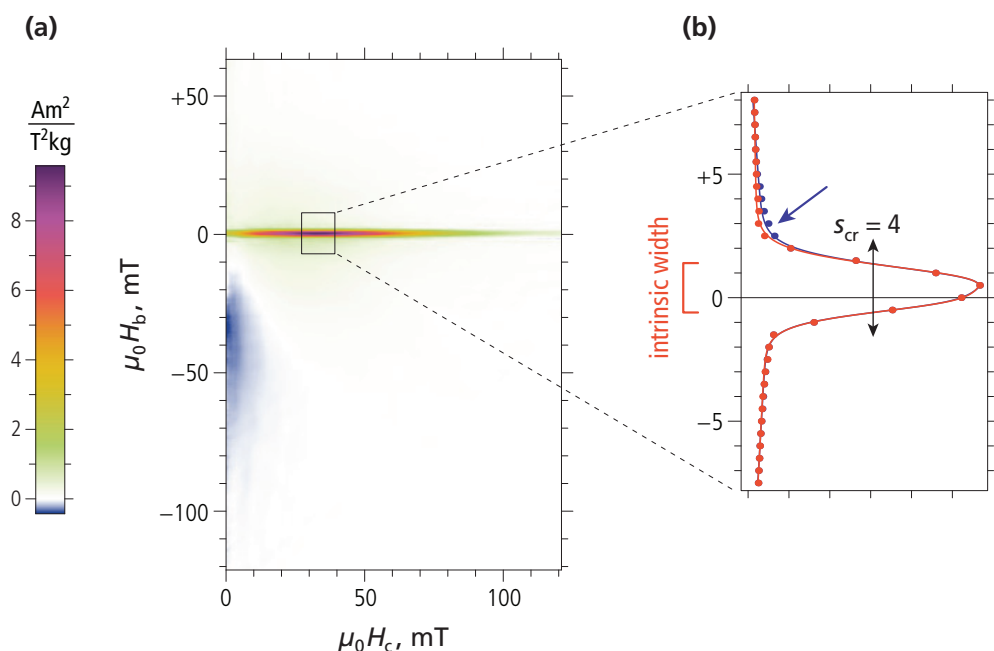


**Fig. 4.22:** (a) FORC diagram obtained from high-resolution FORC measurements of a pelagic carbonate (see the downloadable example “pelagic carbonate”) with variable smoothing and INPUT 13 set to  $0, 4, 0$  (corresponding to a central ridge with zero width along  $H_b=0$ ). (b) Mean vertical profile across the central ridge (blue dots with line representing a best-fit model) obtained with the VARIFORC module IsolateCR as average of all vertical profiles included in the square region shown in (a). A  $\sim 0.4$  mT vertical offset is clearly visible. Furthermore, a  $\sim 1$  mT intrinsic width is deduced from comparison of this profile with the profile generated by an ideal central ridge with zero width using the same smoothing parameters. A second run of CalculateFORC with these intrinsic properties (i.e. INPUT 13 set to  $0, 4, 4, 1$ ) produces a FORC diagram that is practically undistinguishable from the one shown in (a). However, minor differences can be seen on vertical profiles (orange dots with line representing a best-fit model). In particular, the tail indicated by the blue arrow has disappeared. The vertical smoothing factor for all points comprised by the double arrow is limited to  $s_{cr}=4$ , and increases progressively outside of it. If central ridge parameters are correctly chosen with INPUT 13, the whole range of measurements affected by the central ridge is processed with the same vertical smoothing factor. This is important for further calculations involving the central ridge, such as its separation from other FORC contributions with IsolateCR.

- 💡 INPUT 12-13 are essential for decoupling very different processing requirements over horizontal and vertical ridges (i.e. maximum resolution perpendicular to the ridge) from requirements most suited for the remaining parts of the FORC diagram. General processing requirements are controlled by INPUT 10-11, and should be chosen before proceeding with exceptions handled by other options.
- 💡 The intrinsic properties of horizontal and vertical ridges are not yet fully explored.
- 💡 High-resolution measurements of magnetofossil-bearing sediments suggest that central ridges are shifted vertically by ~0.3-0.5 mT and have an intrinsic vertical half-width of ~0.3-0.5 mT. These properties are probably controlled by thermal activations.

#### Updates from version 1.0:

- The variable smoothing procedure has been improved and related options are completely reorganized in version 2.0. Nevertheless, version 2.0 accepts parameter files written for version 1.0, with corresponding functionality limitations.
- As far as INPUT 12 and INPUT 13 are concerned, these options define the whole set of parameters required to process vertical and horizontal ridges, respectively. Accordingly, special ridge-related requirements are no longer tied to main processing parameters, as in version 1.0. This avoids confusions between parameters acting on different FORC features. INPUT 12 introduces processing options for vertical ridges that were unavailable in version 1.0.

### Appendix to INPUT 12-13: Definition of smoothing limits

INPUT 12-13 is defined by the three parameters,  $H_0$ ,  $s_{\min}$ , and  $w_{1/2}$ , which represent the ridge position, the maximum smoothing factor over the ridge, and the ridge intrinsic half-width, respectively. The smoothing factor applied by CalculateFORC in proximity of the ridge and over the ridge itself is the smallest one between the value defined by INPUT 10-11 (eq. 1) and

$$s_{\lim} = s_{\min} \max \left[ 1, \frac{|H - H_0|}{s_{\min} \delta H + w_{1/2}} \right], \quad (2)$$

where  $\delta H$  is the field step size of FORC measurements (Fig. 4.23). This definition is slightly different from that of Egli [2013], in order to make the transition between  $s_{\min}$  and the unlimited smoothing factors wider in proportion to the intrinsic width  $w_{1/2}$  over which the limit is applied. In practice, the range of fields over which the smoothing factor is constant and equal to  $s_{\min}$  coincides with the effective ridge width in the FORC diagram. This means that ridge profiles are equivalent to those obtained with conventional processing.

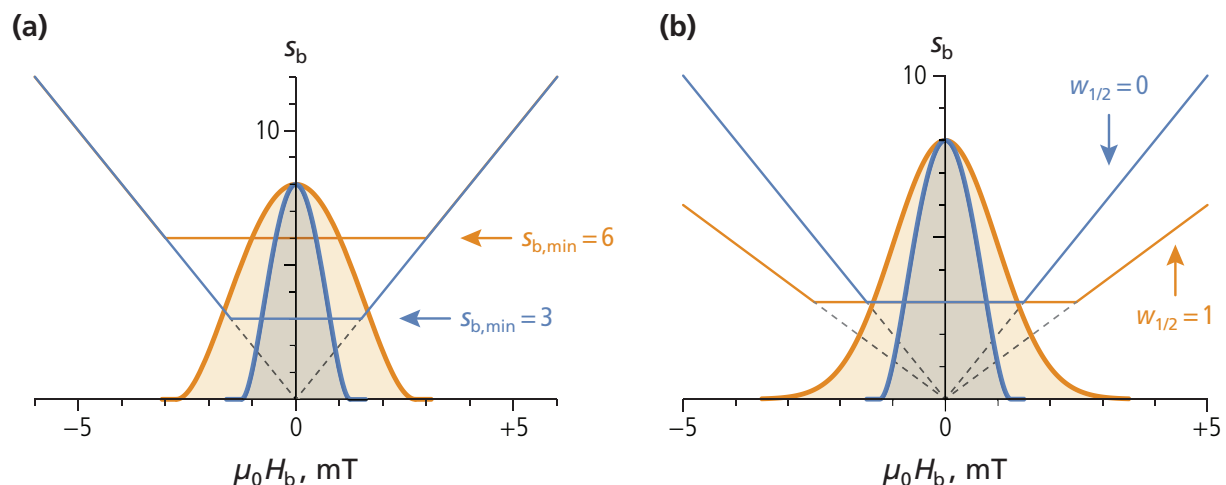


**Fig. 4.23:** Smoothing factor profiles (thin lines) perpendicular to a central ridge (thick lines), according to eq. (2). Both examples assume FORC measurements with 0.5 mT field steps. **(a)** Ideal central ridge with zero intrinsic width (i.e.  $w_{1/2}=0$ ), after FORC processing with a limiting smoothing factor of 3 (blue) and 6 (orange). **(b)** Central ridges characterized by Gaussian intrinsic profiles with  $w_{1/2}=0$  (blue) and  $w_{1/2}=1$  mT (orange), after FORC processing with a limiting smoothing factor of 3. In all cases, the central ridge is processed using a constant smoothing factor over its  $H_b$ -range, so that profiles are equivalent to those obtained with conventional processing.

**INPUT 14. Diagonal smoothing factor limit near coercive fields (new)**

FORC diagram calculation is based on polynomial regression of measured curve sections, whose length is controlled by the smoothing factors chosen with INPUT 10-11. Large smoothing factors, and therefore long curve sections, are often needed to obtain sufficient measurement noise suppression. However, this procedure is limited by the increasing misfit resulting from the fact that polynomials cannot reproduce global features of the measured curves. Such misfits are largest at places where (1) FORCs are steep (i.e.  $M/H$ -maxima), and (2) consecutive FORCs clearly differ from each other (i.e.  $M/H_r$ -maxima). Both conditions correspond to first derivative maxima, which might or might not be related to the FORC function, as shown later with two examples.

In case of FORC measurements of samples with simple hysteresis loop shapes, first derivative maxima occur near the positive and the negative coercive field, i.e.  $\pm H_{coerc}$ . In FORC coordinates, these maxima are distributed along diagonal lines close to  $H_r = -H_{coerc}$  and  $H = +H_{coerc}$ , respectively (Fig. 4.24). Rectangular hysteresis loops generate large first derivative maxima, leading in extreme cases – such as Fig. 4.24 – to evident misfits even with high-resolution measurements and relatively small smoothing factors. In such cases, it is necessary to limit the size of regression rectangles over regions of the FORC diagram where  $\partial M/\partial H_r$  and  $\partial M/\partial H$  are largest. This limitation is controlled by the new option INPUT 14 introduced with version 2.0.

INPUT 14 works in a similar manner as other smoothing factor limitations (e.g. INPUT 12-13). Limitations are avoided with the default option

```
INPUT 14. Smoothing factor limit near coercive fields ( / \ ) ....; None
```

to be used in most cases where processing problems related to large first derivatives are not expected. Otherwise, the simplest way to limit the size of regression rectangles is based on a semi-automatic procedure where an explicitly specified smoothing factor limit (e.g. SF = 5) is applied along diagonals with maximum  $\partial M/\partial H_r$  and  $\partial M/\partial H$  amplitudes. In this case, the first entry of INPUT 14 is Automatic, followed by the limiting smoothing factor. For example,

```
INPUT 14. Smoothing factor limit near coercive fields ( / \ ) ....; Automatic, 5
```

means that the size of regression rectangles along diagonal lines whose position is automatically determined by CalculateFORC is limited to SF = 5.

**Fig. 4.24 (front page):** Example of smoothing artifacts generated by a sample with rectangular hysteresis loop. The sample is a polycrystalline iron film measured in the film plane [courtesy of J.S. McCloy]. (a) High-resolution FORC measurements measured in 0.25 mT steps. Every second curve is shown for clarity. Large curve separation near the negative coercive field corresponds to a  $\partial M/\partial H_r$ -peak near the negative coercive field  $-H_{coerc}$ . On the other hand,  $\partial M/\partial H$  of curves starting at reversal fields  $\leq -H_{coerc}$  peak near the positive coercive field  $H_{coerc}$ .

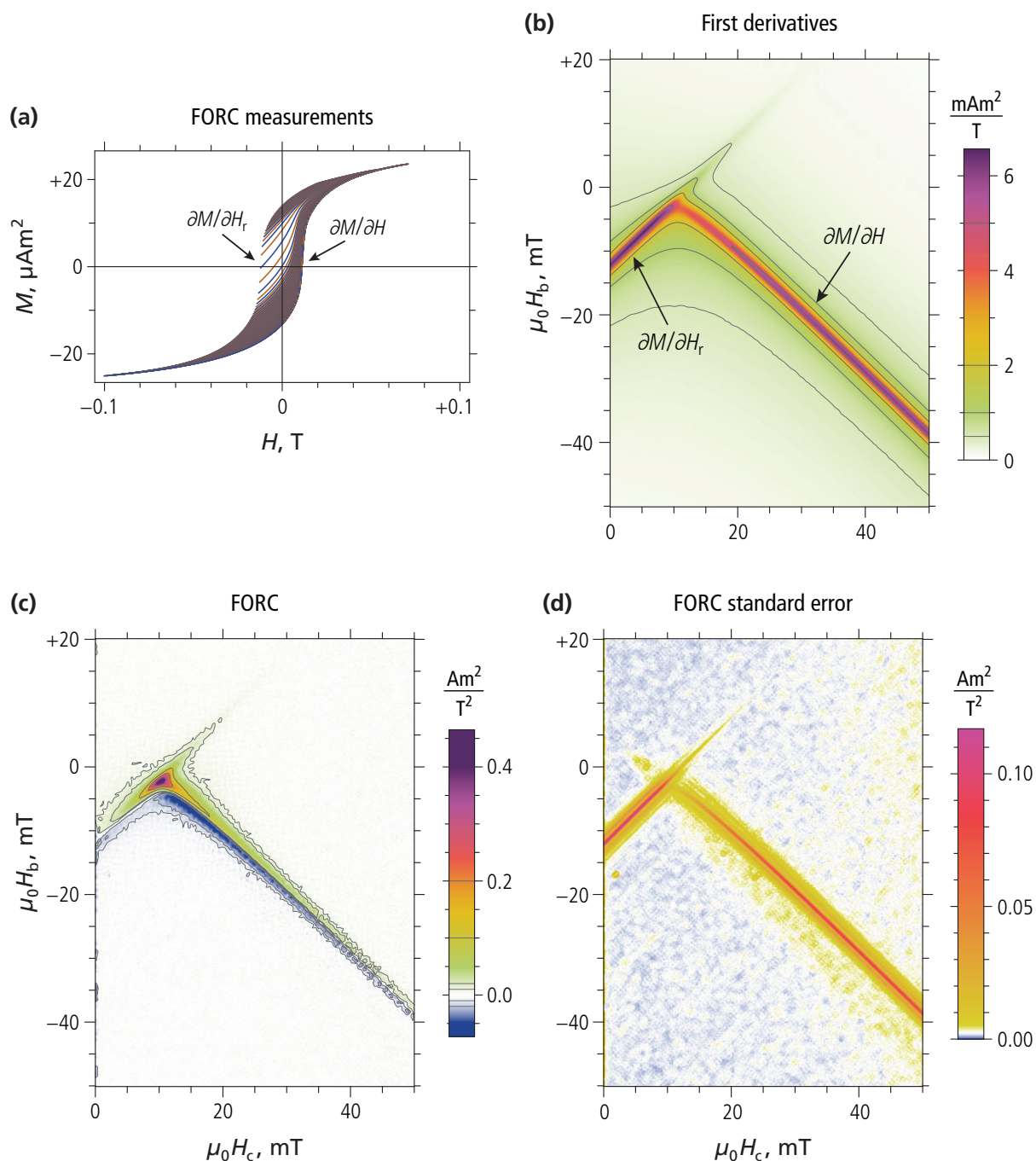


**Fig. 4.24 (continued):** (b) A plot of  $\partial M / \partial H_r + \partial M / \partial H$  in FORC space (obtained by setting INPUT 02 to D) clearly shows the location of first-derivative maxima along diagonal lines defined by  $H_r = -H_{\text{coerc}}$  and  $H = +H_{\text{coerc}}$ , respectively. The resolution of this diagram, obtained with a constant smoothing factor SF = 1.5, is  $\sim 0.4$  mT and the typical width of first derivative maxima is  $\sim 5$  mT. (c) FORC diagram obtained with conventional processing and SF = 1.5. Two positive-negative ridge pairs occur along diagonals with maximum first derivatives. (d) Standard error of the FORC function shown in (c). Error peaks along diagonal lines are of the same order of magnitude as ridge amplitudes in the FORC diagram, whose significance is therefore questionable. Similar results, where most parts of the FORC diagram remaining below the minimum significance threshold, are obtained with any constant smoothing factor.

The size of regression rectangles is limited by “cutting” them along diagonals, so that the resulting octagons fit into the width imposed by the given smoothing factor along  $H_r$  and  $H$ , respectively (Fig. 4.25). Smoothing factor limitations are applied over a range of  $H_r$ - and  $H$ -values where first derivatives are larger than a critical threshold. This threshold corresponds to  $\sim 56\%$  of the first derivative maximum of the upper hysteresis branch obtained from FORC measurements.

In analogy to smoothing factor limits imposed by INPUT 12-13, the transition between unlimited and limited regression rectangles is continuous, providing enhanced resolution along  $H_r$  and  $H$ , where it is most needed (Fig. 4.26d). For this reason, combination of global smoothing options with limits imposed by INPUT 14 enables optimal resolution of ridge-like FORC features related to  $\partial M / \partial H_r$ - and  $\partial M / \partial H$ -maxima (Fig. 4.26e).

The simplest definition of INPUT 14 (i.e. the first parameter of INPUT 14 is set to Automatic) is based on the automatic identification of a first derivative peak in the upper hysteresis branch. The position and width of this peak is stored in the file header of corrected measurement data imported by CalculateFORC. In rare cases, (e.g. extremely noisy data or with uncommon hysteresis loop shapes), the automatic option might fail, generating the following error message:

Hysteresis slope information needed by INPUT 14 is not available from the data file.

In these cases, explicit peak position and width values can be entered with INPUT 14 after inspecting the corrected FORC measurements plotted by ImportFORC.

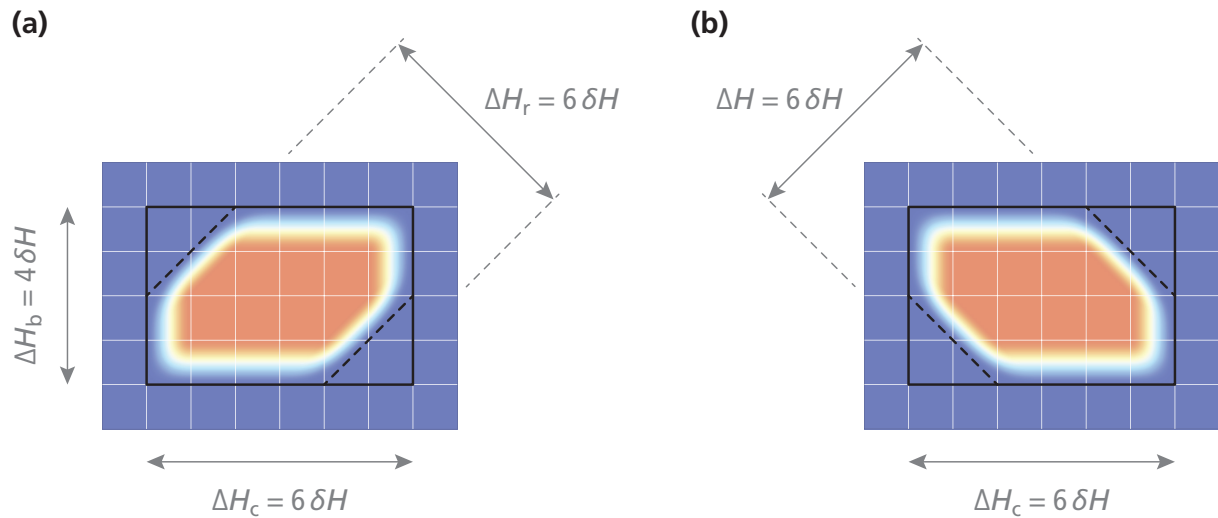


**Fig. 4.25:** Limitation of weighted regression rectangles along diagonals by INPUT 14. The regression rectangles in this example (black) correspond to effective smoothing factors  $s_c = 2.5$  along  $H_c$  and  $s_b = 1.5$  along  $H_b$ , respectively, with a weight function margin of 1 (i.e. INPUT 09 set to 1). Diagonal limits along  $H_r$  (a) and  $H$  (b) (dashed lines) correspond to a limiting smoothing factor  $s = 2.5$  (i.e. the second parameter of INPUT 14 set to 2.5).

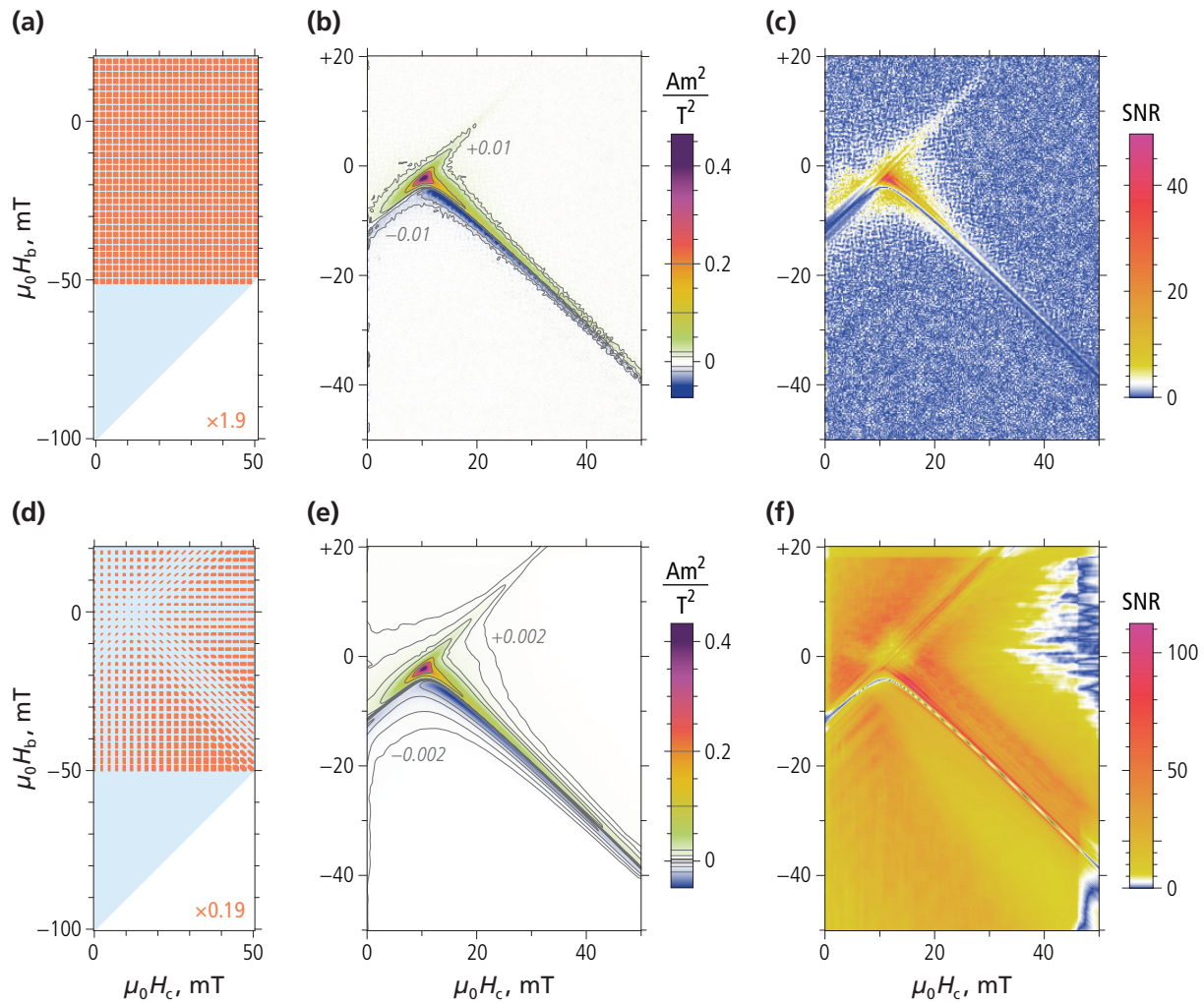


**Fig. 4.26:** FORC processing optimization for the polycrystalline iron film measurements shown in Fig. 4.24. **(a-c)** Conventional processing with a constant smoothing factor SF = 1.5. **(d-f)** Optimized processing with variable smoothing (i.e. INPUT 10 and INPUT 11 set to 5, 0.07), and automatic smoothing factor limitation by SF = 1.5 along diagonals with first derivative maxima (i.e. INPUT 14 set to Automatic, 1.5). **(a,d)** Schematic representation of regression rectangles (orange, scale factor shown on the lower right corner) over the FORC measurement range (light blue). Size limitation along diagonals is clearly distinguishable in (d). **(b,d)** FORC diagrams. Contour lines have been added with the VARIFORC module PlotFORC. In both cases, positive-negative ridge pairs occur along diagonals defined by  $H_r = -H_{\text{coerc}}$  and  $H = +H_{\text{coerc}}$ , respectively. Measurement noise reduction in (e) enabled contour drawing down to 0.5% of the central FORC maximum. **(c,f)** Signal-to-noise ratios (SNR) of the FORC diagrams shown in (b,d). Warm colors (yellow-orange-red) correspond to values of the FORC function that are significantly different from zero, in contrast to insignificant values coded in blue. In case of conventional processing, only the central FORC maximum is significant. Advanced processing, on the other hand, extend the range of significant contributions to the whole diagram, including the two diagonal ridges. The thin blue line in (f) correspond to the transition between negative and positive FORC values, where true zeroes of the FORC function occur. The FORC diagram in (e) contains the typical signatures of strong positive interactions, which originate between Fe grains in the thin film plane (see INPUT 17).

Explicit specifications of the FORC range where the smoothing factor limit of INPUT 14 is applied are entered as sequence of three numbers, e.g.

```
INPUT 14. Smoothing factor limit near coercive fields ( / \ ) ....; 12,2,1.7
```

where the first value is the position  $H_{coerc} > 0$  of the diagonal limits at  $H_r = -H_{coerc}$  and  $H = +H_{coerc}$ , the second value is the smoothing factor limit, and the third value is the width  $w$  of the limiting region.  $H_{coerc}$  and  $w$  are best deduced from the FORC measurement plot produced by ImportFORC. In this case,  $H_{coerc}$  is the absolute value of negative reversal fields corresponding to consecutive curves with largest separation, and  $w$  is the field interval over which the maximum distance between consecutive FORCs is reduced by 50%.

Unlike the particular example of Fig. 4.26, the FORC function is generally not related to particular features of  $\partial M / \partial H_r$  and  $\partial M / \partial H$ . For example, non-interacting single-domain particles are characterized by squared hysteresis loops yielding large first derivative peaks; however, the corresponding FORC diagrams are free of diagonal ridges (Fig. 4.27). Nevertheless, polynomial regression misfits near  $H_r = -H_{coerc}$  and  $H = +H_{coerc}$  produce artifacts that need to be corrected with INPUT 14.

- 💡 INPUT 14 extends the applicability of variable smoothing procedures and enables larger smoothing factor increase rates for better measurement noise suppression at high fields.
- 💡 The best smoothing factor limit in INPUT 14 is a compromise between the opposite needs of measurement noise suppression (large values) and regression artifact suppression (small values). Preliminary runs at low resolution (i.e. INPUT 06 is set to Fast) can be used for this purpose.

#### Updates from version 1.0:

- INPUT 14 is a new feature of version 2.0.
- Automatic INPUT 14 options require additional information stored in corrected measurement files generated by version 2.0 of ImportFORC. Although CalculateFORC can import corrected measurement files generated by older versions of ImportFORC, replacement of old files is recommended in order take advantage of full processing functionality.

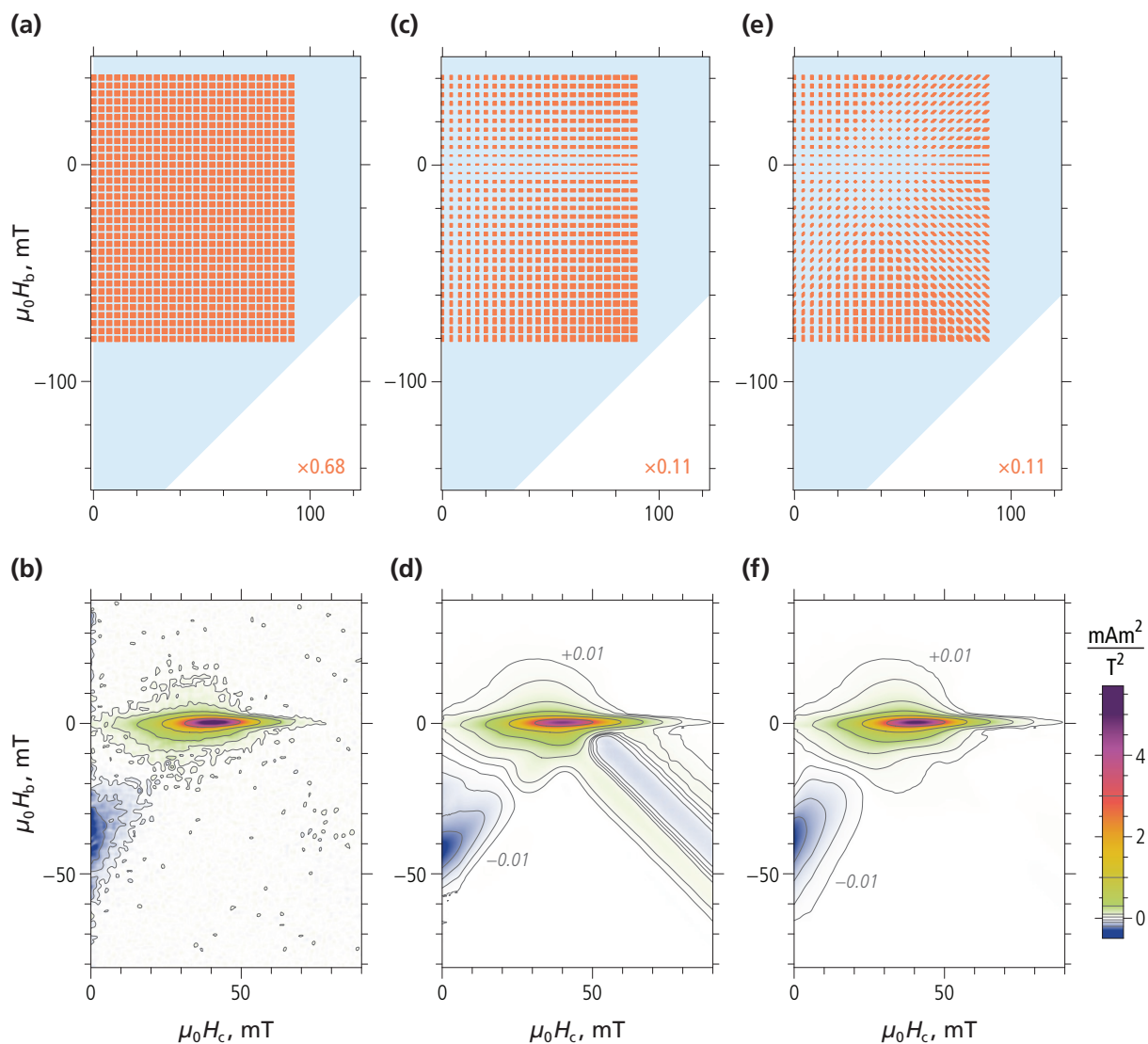


**Fig. 4.27:** FORC processing optimization for high-resolution measurements of cultured magnetotactic bacteria (see the downloadable example “vibrio MV-1”). **Top plots:** Schematic representation of regression rectangles (orange, scale factor shown on the lower right corner) over the FORC measurement range (light blue). **Bottom plots:** FORC diagrams plotted with identical color scales and contour levels. **(a,b)** Conventional FORC processing with constant smoothing factor SF = 3. Most FORC contributions outside the central ridge are dominated by measurement noise. **(c,d)** Variable smoothing obtained with INPUT 10 and INPUT 11 set to 9, 0, 1. Measurement noise is largely suppressed in comparison to (b); for example, non-zero contributions over the upper quadrant are clearly recognizable. On the other hand, the large size of regression rectangles produced regression artifacts along diagonals departing from the central maximum. These diagonals coincide with  $\partial M / \partial H_r$ - and  $\partial M / \partial H$ -maxima. **(e,f)** Regression artifacts in (d) have been suppressed by limiting the smoothing factor to SF = 9 along automatically selected diagonals (i.e. INPUT 14 set to Automatic, 9). Notice the smallest contour level, which represents FORC contributions whose amplitude is ~0.2% of the central maximum.

**INPUT 15-16. Diagonal smoothing factor limits at given  $H$  and  $H_r$  (updated)**

Advanced smoothing options controlled by INPUT 10 and INPUT 11 are based on a Preisach model where the FORC diagram is the product of a pure function of  $H_c$  (e.g. coercivity distribution) and a pure function of  $H_b$  (e.g. interaction field distribution). The typical shape of these functions require maximum resolution at  $H_c=0$  and  $H_b=0$ , so that the size of regression rectangles can be increased when moving away from the high-resolution regions coinciding with the  $H_c$ - and  $H_b$ -axes (Fig. 4.28). This is the principle of the variable (VARIFORC) smoothing procedure introduced by Egli [2013]. A practical limit to this procedure is imposed by the finite capacity of polynomial regression to fit the general shape of magnetization curves over large range of fields. For example, large misfits can arise at places where measured curves are particularly steep (i.e.  $\partial M/\partial H$ -maxima) or very different from each other (i.e.  $\partial M/\partial H_r$ -maxima). Therefore, the optimal size of regression rectangles is also a function of  $H_r$  and  $H$ , which are tied to a coordinate system that is rotated by 45° with respect to the FORC coordinates  $H_c$  and  $H_b$  (Fig. 4.28).

Smoothing limits along  $H_r$  and  $H$  are controlled by INPUT 14 and INPUT 15-16. INPUT 14 limits the size of regression rectangles along first derivative maxima associated with squared hysteresis loops, solving most common regression problems. INPUT 15-16, on the other hand, enable full control of smoothing factor limits along diagonals defined by given values of  $H_r$  and  $H$ , using the same principles of INPUT 14. This possibility is rarely needed and is provided only for completeness, since all common processing requirements are covered by the other options. Therefore, the recommended default option for INPUT 15-16 is

```
INPUT 15. Smoothing factor limit at given H (\ ) ...; None  
INPUT 16. Smoothing factor limit at given Hr (/ ) ...; None
```

A synthetic example is discussed in the following, where a superparamagnetic (SP) contribution has been added to the FORC measurements of single-domain particles (Fig. 4.29). This contribution is characterized by a sharp steepening of all curves at  $H=0$  (i.e. a  $\partial M/\partial H$ -maximum), and produces regression artifacts along the remanence diagonal defined by  $H=0$  (i.e.  $H_b=-H_c$ ). Because all curves share the same SP contribution near  $H=0$ , and because this contribution – not being a function of  $H_r$  – is “invisible” to the FORC diagram, the problem is best solved by subtracting one curve, e.g. the last one, from all measurements (i.e., INPUT 01 set to DF0RC). If this possibility is ignored, a smoothing factor limit along  $H=0$  can be set using INPUT 15, i.e.:

```
INPUT 15. Smoothing factor limit at given H (\ ) ...; 0,4,7
```

(Fig. 4.29e). The first number in INPUT 15 (i.e. 0) sets the value of  $H$  around which the smoothing factor is limited to a value set by the second number (i.e. 4). The third number control the width of the region affected by the smoothing factor limitation (i.e. 7 mT). In this example, 7 mT coincide with the field required to reach 50% of the SP saturation. Position and width of the region affected by smoothing factor limitation must be expressed with same field units used for the FORC measurements, as specified in the file header.

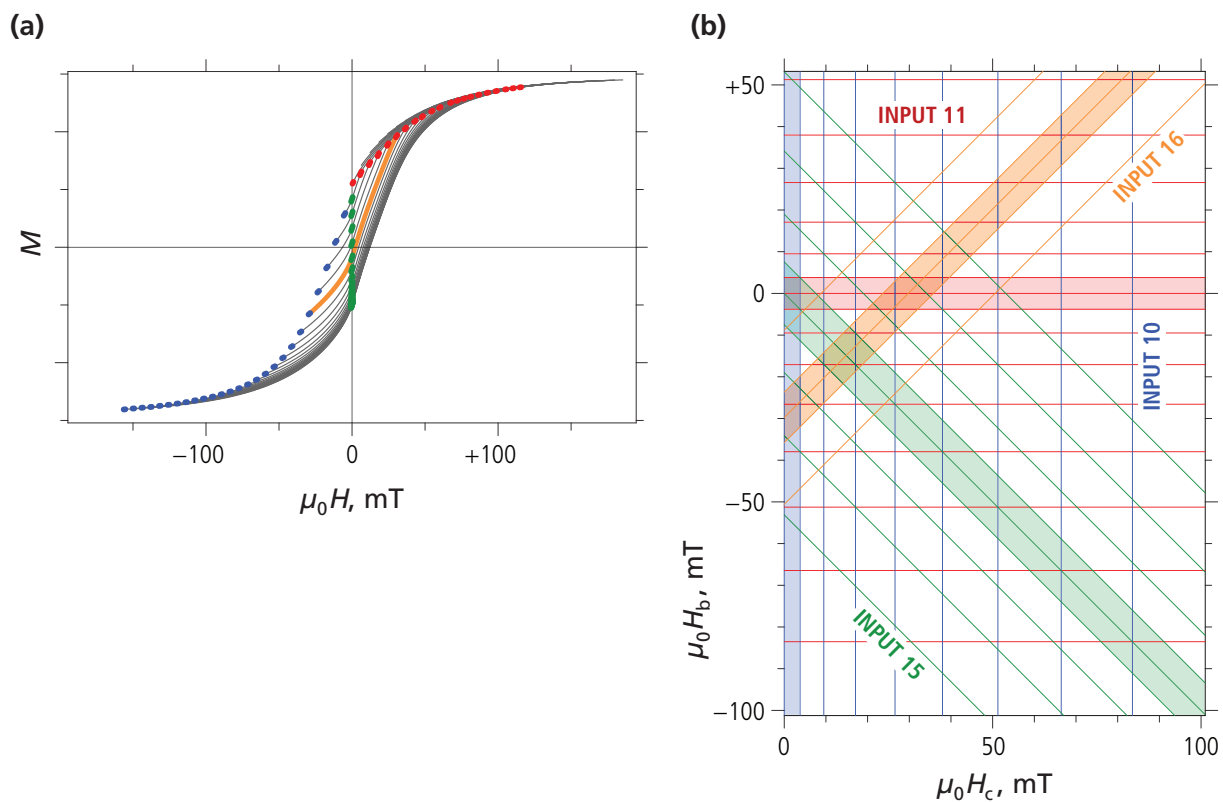


**Fig. 4.28:** Schematic illustration of processing requirements related to measurement coordinates ( $H_r$  and  $H$ ), and Preisach coordinates ( $H_c$  and  $H_b$ ). **(a)** FORC measurements of a sediment sample from the Indian Ocean, containing mainly single-domain particles. Segments of the FORC curves that require high-resolution processing are highlighted in blue, green, red and orange. Blue segments correspond to the beginning  $H=H_r$  of each curve, which might be characterized by anomalous slopes associated with magnetic viscosity effects [Pike *et al.*, 2001]. Green segments at  $H=0$  correspond to remanence measurements. The slope of magnetization curves can increase sharply at  $H=0$ , due to superparamagnetic contributions, or, as in this example, to single-domain particles with vanishing coercivity. Such slope discontinuities produce so-called “wasp-waisted” hysteresis loops [Tauxe *et al.*, 1996]. Red segments at  $H=-H_r$  represent the symmetric counterpart of the beginning of each curve, where “magnetic memory” of the reversal field might produce slopes discontinuities associated with the so-called central ridge [Egli *et al.*, 2010]. The orange curve represents a place where measurement curves are very sensitive to  $H_r$ . **(b)** Grids representing smoothing factor limits imposed by the curve segments highlighted in (a) and controlled by parameters entered with INPUT 10 - 11 and INPUT 15 - 16. Blue dots in (a) define a vertical ridge along  $H_c = 0$  (blue shading), and blue lines represent the horizontal smoothing factor increase towards large values of  $H_c$ . Red dots in (a) define a central ridge along  $H_b = 0$  (red shading), and red lines represent the vertical smoothing factor increase towards large  $H_b$ -amplitudes. Green dots in (a) define a ridge along the remanence diagonal  $H_b = -H_c$  (green shading), and green lines represent the diagonal smoothing factor increase towards large applied field amplitudes  $|H|$ . The orange line in (a) define a ridge along a diagonal with positive slope (orange shading), and orange lines represent the diagonal smoothing factor increase along  $H_r$ . Only some of the limits drawn in this figure are needed for processing typical FORC measurements. Furthermore, automatic diagonal limits that work in most situations can be set automatically with INPUT 14.

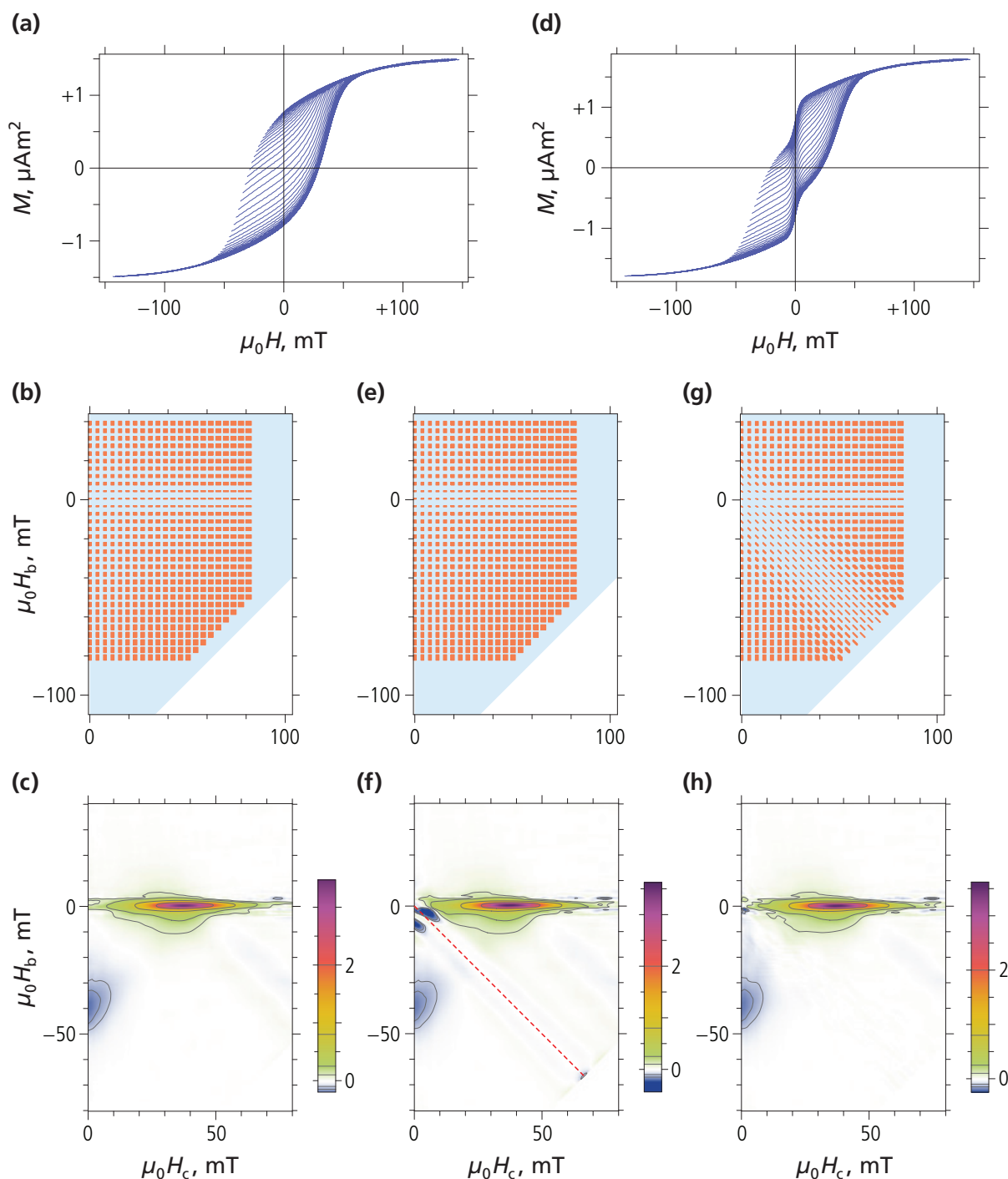


**Fig. 4.29:** FORC processing examples based on cultured magnetotactic bacteria (see the downloadable example “Magnetospirillum 2”). **(a)** FORC measurements. **(b)** Regression rectangles (orange, not to scale) created by a variable smoothing procedure with INPUT 10-11 set to 9, 0.07, and **(c)** corresponding FORC diagram. **(d)** FORC measurements with a superparamagnetic contribution added numerically. **(e,f)** Regression rectangles and FORC diagram obtained with the same settings as in (b,c). Notice the regression artifacts along the remanence diagonal (red dashed line) produced by the added superparamagnetic contribution at  $H = 0$ . **(g)** Regression rectangles (orange, not to scale) created by the same variable smoothing procedure as in (b), and additional smoothing factor limitation along the remanence diagonal (i.e. INPUT 15 set to 0, 4, 7). **(h)** Corresponding FORC diagram. Regression artifacts are almost completely suppressed.

- 💡 For every VARIFORC application known so far, optimal processing parameters have been obtained without the need of additional constraints set by INPUT 15 - 16.
- 💡 Diagonal smoothing factor limits, when needed, are often related to first derivative maxima near positive/negative coercive fields and can be handled automatically with INPUT 14.
- 💡 Processing problems might arise at fields  $H$  where magnetization curves are particularly steep. A typical example are superparamagnetic contributions that saturate in small fields (e.g. Fig. 4.29). If these contributions are similar for all curves, processing problems are best solved by working with FORC measurement differences (i.e. INPUT 01 set to DFORC).

**Updates from version 1.0:**

- INPUT 15 is the updated analogue to INPUT 13 of version 1.0.
- INPUT 16 adds the possibility of limiting the size of regression rectangles along  $H_r$ .
- INPUT 15 - 16 limit the size of regression rectangles along diagonals, instead of acting on their width and height as in version 1.0.

### INPUT 17. Mean field correction parameters

When measuring a magnetic specimen, it is sometimes convenient to distinguish between the external field  $H$  applied by the measuring instrument, and the so-called *internal field*,  $H^i$ , i.e. the magnetic field existing inside the specimen. The internal field is the sum of the external field and any additional field generated by the specimen magnetization (Fig. 4.30). The simplest model for the internal field is thus given by

$$H^i = H + \alpha M(H) \quad (3)$$

where  $M$  is the measured specimen magnetization, and  $\alpha$  is a specimen-specific proportionality constant. Magnetic measurements are expressed as a function of the applied field, i.e.  $M = M(H)$ ; however, the magnetization is an intrinsic response to the field “seen” by the magnetic material, i.e.  $M = M(H^i)$ . This principle applies also to FORC measurements, and it is sometimes desirable to analyze the intrinsic material properties expressed by  $M = M(H_r^i, H^i)$ , where  $H_r^i$  and  $H^i$  are the internal counterparts of  $H_r$  and  $H$ , respectively. The conversion of measured curves  $M(H_r, H)$  into “intrinsic curves”  $M(H_r^i, H^i)$  using eq. (3) is called *mean field correction*. Mean field corrections affect the properties of FORC diagrams calculated from  $M(H_r^i, H^i)$ , because the relationship between internal and external fields is highly non-linear. A mean field correction example based on a thin film made of iron is shown in Fig. 4.31. In this case, an additional, positive (i.e.  $\alpha > 0$ ) field is generated inside the sample by the interaction between individual Fe grains.

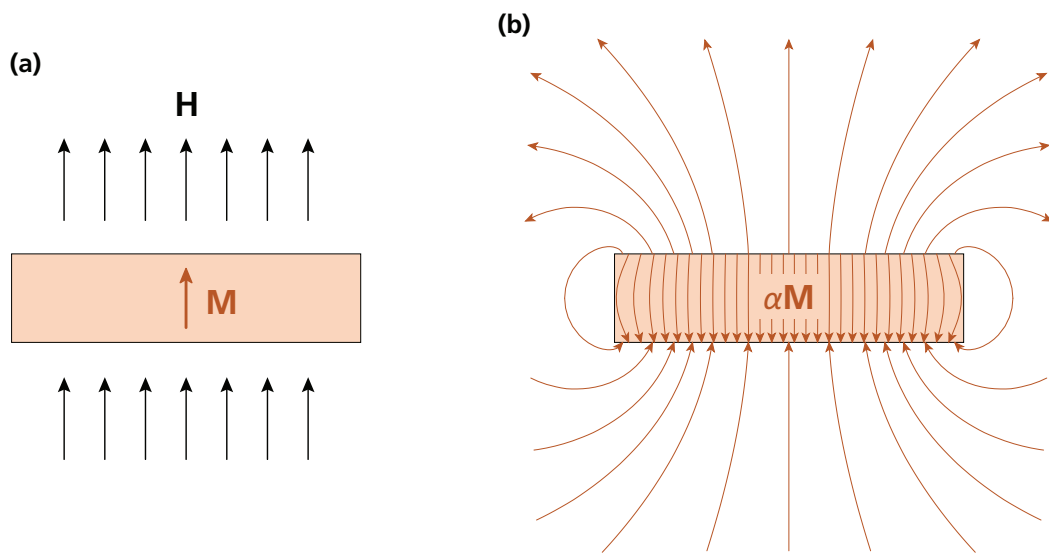


**Fig. 4.30:** General principles of mean field corrections. (a) A platelet-like specimen (shaded) immersed in the external field  $H$  acquires a bulk magnetization  $M$  (i.e. the total magnetic moment divided by the specimen volume). (b) The specimen magnetization generates its own internal and external magnetic fields (arrows). The external field enables measurements of  $M$  based on the equivalent dipole moment, while the mean internal field,  $\alpha M$  adds to the applied field and generates the total internal field  $H^i = \alpha M$  “seen” by the specimen. Accordingly,  $M$  is a function of  $H^i$  and the intrinsic magnetic properties of the specimen material.

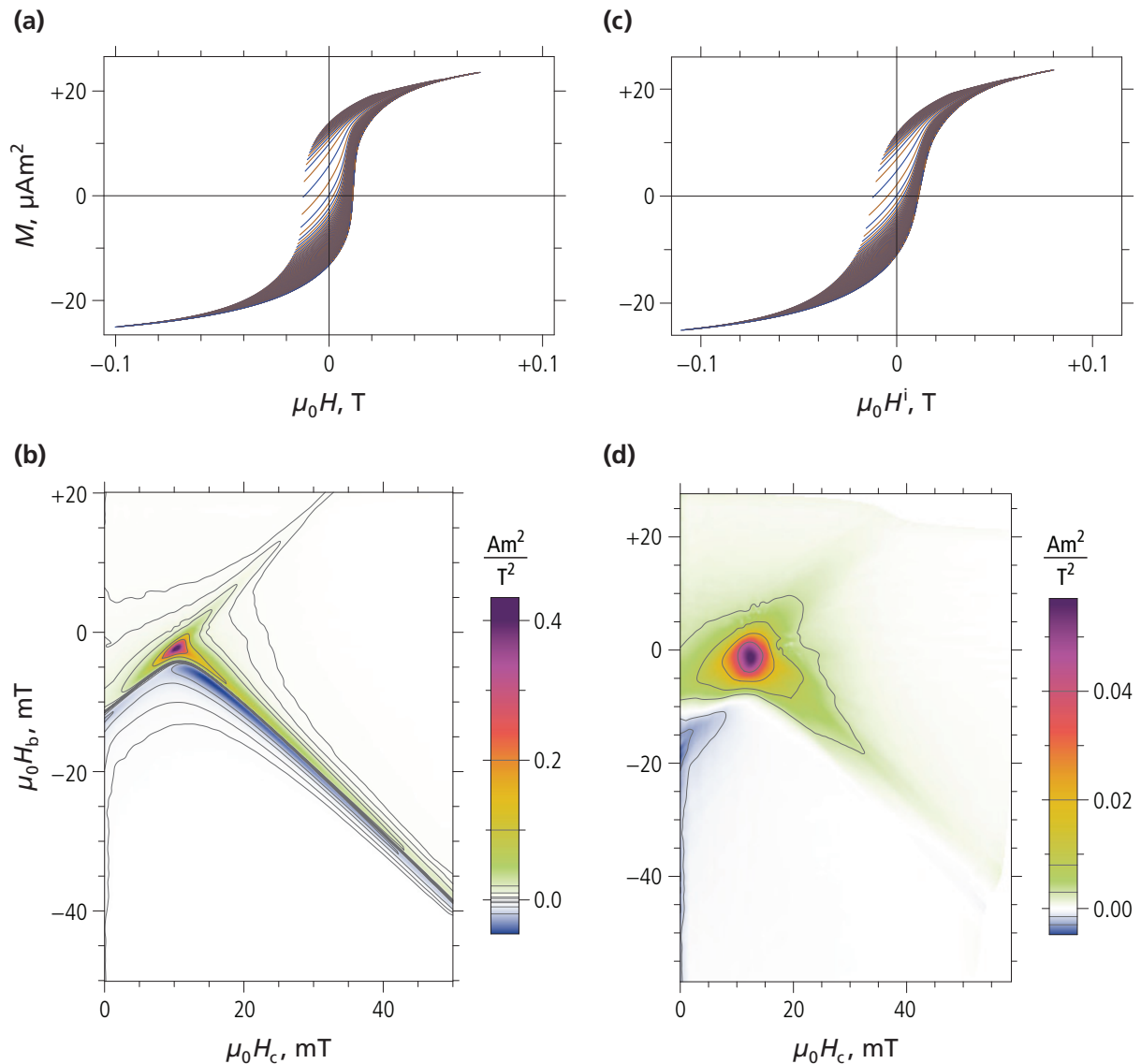


**Fig. 4.31:** Example of mean field correction applied to FORC measurements. The sample is a polycrystalline iron film measured in the film plane [courtesy of J.S. McCloy]. **(a,b)** Original FORC measurements  $M(H_r, H)$  and corresponding diagram. **(c)** Mean-field-corrected FORC measurements  $M(H^i, H^i)$  obtained with eq. (3) and  $\alpha = +0.4 \text{ T/mAm}^2$ . The positive sign of  $\alpha$  means that the internal field is enhanced by the specimen magnetization, as expected from positive interactions between Fe grains within the film plane. **(d)** FORC diagram corresponding to corrected measurements in (c). The diagonal ridges in (b) have been almost completely suppressed, leaving a “smooth” FORC distribution that is more characteristic for single-domain and pseudo-single-domain Fe particles. Accordingly, the FORC diagram in (d) represents the intrinsic signature of Fe particles, i.e. their response to the field in which they are immersed. Residual traces of the diagonal ridges are caused by unremoved internal field contributions. In fact, only the average internal field can be calculated with eq. (3), while field inhomogeneity contributions – described by a distribution of  $\alpha$ -values – continue to affect the FORC diagram. As evident in this example, strong mean field contributions can completely mask intrinsic FORC signatures while having only a modest effect on the hysteresis loop.

Version 2.0 of CalculateFORC enables the application of a mean field correction prior to FORC diagram calculations, with parameters set by INPUT 17. The default option for INPUT 17 is

```
INPUT 17. Mean field correction parameters ....; None
```

if a mean field correction is not required. Otherwise, INPUT 17 is specified by a pair of numbers, e.g.

```
INPUT 17. Mean field correction parameters ....; 1,0.4
```

for the example of Fig. 4.31. The first number (e.g. 1) is the smoothing factor used to fit the measured magnetization  $M(H_r, H)$ , which is required by eq. (3). Because magnetization fits are much less sensitive than the mixed second derivative required for calculating the FORC diagram, conventional processing with a constant smoothing factor is sufficient for obtaining excellent results. In fact, this smoothing factor can be very small (e.g. equal to the minimum value of 1) while still providing excellent results. The second INPUT 17 parameter (e.g. 0.4) is the value of the constant  $\alpha$  in eq. (3) used for performing the mean field correction. The value of  $\alpha$  has to be expressed in (field)/(magnetization) units according to the units listed in the file header of the imported FORC data. For example, the original field and magnetization units for the example of Fig. 4.31 are T and mAm<sup>2</sup>, respectively, so that the proper unit of  $\alpha$  is T/mAm<sup>2</sup>. Another way to enter  $\alpha$  is by normalizing it with the saturation magnetization or the saturation remanence of the specimen, for example

```
INPUT 17. Mean field correction parameters ....; 1,0.8/MS
```

if the entered value (e.g. 0.8) is to be normalized by the saturation magnetization stored along with the imported FORC data. In this case, the entered value has the same unit as the magnetic field of the imported data. This option is particularly useful when mean fields are caused by the exchange bias, in which case  $\alpha$ , when normalized by  $M_s$ , can be identified with the exchange field.

Units should be examined carefully when mean field corrections are performed. A proper physical meaning for eq. (3) is only given if  $\alpha$  is entered as exchange field and normalized by  $M_s$ , or if  $M$  is the volume-normalized magnetization (S.I. unit: A/m, c.g.s. unit: emu/cm<sup>3</sup>) and  $H$  is the magnetic field (S.I. unit: A/m, c.g.s. unit: Oe). In this case,  $\alpha$  is a unitless number comprised between -1 and +1 (S.I. system), or -1/4π and +1/4π (c.g.s. system). Meaningful values of  $\alpha$  are either guessed, or deduced after proper unit transformations (see the Appendix at the end of this section). Only a finite range of values yields meaningful corrections. In case  $\alpha$  is guessed, the correct value is deduced from the signature of the resulting FORC diagram, implying some knowledge about the specimen properties.

The mean field correction procedure used by CalculateFORC is based on few processing steps based on the interplay between original and corrected FORC coordinates (Fig. 4.32). The first step consists in calculating magnetization values  $M(H_c, H_b)$  over the whole range covered by measurements, using the constant smoothing factor entered with INPUT 17. These values are used in combination with eq. (3) to calculate internal field coordinates  $(H_c^i, H_b^i)$  for each measurement point, according to the value of  $\alpha$  entered with INPUT 17 (Fig. 4.32b).

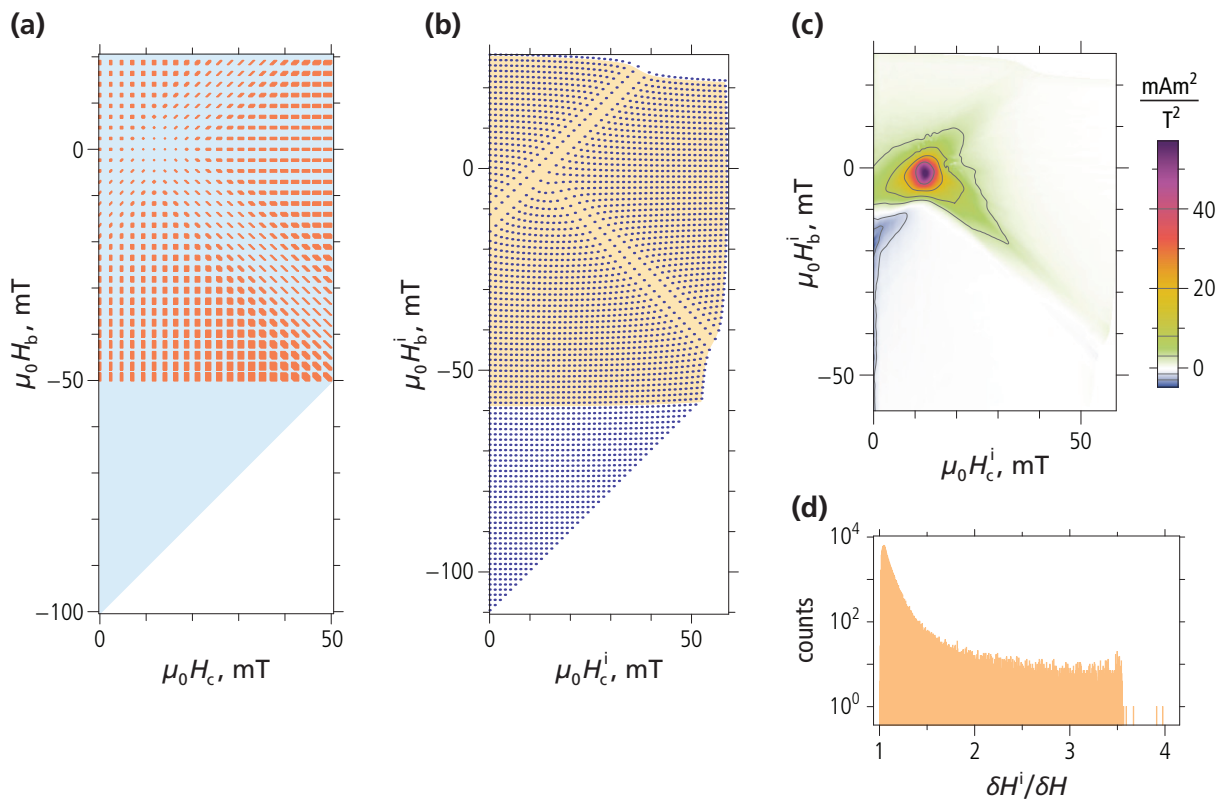


**Fig. 4.32:** Mean field correction procedure used by CalculateFORC, illustrated with the example of the polycrystalline iron film shown in Fig. 4.31. **(a)** Schematic representation of regression rectangles (orange, not to scale) over the chosen output range. The FORC range covered by measurements is shown as light blue background. The size of regression rectangles is optimized with respect to the peculiar properties of the uncorrected FORC diagram, providing higher resolution along diagonal lines characterized by  $\partial M / \partial H_r$ - and  $\partial M / \partial H$ -maxima near the positive and negative coercive fields. **(b)** Location of measurement points (dots, every second shown for clarity) in internal field coordinates  $(H_c^i, H_b^i)$ . The shaded area represents the output range covered by measurements. Notice the large separation between measurement points across diagonals with first derivative maxima. **(c)** Mean-field-corrected FORC diagram, obtained by polynomial regression of measurement points in internal field coordinates  $(H_c^i, H_b^i)$ . The FORC diagram is calculated for the smallest regular matrix of output points that encloses the shaded output range in (b). While polynomial regression is performed with internal field coordinates, the choice of regression rectangles and corresponding weight factors occurs in original measurement coordinates according to (a). **(d)** Histogram of “internal” field steps  $\delta H^i$  of measurements, normalized by the step  $\delta H$  of applied fields. Most steps are unaffected by the mean field correction, as seen from the peak at  $\delta H^i / \delta H \approx 1$ , corresponding to FORC regions where the grid of measurement points in (c) is undistorted. Grid distortions are proportional to  $\partial M / \partial H_r$  and  $\partial M / \partial H$ , and are therefore maximal near positive/negative coercive fields, and minimal near saturation. Large  $\delta H^i$ -values reduce the amplitude of derivatives across the diagonals mentioned above, eliminating the diagonal ridges visible in the uncorrected FORC diagram.

The transformed coordinates no longer form a regular measurement grid as with the original coordinates did, because the distance between neighbor points, corresponding originally to field measurement steps  $\delta H$ , is modified according to local magnetization differences. A histogram of the “internal” field steps  $\delta H^i$  (Fig. 4.32d) gives an idea of how the total internal field is affected by the specimen magnetization. In general,  $\alpha > 0$  expands the field steps, and  $\alpha < 0$  makes them smaller. If negative values of  $\alpha$  are entered, it is important to verify that internal field steps remain positive, since the time sequence of measurements cannot be reversed. This check is performed automatically. The following error message is produced if negative  $\delta H^i$  are encountered

**More than 5% of all corrected field steps are negative!**

**Mean field effects resulting from INPUT 17 specifications are unphysical. Program aborted.**

and the program is aborted. In this case, less negative values of  $\alpha$  must be chosen. Once the measurement grid and the chosen output range have been expressed in internal field coordinates, a regular grid of output points is built over the output range. This grid will support the output FORC diagram through polynomial regression of measurement points in  $(H_c^i, H_b^i)$ -coordinates.

While polynomial regression is performed on internal field coordinates, the choice of regression rectangles and corresponding weight factors is based on original measurement coordinates and the smoothing options chosen with INPUT 10-16. This means that the  $(H_c^i, H_b^i)$ -coordinates of each output point of the FORC diagram need to be transformed into  $(H_c, H_b)$ -coordinates, so that both coordinate systems are used for polynomial regression. This procedure ensures that the smoothing procedure fulfill the same criteria used for processing FORC diagrams without mean field correction. Therefore, a preliminary CalculateFORC run without mean field correction is recommended for optimizing the choice of processing parameters.

Mean field correction can also be used for simulation purposes, i.e. for simulating the effect of a given mean field on existing FORC data. Such simulations are based on

$$H = H^i - \alpha M(H^i) \quad (4)$$

where  $H^i$  is the internal field, supposed to coincide with the measurement field, and  $H$  is the simulated applied field. Eq. (4) formally equivalent to eq. (3) after reversing the sign of  $\alpha$ . This means that internal field enhancement is simulated with negative values of  $\alpha$  and vice versa. For example, positive/negative mean field effects on single-domain particles can be simulated using FORC data of specimens containing non-interacting particles (Fig. 4.33), reproducing the typical mean field signatures predicted by theoretical models.

**Fig. 4.33 (front page):** Simulation of mean field effects on a dispersion of single-domain (SD) particles. The starting dataset for these simulations is a pelagic carbonate whose magnetic properties are equivalent to those of isolated (non-interacting) SD particles with uniaxial anisotropy, as shown in (a,b) (see the downloadable example “pelagic carbonate”). The non-interacting SD signature consists of a horizontal ridge along  $H_b = 0$  [Newell, 2005]. (c,d) Negative mean field interactions have been simulated by setting INPUT 17 to  $2, 0, 0.008$  (i.e.  $\alpha = -0.008 \text{ T/mAm}^2$  ).

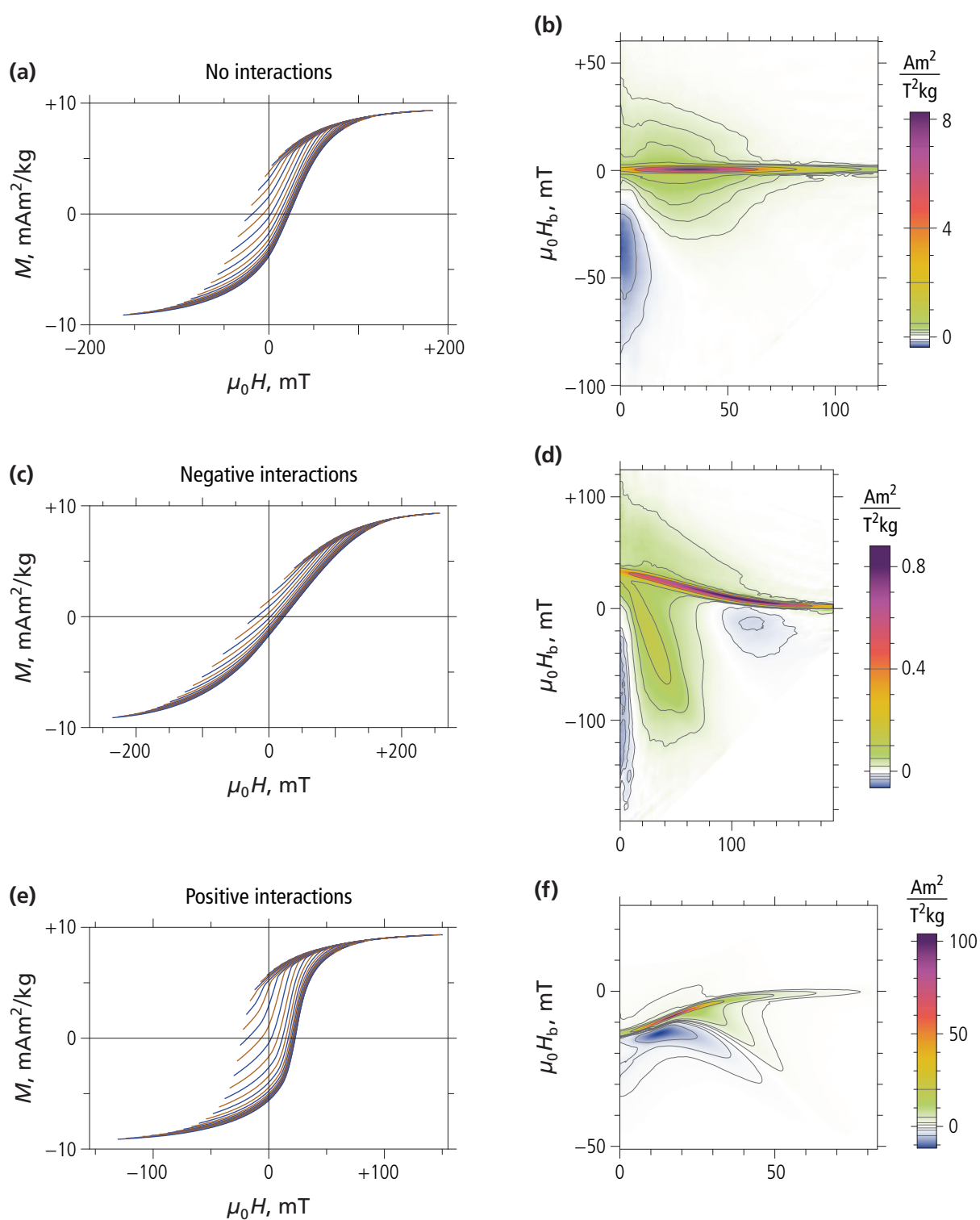


**Fig. 4.33 (continued): (c,d)** The hysteresis loop loses its SD signature, while an upward shifted central ridge is preserved in the FORC diagram, whose signature matches model predictions [Pike *et al.*, 2005]. **(e,f)** Positive mean field interactions have been simulated by setting INPUT 17 to 2, -0.0035 (i.e.  $\alpha = +0.0035 \text{ T/mAm}^2$ ). The hysteresis loop has become rectangular, with increased coercivity and saturation remanence reflecting the stabilizing effect of positive interactions. The central ridge is shifted downwards and diagonal positive/negative ridge pairs similar to those of Fig. 4.31b begin to appear.

- 💡 Mean field corrections are always based on an (implicit) model for the internal properties of the measured specimen. These are rarely known in advance, so that mean field corrections are often obtained with guesses of the proportionality constant  $\alpha$  in eq. (3). In this case, the guess is based on the disappearance of FORC signatures considered typical for positive/negative mean fields. Because of the iterative nature of such guesses, preliminary runs are best performed at low resolution (i.e. INPUT 06 is set to Fast).
- 💡 The Appendix at the end of this section describes useful methods for obtaining meaningful initial guesses of the proportionality constant  $\alpha$  in eq. (3).
- 💡 Selection of proper smoothing parameters is best performed on preliminary runs without mean field correction (i.e. INPUT 17 is set to None). These runs are also useful for recognizing typical positive/negative mean field signatures in the FORC diagram, which can serve as a guide for choosing a proper correction.
- 💡 INPUT 17 can also be used as a modeling tool for predicting the effects of mean interaction fields on given magnetic systems (e.g. Fig. 4.33). In this case, the sign of the proportionality constant  $\alpha$  is reversed with respect to the case of mean field corrections (i.e. positive values for simulating negative mean fields and vice versa).

**Updates from version 1.0:**

- Mean field correction is a new feature of version 2.0.

## Appendix: Calculation of appropriated mean field corrections

The definition of internal field is straightforward in case of homogeneous magnetic materials (Fig. 4.30), where this field is the sum of the applied field and the field produced by the specimen magnetization. In such cases, the proportionality factor  $\alpha$  in eq. (3) depends only on specimen shape and is called *demagnetizing factor* [e.g. Morrish, 1965]. Heterogeneous materials, such as magnetic particle dispersions, represent a more complicated case where two definitions of internal field are possible, depending on whether “internal” is referred to the specimen (specimen field) or to the magnetic particles themselves (crystal field). Furthermore, magnetic measurements of particle dispersions are typically expressed with mass-normalized magnetization units (S.I.: Am<sup>2</sup>/kg, c.g.s.: emu/g). In such cases, the proportionality factor  $\alpha$  in eq. (3) has no direct physical meaning, unless proper unit conversion is considered as discussed in the following.

### Case 1: Specimen internal field

In this case, the internal field is the total field “seen” by the magnetic particles, and is usually regarded as the superposition of a mean field over the whole specimen volume and a local field dictated by the stray fields produced by neighbor particles in what is known as *magnetostatic interaction field*. The mean component of this field is corrected with eq. (3) and an appropriated proportionality factor  $\alpha = \alpha_{si}$  that can be derived from simple specimen properties. For this purpose, consider a specimen of mass  $m$ , volume  $V$ , and mass-normalized saturation magnetization  $M_s$ , which contains a uniform dispersion of magnetic particles made of a material with volume-normalized spontaneous magnetization  $\mu_s$ . The magnitude of interaction fields is a function of  $\mu_s$  and of the volume concentration  $0 < p < 1$  of magnetic particles. In case of uniform particle dispersions, this concentration is given by:

$$p = \frac{M_s m}{\mu_s V} \quad (4)$$

Because the intensity of local interaction fields is of the order of magnitude of  $0.3p\mu_s$  [Egli, 2006], typical starting values of  $\alpha$  to be used with eq. (3) in combination with mass-normalized specimen magnetizations are given by:

$$\alpha_{si} \left[ \frac{T}{Am^2/kg} \right] \approx 0.3\mu_0 \times \frac{m [kg]}{V [m^3]} \quad \alpha_{si} \left[ \frac{Oe}{emu/g} \right] \approx \frac{0.3}{4\pi} \times \frac{m [g]}{V [cm^3]} \quad (5)$$

in S.I. and c.g.s. units respectively, with  $\mu_0 = 4\pi \times 10^{-7}$  Vs/(Am). Inhomogeneous particle dispersions are characterized by locally higher concentrations, with correspondingly larger values of  $\alpha_{si}$ .

### Case 2: Crystal field

In some cases, the intrinsic properties of magnetic particles are better described in terms of reaction of the magnetic material they are made of to the total field inside them. For example, domain wall pinning/unpinning is controlled by this field, rather than the field existing outside the

particles. Mean field corrections are then based on eq. (3) using a “total”  $\alpha = \alpha_{si} + \alpha_{pi}$  which accounts for additional magnetic fields inside the specimen ( $\alpha_{si}$ , see case 1) and inside the particles ( $\alpha_{pi}$ ). If particles are made of a homogeneous magnetic material,  $\alpha_{pi}$  corresponds to the demagnetizing factor  $D$  of a magnetized volume with given shape. Assuming that the mean magnetization of all particles is proportional to the specimen magnetization, one obtains the following values of  $\alpha_{pi}$  to be used in combination with mass-normalized specimen magnetization:

$$\alpha_{pi} \left[ \frac{T}{Am^2/kg} \right] = -\mu_0 D[S.I.] \times \frac{\mu_s [A/m]}{M_s [Am^2/kg]} \quad \alpha_{pi} \left[ \frac{Oe}{emu/g} \right] = -D[c.g.s.] \times \frac{\mu_s [emu/cm^3]}{M_s [emu/g]} \quad (6)$$

in S.I. and c.g.s. units respectively, where  $\mu_s$  is the volume-normalized spontaneous magnetization of the material inside the magnetic particles,  $M_s$  is the mass-normalized saturation magnetization, and  $\mu_0 = 4\pi \times 10^{-7} Vs/(Am)$ . Furthermore,  $0 < D[S.I.] < 1$  is the demagnetizing factor in S.I. units, and  $D[c.g.s.] = D[S.I.] / 4\pi$  the demagnetizing factor in c.g.s. units.

### *Case 3: Exchange field*

Interfaces between antiferromagnetic and ferrimagnetic phases can produce a phenomenon called exchange bias, when the anisotropy of the antiferromagnetic phase modifies the field required for switching the magnetization of the ferrimagnetic phase. The amount by which the switching field is decreased or increased is called exchange field  $H_{ex}$ . This field is phenomenologically equivalent to an internal field. In case of randomly oriented interfaces, the net effect of the exchange bias is largest when the specimen is saturated, so that eq. (3) might be rewritten as:

$$H^i = H + \alpha \frac{M(H)}{M_s} \quad (3)$$

with  $\alpha \approx H_{ex}$ .

### INPUT 18. Error plots and significance threshold (updated)

Measurement error and significance level calculations are part of the standard FORC processing procedure of CalculateFORC. FORC diagram error estimates represent a useful guide for the choice of optimal processing parameters. Furthermore, significance levels derived from error estimates represents an essential tool for discriminating between weak FORC signatures and measurement noise [Heslop and Roberts, 2012]. For this reason, the standard CalculateFORC output contains two diagrams representing the estimated standard error of the FORC function (error plots) and the signal-to-noise ratio (SNR plots), defined as the ratio between FORC amplitudes and standard error. Since version 2.0, both plots are generated as part of the same standard output, and the user is no longer asked to choose one.

The standard error is plotted with a color scale ranging from blue (zero) to magenta (maximum error) through white, yellow, orange, and red for intermediated values (Fig. 4.34). White pixels coincide with the quadratic mean of the standard error over measured regions of the plotted FORC space. Accordingly, regions plotted with cold/warm colors are characterized by standard errors below/above the average. Standard error plots are very useful for discriminating between measurement error contributions and polynomial regression misfits. The former contributions are characterized by a “grainy” appearance with high-amplitude “stripes” corresponding to trajectories of curves affected by transient measurement instabilities. Measurement errors might increase towards the right end of the FORC diagram (i.e. large  $H_c$ ) because of field-proportional error contributions. Polynomial regression misfits, on the other hand, form patterns that are highly correlated with particular FORC diagram features (e.g. the central ridge) and first derivative maxima, i.e. places where the measured curves change their shape most rapidly.

As a general role, measurement error contributions decrease and regression misfits increase when larger smoothing factors are chosen. Accordingly, optimal processing parameters are found when the two contributions become nearly equal. The advantage of error plots over global goodness-of-fit parameters [Harrison and Feinberg, 2008] resides in the possibility of discriminating between different error sources and adapt smoothing parameters to local needs over high- and low-resolution parts of the FORC diagram.

Large misfit errors call for the use of appropriated smoothing factor limitations through INPUT 12-16. For example, large misfit errors along diagonals in Fig. 4.34e are caused by first derivative maxima near the positive/negative coercive fields, and can be removed by local smoothing factor limitations with INPUT 14. 1-D FORC features such as the central ridge are by definition not exactly reproducible by polynomials and produce misfit errors even in combination with smallest smoothing factors (Fig. 4.34b). Therefore, error signatures related to horizontal/vertical ridges cannot be removed and the choice of smoothing parameter limitations along such ridges (i.e. INPUT 12-13) is guided by the best compromise between resolution requirements and noise suppression.

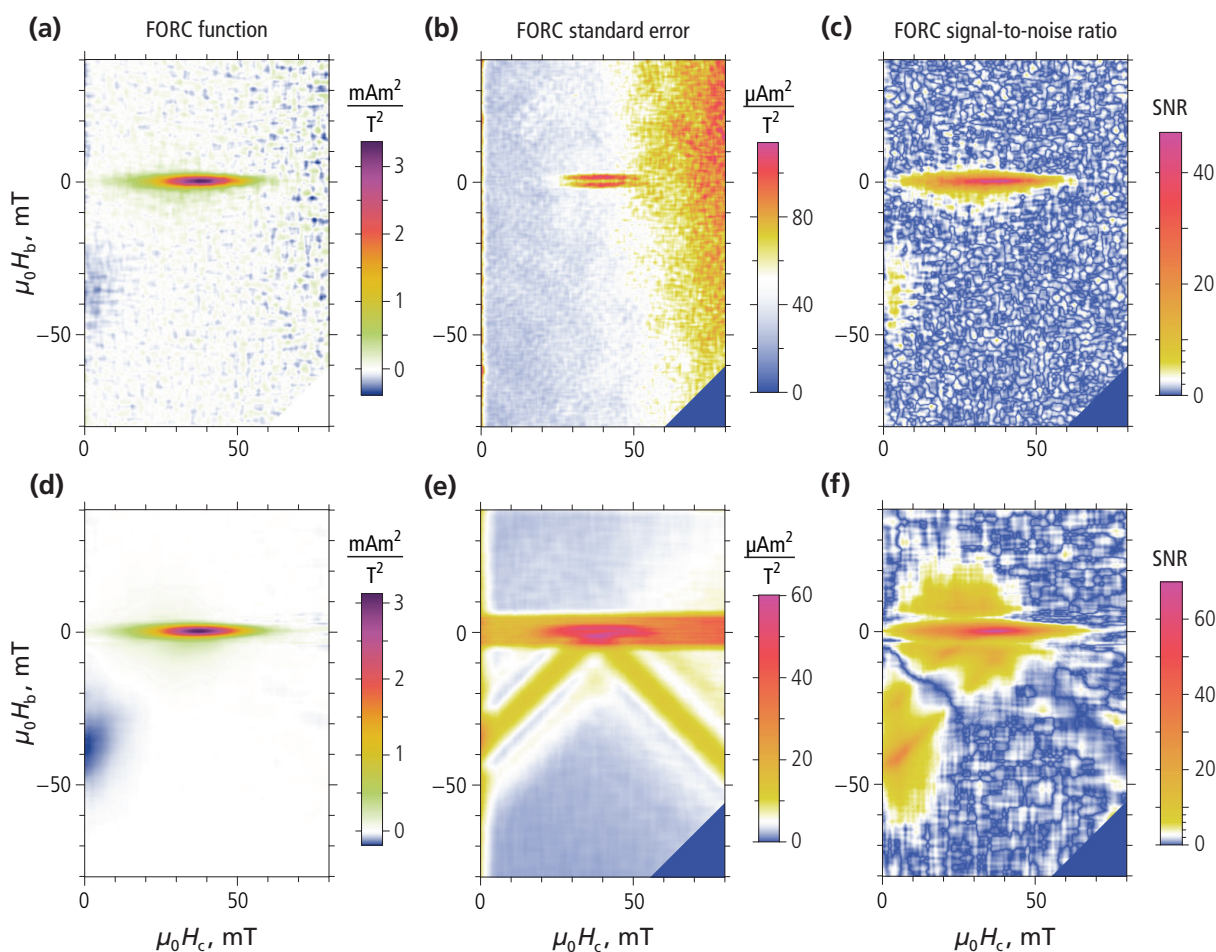


**Fig. 4.34:** Example of FORC diagrams (left), corresponding standard error (middle), and signal-to-noise ratios (SNR, right) obtained with CalculateFORC from measurements of cultured magnetotactic bacteria (see the downloadable example “Magnetospirillum 2”). The significance threshold of SNR plots has been set to 3 ( $\geq 99\%$  confidence level). **(a-c)** Conventional FORC processing results obtained with a constant smoothing factor SF = 5. The standard error contains patterns related to field-induced measurement noise (i.e. a vertical ridge at  $H_c=0$  due to field sweep reversal at the beginning of each curve, and error increase toward large  $H_c$ -values). Errors along the central ridge (i.e.  $H_b=0$ ) are produced by regression misfits. Blue-white regions of the SNR plot show that most parts of the FORC diagram are not significant. **(d,f)** Variable smoothing results (INPUT 10-11 set to 10, 0.03) with smoothing factor limitation along the central ridge (INPUT 13 set to 0.5, 5, 0.5). The standard error is dominated by regression misfit patterns along the central ridge and along diagonals with maximum  $\partial M / \partial H_r$  - and  $\partial M / \partial H$  - amplitudes. The maximum error outside the central ridge is  $\sim 10 \text{ Am}^2/\text{T}^2$ , instead of  $\sim 80 \text{ Am}^2/\text{T}^2$ , as with conventional FORC processing. The range of significant FORC measurements is expanded by the variable smoothing procedure: in this example, it covers all relevant features of the FORC function. The blue triangle on the lower left corner of error and SNR plots is not covered by FORC measurements and is set to zero by default.

The signal-to-noise ratio is plotted with a color scale ranging from blue (zero) to magenta (maximum SNR) through white, yellow, orange, and red for intermediate values (Fig. 4.34). White pixels coincide with the user-defined threshold above which FORC amplitudes are significantly  $>0$  at a given confidence level (e.g. SNR = 3 at  $\geq 99\%$  confidence level). This threshold is set with INPUT 18, e.g.

```
INPUT 18. Significance threshold of signal-to-noise ratio ....; 3
```

for the examples of Fig. 4.34. Accordingly, regions plotted with cold/warm colors are characterized by insignificant/significant FORC contributions. The SNR threshold corresponding to a given confidence level depends on the number of measurements considered for polynomial regression. This number is  $>25$  for common choices of the smoothing factors (i.e.  $s_c \geq 2$  and  $s_b \geq 2$ ), so that significance thresholds corresponding to a 99% confidence level are always  $<3$  [Egli, 2013]. This means that FORC amplitudes characterized by  $\text{SNR} \geq 3$  are significant at a confidence level of at least 99%. Significance thresholds corresponding to common confidence levels are listed in Tab. 4.3 and two examples are shown in Fig. 4.35.

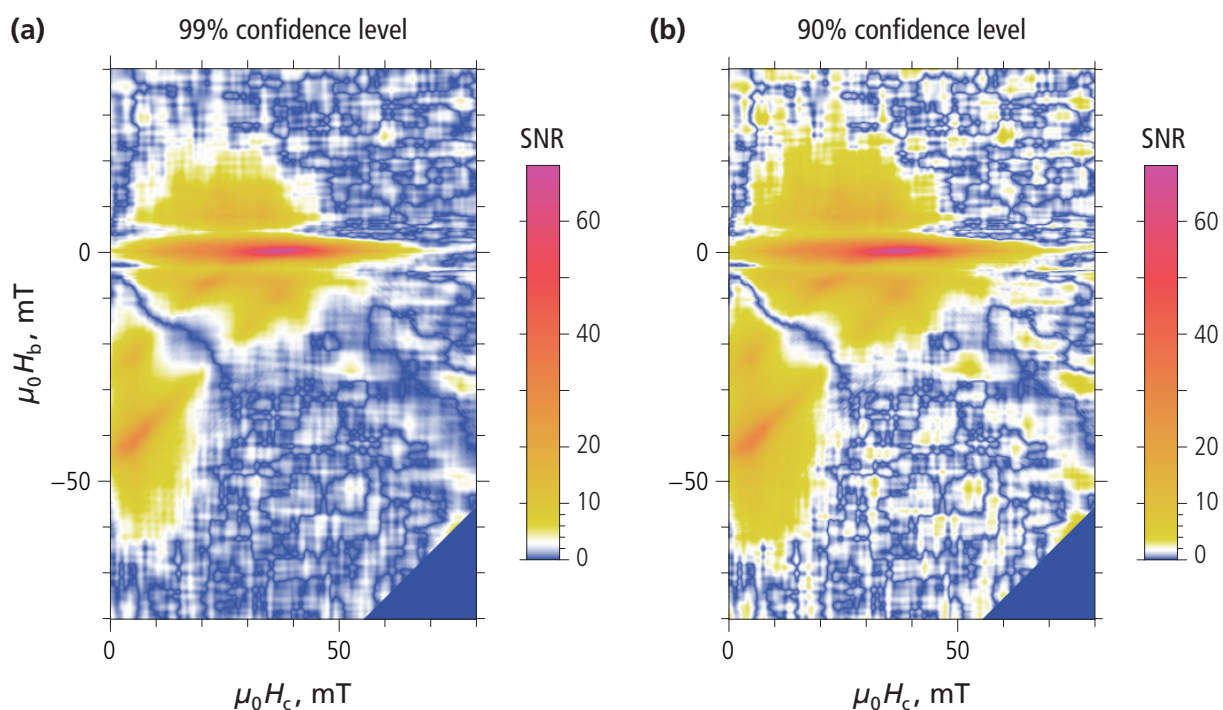


**Fig. 4.35:** Examples of signal-to-noise ratio (SNR) plots produced by CalculateFORC using two different color scales where white corresponds to a significance level of (a) 3 (i.e. INPUT 18 is set to 3), and (b) 1.75 (i.e. INPUT 18 is set to 1.75). Both plots have been obtained with the same FORC measurements of cultured magnetotactic bacteria shown in Fig. 4.34. The significance thresholds correspond to confidence levels of  $\sim 99\%$  (a) and  $\sim 90\%$  (b) (Tab. 4.3). The significant range of the FORC diagram coincides with regions of the SNR plot that are consistently orange, red, or magenta. The size of these regions is similar in the two plots, demonstrating that the choice of a significance threshold  $> 1$  is not particularly critical.

SNR plots with the abovementioned color scale are very useful for identifying significant regions of the FORC diagram and distinguish real low-amplitude FORC features from measurement error artifacts. Important regions of the FORC diagram should be characterized by consistent warm colors in SNR plots (orange-red without blue spots). Furthermore,  $\text{SNR} \geq 15$  is required for drawing meaningful contours. As a general role, SNR increases when larger smoothing factors are chosen, up to the point where smoothing artifacts start to appear. Such artifacts are best identified in plots of the standard error.

FORC diagrams featuring positive and negative contributions forcefully contain transition regions where the FORC function is exactly zero (Fig. 4.34f). Such regions will always appear as insignificant (i.e. blue) in SNR plots, regardless of the processing parameters used.

CalculateFORC exports an error matrix file along with FORC data (see section 4.6).

**Tab. 4.3:** Significance thresholds of the signal-to-noise ratio of the FORC function at given confidence levels  $1 - \alpha$ . Thresholds are weak functions of the horizontal ( $s_c$ ) and vertical ( $s_b$ ) smoothing factors. Significance thresholds correspond to the  $1 - \alpha/2$  quantile of the Student  $t$ -distribution with  $v$  degrees of freedom, where  $v = 8(s_c - 1)(s_b - 1) + 6(s_c + s_b) - 13$ . Signal-to-noise ratios larger than the given significance threshold represent values of the FORC function that are  $\neq 0$  at a given confidence level.

|                      | $s_c = s_b = 2$ | $s_c = 5, s_b = 2$ | $s_c = s_b = 10$ |
|----------------------|-----------------|--------------------|------------------|
| Degrees of freedom   | 19              | 61                 | 755              |
| 99% confidence level | 2.86            | 2.66               | 2.58             |
| 95% confidence level | 2.09            | 2.00               | 1.96             |
| 90% confidence level | 1.73            | 1.67               | 1.65             |

- 💡 FORC diagram features are significant only if the corresponding FORC region is systematically filled with yellow, red and magenta pixels in signal-to-noise plots.
- 💡 Error estimates are themselves affected by errors. Therefore, short-range fluctuations of the standard error and the signal-to-noise ratio are not significant. If fluctuations of the signal-to-noise ratio within a certain FORC region include blue spots, the corresponding FORC feature should be considered insignificant.
- 💡 Plots of the standard error and signal-to-noise ratio produced by CalculateFORC serve as diagnostic tools for optimizing the processing options. Information about the significance of plotted data can be added to the FORC diagram using the VARIFORC function PlotFORC, along with other plotting options. In this case, significant regions of the FORC diagram are outlined by a contour line corresponding to the given significance threshold (e.g. 3) of the signal-to-noise ratio.

**Updates from version 1.0:**

- Both the error plot and the signal-to-noise ratio plot are generated as part of the standard CalculateFORC output since version 2.0. Accordingly, the only error parameter to be entered by the user with INPUT 18 is the significance threshold of the signal-to-noise ratio.

### INPUT 19. Error matrix size limit

The FORC error calculation procedure of CalculateFORC is based on the inversion of  $N \times N$  matrices, where  $N = (2s_c + 1)(2s_b + 1)$  is the number of measurements used for polynomial regression with smoothing factors  $s_c$  and  $s_b$  [Egli, 2013]. For example,  $N \times N = 121$  for conventional FORC processing with  $SF = s_c = s_b = 5$ . If advanced smoothing options are chosen,  $N$  becomes very large (up to  $>10^4$ ) over parts of the FORC space, so that operations involving  $N \times N$  matrices require excessive computer memory. Therefore, an upper limit  $N_{\max}$  for the size of error matrices must be set with INPUT 19. For example,

```
INPUT 19. Error matrix size limit ....; 2000
```

limits the size of error matrices to  $2000 \times 2000$ , so that memory usage does not exceed 1 GB.

If polynomial regression is performed over  $N > N_{\max}$  measurement points, where  $N_{\max}$  is the limit set with INPUT 19, CalculateFORC will still use all points to calculate the FORC value, prior to randomly pick  $N_{\max}$  measurement points for error calculation.  $N_{\max} >> 100$  ensures that the chosen points provide a representative sample of measurement errors. Therefore, the limit entered with INPUT 19 must be an integer  $\geq 100$ .

If the limit set by INPUT 19 exceeds the available system memory, CalculateFORC will be aborted as soon as the evaluated error matrices become excessively large, and the following message appears:

```
No more memory available.  
Mathematica kernel has shut down.  
Try quitting other applications and then retry.
```

In this case close the Mathematica® notebook where your CalculateFORC session was running, and try again after lowering the limit set by INPUT 19.

- 💡 The maximum memory of a PC with 2 GB RAM is exceeded with  $N = 10'000$ . In this case, a safe limit to be set with INPUT 19 is 5000.
- 💡 A convenient default setting for INPUT 19 is given by  $N_{\max} = 2'500 \times \text{RAM}$ , where RAM is the available RAM memory in GB.
- 💡 Very large matrix size limits do not increase the precision of error estimates significantly, but increase the processing time. Matrix size limits around 2000 are sufficient for all processing purposes, avoiding excessive memory usage on modern PC's.

## INPUT 20. Outlier detection threshold

FORC diagram calculations are based on polynomial regression of measurement points lying within selected areas around given FORC coordinates (Fig. 4.15). If the second-order polynomial used for regression is a suitable local approximation of the FORC function, regression residuals coincide with measurement errors. Outliers, defined as points with unusually large errors, appear as measurement points with anomalously large regression residuals.

Outliers can be identified and removed with CalculateFORC, as far as not previously done when importing raw measurement data with the VARIFORC module ImportFORC (see Chapter 3). Outliers are defined as measurement points whose regression residuals are larger than a given multiple  $\lambda$  of the quadratic mean of all other residuals. The multiple  $\lambda$  is entered with INPUT 20, e.g.:

```
INPUT 20. outlier detection threshold ....; 3
```

and is limited to values  $\geq 2$ . If measurement errors are described by a Gaussian distribution, the probability of identifying a regression residual as an outlier is given by the  $2\lambda$ -quantile of the error function (Tab. 4.4). Values of  $\lambda$  comprised between 2 and 3 correspond to probabilities of 1-5%. Large value of  $\lambda$ , can be entered in order to keep all measurement points. Using

```
INPUT 20. outlier detection threshold ....; 5
```

only one Gaussian measurement error out of 1.7 million is considered as an outlier.

**Tab. 4.4:** Selected outlier detection limits and the corresponding probability that a Gaussian measurement error is considered an outlier by CalculateFORC.

| Outlier detection threshold $\lambda$ | % of Gaussian errors considered as outliers |
|---------------------------------------|---------------------------------------------|
| 1.645                                 | 10%                                         |
| 1.960                                 | 5%                                          |
| 2.576                                 | 1%                                          |
| 3.291                                 | 0.1%                                        |
| 3.891                                 | 0.01%                                       |

### INPUT 21. Clip negative coercivity distribution values

In addition to the FORC diagram and corresponding error plots, CalculateFORC processes subsets of FORC measurements that define two types of coercivity distributions associated with the backfield demagnetization curve and with irreversible processes occurring at the reversal field  $H_r$ , respectively (see Chapter 8). Coercivity distributions derived from magnetization curves can be negative over some field ranges. In most magnetic materials, however, negative elemental contributions are masked by superposition with much larger positive contributions, so that the resulting coercivity distributions are strictly positive functions. Therefore, negative coercivity distribution values arise from measurement noise in most cases, and do not need to be plotted. Negative amplitudes in coercivity distribution plots are clipped with

INPUT 21. Clip negative coercivity distribution values ....; Yes

(Fig. 4.36b) and preserved with:

INPUT 21. clip negative coercivity distribution values ....; No

(Fig. 4.36a). INPUT 21 is conveniently set to Yes when processing measurements of common magnetic materials and geologic samples.

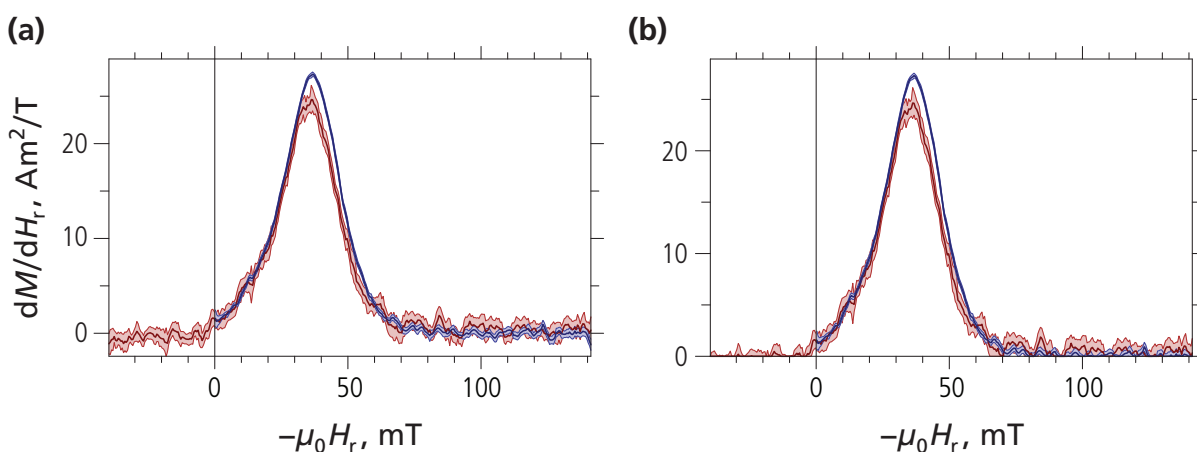


**Fig. 4.36:** Coercivity distributions obtained from FORC measurements of cultured magnetotactic bacteria (see the downloadable example “Magnetospirillum 2”), Measurements have been processed with a constant smoothing factor SF = 3. Shaded regions around each curve are confidence intervals corresponding to two times the estimated standard error. Blue curves: coercivity distribution  $dM(H_r, 0)/dH_r$  calculated from the backfield demagnetization curve  $M(H_r, 0)$ . Red curves: coercivity distribution  $\partial M(H_r, H_r)/\partial H$  derived from the irreversible component of the upper branch of the hysteresis loop. This example has been intentionally created using insufficient smoothing for demonstration purposes. **(a)** Unconstrained plot with negative values (i.e. INPUT 21 set to No). **(b)** Constrained plot where negative values are set to 0 (i.e. INPUT 21 set to Yes).

- INPUT 21 does not affect the coercivity distribution data exported by CalculateFORC, which always correspond to unconstrained values.

💡 Setting INPUT 21 to Yes when processing very noisy data avoids wasting some of the plotted range with insignificant negative amplitudes.

### INPUT 22. Confidence interval of coercivity distributions

In addition to the FORC diagram and the corresponding error plots, CalculateFORC processes subsets of FORC measurements that define two types of coercivity distributions associated with the backfield demagnetization curve and with irreversible processes occurring at the reversal field  $H_r$ , respectively (see Chapter 8). The error estimate for these coercivity distributions is plotted in form of a confidence interval, which is defined as a given multiple  $\lambda > 0$  of the standard error. This multiple is specified by INPUT 22, e.g.

```
INPUT 22. Confidence interval factor for distribution plots .....; 2
```

Common choices of INPUT 22 are  $\lambda = 1$  for plotting the standard error (Fig. 4.37a) and  $\lambda = 2$  for the 95% confidence interval in case of Gaussian errors (Fig. 4.37b).

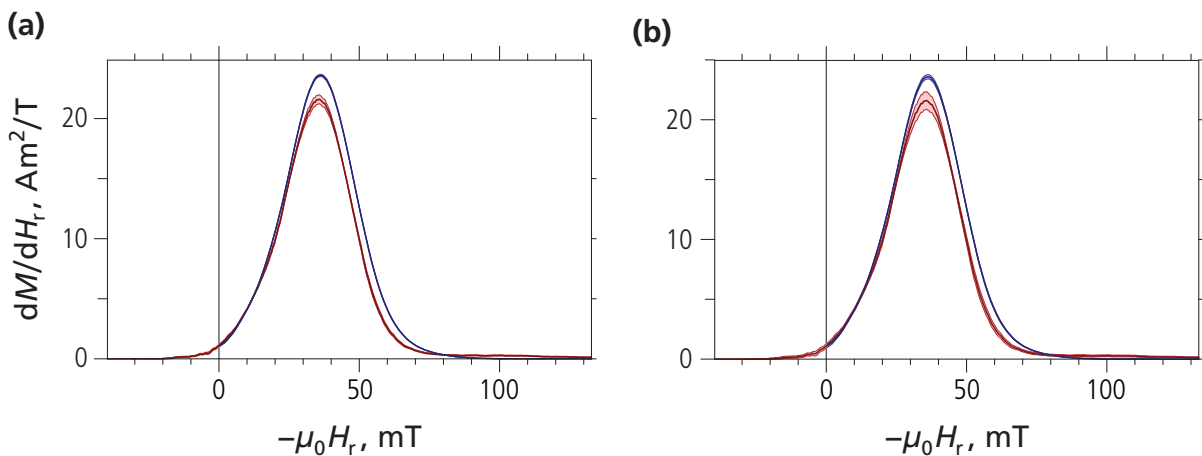


**Fig. 4.37:** Coercivity distributions of cultured magnetotactic bacteria (see the downloadable example “*Magnetospirillum 2*”) produced by CalculateFORC with a variable smoothing procedure (i.e. INPUT 10-11 set to 10, 0.07 and INPUT 13 set to 0.5, 5, 0.5). Confidence intervals (shaded bands) are expressed as (a) standard error (i.e. INPUT 22 is set to 1), and (b) double standard error (i.e. INPUT 22 is set to 2). Blue curves: coercivity distribution  $dM(H_r, 0)/dH_r$  calculated from the backfield demagnetization curve  $M(H_r, 0)$ . Red curves: coercivity distribution  $\partial M(H_r, H_r)/\partial H$  derived from the irreversible component of the upper branch of the hysteresis loop.

### INPUT 23. FORC diagram ticks specifications

INPUT 23 is used to set the ticks of the  $H_c$ - and  $H_b$  field scales in the FORC diagram. The default setting is

```
INPUT 23. FORC plot ticks specifications ....; Automatic
```

for placing field ticks automatically. In this case, CalculateFORC uses the same tick intervals (e.g. 50 mT for major ticks and 10 mT for minor ticks) for both  $H_c$  and  $H_b$ , as customary in FORC plots (Fig. 4.38a). This option yields reasonable tick spacing in most cases. Although plotting refinements, including tick specifications, are usually performed with the VARIFORC module PlotFORC, custom tick specifications can be entered with INPUT 23 in two ways. The simplest form consists of a number pair, e.g.:

```
INPUT 23. FORC plot ticks specifications ....; 10, 2
```

where the first number is the field interval used for major ticks, and the second number is an integer  $>0$  that specify the number of minor intervals by which major tick intervals are divided. The major tick interval is assumed to have the same unit as magnetic fields in FORC measurements (e.g. mT). The specification of the above example applies to both  $H_c$  and  $H_b$ , so that that major ticks are drawn every 10 mT, and the 10 mT intervals are divided by two with 1 minor tick. Minor ticks are avoided by setting the second number to 1.

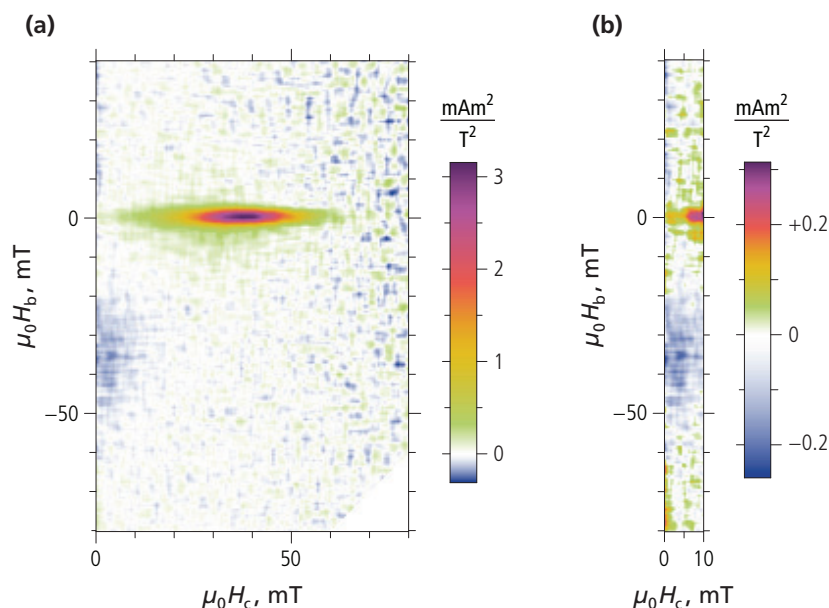


**Fig. 4.38:** Examples of FORC diagrams obtained from the same measurements of cultured magnetotactic bacteria (see the downloadable example “Magnetospirillum 2”) over different ranges of the FORC space. The field ticks in (a) were produced with INPUT 23 set to Automatic. The same result would be obtained with INPUT 23 set to 50, 5 (i.e. major ticks every 50 mT with major tick intervals divided by five by minor ticks). The ticks in (b) have been specified by setting INPUT 23 to 10, 2, 50, 5.

Individual  $H_c$ - and  $H_b$ -tick specifications, as for instance in case of FORC spaces with very different horizontal and vertical ranges, can also be entered with INPUT 23. In this case, four parameters are needed, e.g.:

```
INPUT 23. FORC plot ticks specifications ....; 10, 2, 50, 5
```

(Fig. 4.38b). In this case,  $H_c$ - and  $H_b$ -ticks are defined by the first two and the second two numbers, respectively, in the same manner as for single tick specification. In the above example, major  $H_c$ -ticks are drawn every 10 mT (first number), and major  $H_b$ -ticks are drawn every 50 mT (third number). Major  $H_c$ - and  $H_b$ -tick intervals are divided in 2 and 5 equal intervals, respectively, by minor ticks (second and fourth number).

- 💡 Extended FORC diagrams plotting options, including tick specifications, are available with the VARIFORC function PlotFORC.
- 💡 The default tick specification `Automatic` generate satisfactory results in all cases where the FORC space covers similar  $H_c$ - and  $H_b$ -ranges.
- 💡 Explicit tick specifications are useful when plotting FORC diagrams with very large or very small aspect ratios (e.g. FORC diagrams of multidomain hysteresis).

#### INPUT 24. FORC diagram color saturation

CalculateFORC uses two standard color scales for plotting FORC diagrams and corresponding errors or signal-to-noise ratios. The color scales are specially designed to give best performances with the special characteristics of FORC functions, as explained in detail in Chapter 5. The color scales are created by blending printable colors for reproducible printing results. Because the printable color gamut can vary significantly, it might be necessary to reduce color saturation for best results. Color saturation can be controlled with INPUT 24. The default option corresponding to 95% of full saturation is obtained with

```
INPUT 24. FORC diagram color saturation ....; Automatic
```

(Fig. 4.39). This option yields good results on monitors as well as with printing. Alternatively, an explicit color saturation value comprised between 0 and 1, can be entered, e.g.:

```
INPUT 24. FORC diagram color saturation ....; 0.7
```

for 70% of full saturation (Fig. 4.39d).

Although color saturation can be set to any value between 1 (maximum saturation) and 0 (pure white), practical saturation values are comprised between 0.8 and 1.

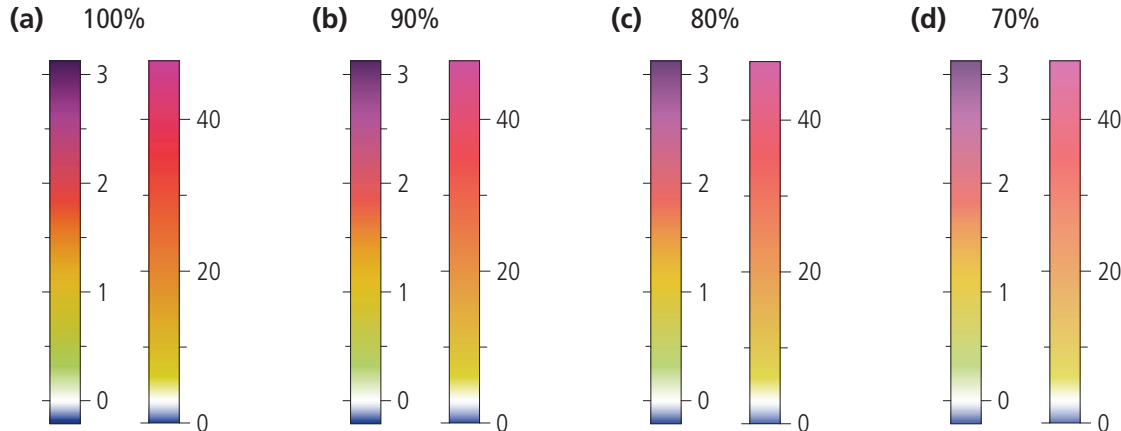


**Fig. 4.39:** Examples of CalculateFORC color scales obtained with different saturation levels specified by INPUT 24, from 100% (a) to 70% (d). The left color scale in each example is used for FORC diagrams, while the right color scale corresponds to plots of FORC errors and signal-to-noise ratios.

💡 Color printing problems are created by the need of converting the original RGB color space into the much smaller color gamut of the CMYK space used for printing. They are best solved by reducing the color saturation of original plots.

### INPUT 25. FORC diagram color scale clipping

The FORC diagram color scale used by CalculateFORC is controlled by the full range of FORC amplitudes and by INPUT 25, which represents the fraction of smallest and largest FORC values lying outside the regular color range. These values are plotted with the color corresponding to minimum (blue) and maximum (purple) values. The color scale is extended to the entire range of FORC amplitudes with

```
INPUT 25. Fraction of FORC diagram pixels with clipped colors ...; 0
```

(Fig. 4.40a). Color scales covering smaller ranges of FORC values are obtained by entering a number comprised between 0 and 1, e.g.

```
INPUT 25. Fraction of FORC diagram pixels with clipped colors ...; 0.05
```

for excluding the 5% smallest and largest values from the regular range (Fig. 4.40b). This option is used with noisy FORC diagrams in order to avoid “wasting” part of the color scale with the need of covering extreme values amplified by measurement errors.

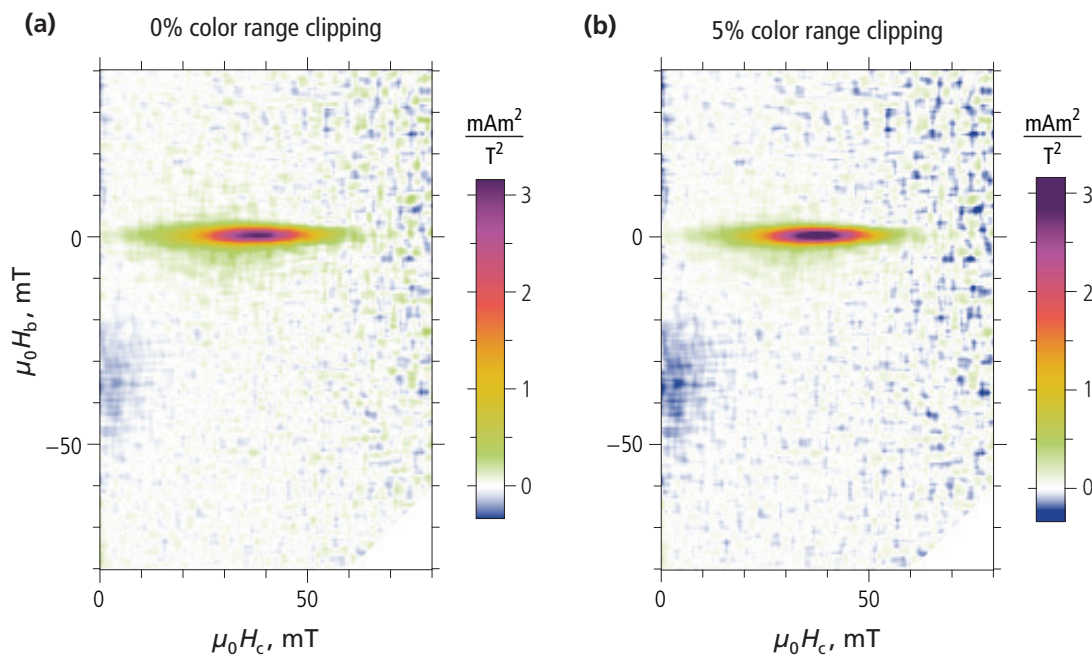


**Fig. 4.40:** Color range clipping examples generated with FORC measurements of cultured magnetotactic bacteria (see the downloadable example “Magnetospirillum 2”). Both diagrams have been calculated with conventional processing and SF = 5. (a) Color scale extends over the entire range of FORC values (i.e. INPUT 25 is set to 0). Minimum values (blue) are determined by measurement noise over the right part of the FORC diagram, instead of true negative FORC contributions near  $H_c=0$ . (b) The color scale is clipped over the smallest and largest 5% of all FORC amplitudes (i.e. INPUT 25 is 0.05). FORC values  $>2.8 \text{ mAm}^2/\text{T}^2$  and  $<-0.281 \text{ Am}^2/\text{T}^2$  are represented with the same purple and blue color, respectively. True negative FORC contributions near  $H_c=0$  are more evident than in (a).

INPUT 25 can be used to enhance the color contrast of small FORC amplitudes at cost of high-amplitude features (e.g. the central ridge). Because the color scale used by CalculateFORC is optimized for the representation of typical FORC functions, good results are generally obtained with any value of INPUT 25 comprised between 0 and 0.05.

The fraction of minimum/maximum FORC values excluded from the regular color range is applied to groups of pixels corresponding to the maximum FORC diagram resolution. For example, if this resolution corresponds to a central ridge covering  $500 \times 2$  pixels and INPUT 25 is set to 0.01, the smallest and largest 10 values (corresponding to  $500 \times 2 \times 0.01$ ) are excluded.

- 💡 The VARIFORC function PlotFORC should be used for advanced color scale options.
- 💡 INPUT 25 can be set to 0.01 with good results in most cases.
- 💡 Relatively large values of INPUT 25 (but still <1) can be used to enhance the color contrast over FORC features with very small amplitudes.
- 💡 INPUT 25 has no effects on exported FORC data. FORC diagrams with different color scales can always be generated using PlotFORC.



## 4.6 Data formats exported by CalculateFORC

Depending on the output function chosen with INPUT 02, CalculateFORC exports processing results to two or six files. If INPUT 02 was set to FORC, six files with the following name endings are exported:

- 1) \_FORC\_VARIFORC.txt for the FORC matrix,
- 2) \_FORCStandardError\_VARIFORC.txt for the matrix of FORC standard errors,
- 3) \_Backfield\_Linear\_VARIFORC.txt for the coercivity distribution corresponding to back-field demagnetization on a linear field scale,
- 4) \_Backfield\_Log10\_VARIFORC.txt for the coercivity distribution corresponding to backfield demagnetization on a  $\log_{10}$  field scale,
- 5) \_Reversal\_Linear\_VARIFORC.txt for the coercivity distribution corresponding to the irreversible component of the upper hysteresis branch on a linear field scale,
- 6) \_Reversal\_Log10\_VARIFORC.txt for the coercivity distribution corresponding to the irreversible component of the upper hysteresis branch on a  $\log_{10}$  field scale.

If INPUT 02 was set to any function *func* except FORC, two files with the following name endings are exported:

- 1) \_*func*\_VARIFORC.txt for the matrix of *func* values,
- 2) \_*func*StandardError\_VARIFORC.txt for the matrix of *func* standard errors.

Abovementioned files are required by other VARIFORC modules for further processing. They also provide data for other applications, and contain useful summary information. The files are produced with a specific format that is explained in the following.

### 4.6.1 FORC matrices

FORC matrices (\_FORC\_VARIFORC.txt and \_FORCStandardError\_VARIFORC.txt) are exported to files with the structure shown in Fig. 4.41. The file header contains summary information about FORC processing options and magnetizations derived from FORC data, followed by a matrix of FORC values corresponding to points of the output grid. The beginning of the data matrix section is univocally located by the title line `Data matrix`, regardless of the actual row number.

Information blocks in the file header begin with a title (e.g. Field unit, magnetization unit, and FORC unit), followed by comma-separated parameter lists. Empty lines are used to separate blocks. Line widths are unlimited and might therefore be wrapped by some text editors. The content of individual blocks is explained in the following.

```
VARIFORC v.2.00. FORC function -1/2 ddM/(dHr dH) from corrected FORC measurements.

Source file
E:\...\Leg138_848_S0_CorrectedMeasurements_VARIFORC.frc

Field unit, magnetization unit, and FORC unit
T,mAm2/kg,1e-3 Am2/(T2 kg)

Field step of FORC measurements, first point offset, field measurements regularization
0.0005015553545586107,0.00007597585780746107, False

Last FORC begins at
-0.16213794366264145

Hc-range of data matrix
0.00025,0.12075

Hb-range of data matrix
-0.121,0.063

Data matrix size
242,369

Mesh size of data matrix
0.0005

Origin of data matrix
0.00025,0

Weighted margin of regression rectangles
2

Horizontal smoothing factor (effective) and increase rate
10.,0.09

Vertical smoothing factor (effective) and increase rate
10.,0.09

Horizontal smoothing factor limit (effective), at given Hc, plus/minus
None,0.,0.

Vertical smoothing factor limit (effective), at given Hb, plus/minus
4.,0.0004,0.0005

[...]

Mrs from FORC measurements and standard error
3.897134730097964,0.0006913444803027636

Mrs from backfield curve and standard error
3.8496819505448734,0.0005754758112584479

Total irreversible magnetization at reversal field and standard error
3.8878277315457086,0.001957678649939554

Data matrix
160.06739183958143,118.37842663606989,115.95472514390212,87.88558329784428,86.993797140831
0653501062625,6.303779035918211,8.388267301388282,10.37817057290107,13.40406065855936,16.7
174646,2.6944584311521567,1.4183993690578518,3.1708407393339257,4.79025426467615,5.9296297
159.4938593035847,143.44697925228684,142.87396996126608,105.85918269503964,93.310231971413
```

**Fig. 4.41:** Example of FORC matrix file produced by CalculateFORC. Information blocks begins with a title (highlighted in blue), followed by a list of parameters. FORC data begin after **Data matrix**.

### Block 1: File title

The first line contains the file title VARIFORC v2.00. *Type*, where *Type* represents the type of FORC data, e.g. FORC function  $-1/2 \text{ ddM}/(\text{dHr dH})$  from corrected FORC measurements or M from corrected FORC measurements.

### Block 2: Source file

This block contains information about the source of corrected FORC measurement data used for processing. Usually, corrected FORC data are generated by the VARIFORC module Linear CombineFORC as a preprocessing step. In this case, this block is titled “Source file” and contains the complete path of the source file. If Corrected FORC measurements generated by the VARIFORC module LinearCombineFORC have been used, this block is titled “linear combination factors for listed source files” and contains a list of corrected FORC measurement file paths preceded by corresponding linear combination factors.

### Block 3: Units

This block contains the field and magnetization units of the source data, as well as the unit of output data contained in the file. Units can be preceded by S.I. prefixes or numerical unit multipliers. The type of units (e.g. field, magnetization, FORC, coercivity distribution) are explicitly mentioned in the block title in same sequence as listed below.

### Block 4: Measurement field steps

This block contains information about field steps of corrected measurements, i.e. the mean field step, first point offset, and field measurement regularization. The first point offset is defined as the difference between the mean first field step in every curve and successive field steps. For instance, -0.1 means that the first step of each curve is smaller by 0.1 mT with respect to the following steps. Field measurement regularization refer to processing option INPUT 08: False means that original field measurements have been used for processing, while True indicates that field measurements have been replaced with interpolated values.

### Block 5: Last FORC specifications

This block specifies the reversal field corresponding to the last measured curve. Together with block 4, this provides complete information about the position of measurement points in FORC space.

### Block 6: $H_c$ -range of data matrix

This block contains the smallest and largest  $H_c$ -coordinates among all FORC matrix points. Because each matrix point is understood as a pixel center, the FORC range is extended by  $\Delta H/2$  on each side, where  $\Delta H$  is the mesh size of the output points.

**Block 7:  $H_b$ -range of data points**

This block contains the smallest and largest  $H_b$ -coordinates among all FORC matrix points. Because each matrix point is understood as a pixel center, the FORC range is extended by  $\Delta H/2$  on each side, where  $\Delta H$  is the mesh size of the output points.

**Block 8: Data matrix size**

This block contains the FORC matrix dimensions, expressed as number of grid points along  $H_c$  (first entry), and number of grid points along  $H_b$  (second entry).

**Block 9: Mesh size of data matrix**

This block contains the mesh size  $\Delta H$  of the output grid points represented by the FORC matrix, as specified with the processing option INPUT 06.

**Block 10: Origin of data matrix**

This block contains the  $(H_c, H_b)$ -coordinate of the output grid origin, as specified with the processing option INPUT 07. Blocks 9 and 10 specify the FORC coordinates of all data matrix points.

**Block 11: Weighted margin of regression rectangles**

This block contains the width of the weighted margin of regression rectangles, as specified with the processing option INPUT 09.

**Block 12: Horizontal smoothing factor specifications**

This block contains horizontal smoothing factor specifications as specified with the processing option INPUT 10 (with same format, i.e. minimum effective smoothing factor and increase rate).

**Block 13: Vertical smoothing factor specifications**

This block contains vertical smoothing factor specifications as specified with the processing option INPUT 11 (with same format, i.e. minimum effective smoothing factor and increase rate).

**Block 14: Horizontal smoothing factor limits**

This block contains horizontal smoothing factor limits as specified with the processing option INPUT 12 (i.e. smoothing factor limit, position of the limit along  $H_c$ , and half-width of the limited region along  $H_c$ ).

**Block 15: Vertical smoothing factor limits**

This block contains vertical smoothing factor limits as specified with the processing option INPUT 13 (i.e. smoothing factor limit, position of the limit along  $H_b$ , and half-width of the limited region along  $H_b$ ).

### Block 16: Diagonal smoothing factor limits under first derivative maxima

This block contains diagonal smoothing factor limits at values of  $H_r$  and  $H$  characterized by maximum first derivatives of  $M(H_r, H)$ , as specified with the processing option INPUT 14 (i.e. smoothing factor limit, position of the limit along the diagonals  $|H_r| = |H|$ , and half-width of the limited region).

### Block 17: Diagonal smoothing factor limits at given $H$

This block contains diagonal smoothing factor limits at given  $H$  as specified with the processing option INPUT 15 (i.e. smoothing factor limit, position of the limit along  $H$ , and half-width of the limited region along  $H$ ).

### Block 18: Diagonal smoothing factor limits at given $H_r$

This block contains diagonal smoothing factor limits at given  $H_r$  as specified with the processing option INPUT 16 (i.e. smoothing factor limit, position of the limit along  $H_r$ , and half-width of the limited region along  $H_r$ ).

### Block 19: Smoothing factor and proportionality constant used for mean field correction

This block contains mean field correction parameters (i.e. smoothing factor used for mean field calculation and mean field proportionality constant) as specified with the processing option INPUT 17.

### Block 20: $M_{rs}$ from FORC measurements and standard error

This block contains the saturation remanence  $M_{rs}$  estimated from FORC measurements and the corresponding standard error estimate. If estimates are not available, numerical values are replaced by None.

### Block 21: $M_{rs}$ from backfield curve and standard error

This block contains the integral

$$M_{bf} = \int_{H_{min}}^{H_{max}} f_{bf}(H) dH \quad (7)$$

of the backfield coercivity distribution  $f_{bf}$  (see Chapter 8) and the corresponding standard error estimate.  $H_{min}$  and  $H_{max}$  are the minimum and maximum fields, respectively, for which  $f_{bf}$  has been calculated. Generally,  $H_{min}=0$ . For sufficiently large values of  $H_{max}$ ,  $M_{bf}$  coincides with the saturation remanence  $M_{rs}$ . If an output function other than FORC has been chosen with INPUT 02, entries in this block are set to None.

### Block 22: Total irreversible magnetization at reversal field and standard error

This block contains the integral

$$M_{\text{irs}} = \int_{H_{\min}}^{H_{\max}} f_{\text{irr}}(H) dH \quad (8)$$

of the reversal field coercivity distribution  $f_{\text{irr}}$  (see Chapter 8) and the corresponding standard error estimate.  $H_{\min}$  and  $H_{\max}$  are the minimum and maximum fields for which  $f_{\text{irr}}$  has been calculated. For sufficiently large  $H_{\min}$ - and  $H_{\max}$ -amplitudes, this integral coincides with the total irreversible magnetization of the major hysteresis loop. If an output function other than FORC has been chosen with INPUT 02, entries in this block are set to None.

### Block 23: Integral of the FORC function and standard error

This block contains the integral

$$I = 2 \int_{H_{c,\min}}^{H_{c,\max}} \int_{H_{b,\min}}^{H_{b,\max}} \rho(H_c, H_b) dH_c dH_b \quad (9)$$

of the FORC function  $\rho(H_c, H_b)$  over the output FORC space, and the corresponding standard error estimate. Ideally, this integral coincides with the total irreversible magnetization of the major hysteresis loop. If an output function other than FORC has been chosen with INPUT 02, entries in this block are set to None.

### Block 24: Integral of the FORC function over $H_r > 0$ and standard error

This block contains the integral

$$I_{H_r \geq 0} = 2 \int_{H_{c,\min}}^{H_{c,\max}} \int_{H_c}^{H_{b,\max}} \rho(H_c, H_b) dH_c dH_b \quad (10)$$

of the FORC function  $\rho(H_c, H_b)$  over the FORC space limited by  $H_r \geq 0$  (i.e.  $H_b \geq H_c$ ), and the corresponding standard error estimate. Ideally, this integral coincides with the integral of  $f_{\text{irr}}$  over negative arguments. If an output function other than FORC has been chosen with INPUT 02, entries in this block are set to None.

### Block 25: Integral of the FORC function over $H_b > 0$ and standard error

This block contains the integral

$$I_{H_b \geq 0} = 2 \int_{H_{c,\min}}^{H_{c,\max}} \int_0^{H_{b,\max}} \rho(H_c, H_b) dH_c dH_b \quad (11)$$

of the FORC function  $\rho(H_c, H_b)$  over the upper quadrant of the FORC space (i.e.  $H_b \geq 0$ ), and the corresponding standard error estimate. If an output function other than FORC has been chosen with INPUT 02, entries in this block are set to None.

### Block 26: Integral of FORC function over negative contributions and standard error

This block contains the integral

$$I_{\rho < 0} = 2 \int_{H_{c,\min}}^{H_{c,\max}} \int_{H_{b,\min}}^{H_{b,\max}} \min[0, \rho(H_c, H_b)] dH_c dH_b \quad (12)$$

of negative values of the FORC function  $\rho(H_c, H_b)$  over the output FORC space, and the corresponding standard error estimate. If an output function other than FORC has been chosen with INPUT 02, entries in this block are set to None.

### Block 27: Data matrix

This is the last block and contains the data matrix with matrix elements

$$\rho_{k,j} = \rho(H_{c,j}, H_{b,k}) \quad (13)$$

corresponding to FORC function values at the  $j$ -th  $H_c$ -coordinate and the  $k$ -th  $H_b$ -coordinate of the output grid.  $H_c$ -coordinates are sorted in ascending order from smallest to largest value.  $H_b$ -coordinates are sorted in descending order from largest to smallest value. Each matrix row is a list of comma-separated values and matrix rows are separated by empty lines. The first and last rows correspond to the topmost and bottommost pixel rows in the FORC diagram.

#### 4.6.2 Coercivity distributions

Coercivity distributions (\_Backfield\_Linear\_VARIFORC.txt, \_Backfield\_Log10\_VARIFORC.txt, \_Reversal\_Linear\_VARIFORC.txt, \_Reversal\_Log10\_VARIFORC.txt) are exported to files with the structure shown in Fig. 4.42. The file header contains summary information about FORC processing options and magnetization derived from coercivity distribution data, followed by coercivity distribution values listed in a comma-separated three-column format with no empty lines. The beginning of the data section is univocally located by the title line Coercivity distribution on linear field scale, or Coercivity distribution on log10 field scale, regardless of the actual row number.

Information blocks in the file header begin with a title (e.g. Field unit, magnetization unit, and coercivity distribution unit), followed by comma-separated parameter lists. Empty lines are used to separate blocks. Line widths are unlimited and might therefore be wrapped by some text editors. The content of blocks is explained in the following.

#### Block 1: File title

The first line contains the file title VARIFORC v2.00. Type, where Type represents the type of FORC data, e.g. Backfield coercivity distribution  $f(x) = 1/2 dM/dH_r @ (H_r=-x, H=0)$  or Reversal coercivity distribution  $f(x) = 1/2 dM/dH_r @ (H_r=-x, H=-x)$ .

```
VARIFORC v.2.00. Backfield coercivity distribution f(x) = 1/2 dM/dHr @ (Hr=-x,H=0).  
Source file  
E:\...\Leg138_848_S0_CorrectedMeasurements_VARIFORC.frc  
Field unit, magnetization unit, and FORC unit  
T,mAm2/kg,1e-3 Am2/(T2 kg)  
Field step of FORC measurements, first point offset, field measurements regularization  
0.0005015553545586107,0.00007597585780746107, False  
Last FORC begins at  
-0.16213794366264145  
Hc-range of data matrix  
0.00025,0.12075  
Hb-range of data matrix  
-0.121,0.063  
Data matrix size  
242,369  
Mesh size of data matrix  
0.0005  
origin of data matrix  
0.00025,0  
Weighted margin of regression rectangles  
2  
Horizontal smoothing factor (effective) and increase rate  
10.,0.09  
Vertical smoothing factor (effective) and increase rate  
10.,0.09  
Horizontal smoothing factor limit (effective), at given Hc, plus/minus  
None,0.,0.  
Vertical smoothing factor limit (effective), at given Hb, plus/minus  
4.,0.0004,0.0005  
[...]  
Mrs from FORC measurements and standard error  
3.897134730097964,0.0006913444803027636  
Mrs from backfield curve and standard error  
3.8496819505448734,0.0005754758112584479  
Coercivity distribution on linear field scale  
0.00025,20.167830708547697,0.5639101182919285  
0.00075,21.46670335540199,0.5089310775518388  
0.00125,22.778501821403644,0.4204904977933693  
0.00175,24.0655552590083,0.391853686875105  
0.00225,25.087941766374634,0.361261262798524  
0.00275,26.505976188888432,0.19585399003342707  
...
```

**Fig. 4.42:** Example of coercivity distribution file produced by CalculateFORC. Information blocks begins with a title (highlighted in blue), followed by a list of parameters. Coercivity distribution data begin after **Coercivity distribution on linear field scale**.

### Blocks 2-20: From “source files” until “ $M_{rs}$ from FORC measurements”

These blocks in the file header are identical to those of the output function file (see [section 4.6.1](#)).

### Block 21: Total magnetization obtained by integrating the coercivity distribution

This block contains the total magnetization obtained by integrating the coercivity distribution and the associated standard error. In case of backfield coercivity distributions, this magnetization corresponds to the saturation remanence  $M_{rs}$  and the block is titled  $M_{rs}$  from backfield curve and standard error. In case of reversal coercivity distributions, the listed magnetization corresponds to the total irreversible magnetization associated with the hysteresis loop and the block is titled Total irreversible magnetization at reversal field and standard error.

### Block 22: Coercivity distribution

This last block, entitled Coercivity distribution on a linear field scale, or Coercivity distribution on a log10 field scale, contains coercivity distribution data in a comma-separated, three-column format, without empty lines. In case of linear field scales, lines are of the form  $H_k, f_k, \varepsilon_k$ , where  $f_k = f(H_k)$  is the value of the coercivity distribution for the  $k$ -th field  $H_k$ , and  $\varepsilon_k$  is the corresponding standard error. In case of logarithmic field scales, lines are of the form  $\log_{10} H_k, f_k^{\log}, \varepsilon_k^{\log}$ , where  $f_k^{\log} = f(H_k) \ln 10$  is the value of the logarithmic coercivity distribution for the  $k$ -th field  $H_k$ , and  $\varepsilon_k^{\log}$  is the corresponding standard error.

Logarithmic coercivity distributions are defined over positive fields only. Therefore, the logarithmic reversal coercivity distribution is incomplete with respect to its linear counterpart.

## 4.7 Literature

- Acton, G.A., Q.Z. Yin, K.L. Verosub, L. Jovane, A. Roth, B. Jacobsen, and D.S. Ebel (2007). Micromagnetic coercivity distributions and interactions in chondrules with implications for paleointensities of the early solar system, *Journal of Geophysical Research*, 112, B03S90, doi:10.1029/2006JB004655.
- Egli, R. (2006). Theoretical aspects of dipolar interactions and their appearance in first-order reversal curves of thermally activated single-domain particles, *Journal of Geophysical Research*, 11, B12S17, doi:10.1029/2006JB004567.
- Egli, R. (2013). VARIFORC: an optimized protocol for the calculation of non-regular first-order curves (FORC) diagrams, *Global and Planetary Change*, 210, 302-320, doi: 10.1016/j.gloplacha.2013.08. 003.
- Harrison, R.J., and J.M. Feinberg (2008). FORCinel: An improved algorithm for calculating first-order reversal curve distributions using locally weighted regression smoothing, *Geochemistry, Geophysics, Geosystems*, 9, Q05016, doi:10.1029/2008GC001987.
- Heslop, D., and A. Muxworthy (2005). Aspects of calculating first-order reversal curve distributions, *Journal of Magnetism and Magnetic Materials*, 288, 155-167.
- Heslop, D., and A.P. Roberts (2012). Estimation of significance levels and confidence intervals for first-order reversal curve distributions, *Geochemistry Geophysics Geosystems*, 13, Q12Z40, doi: 10.1029/2012GC00 4115.
- Morrish, A.H. (1965). *The physical properties of magnetism*, Wiley, 1965.
- Newell, A.J. (2005). A high-precision model for first-order reversal curve (FORC) functions for single-domain ferromagnets with uniaxial anisotropy, *Geochemistry Geophysics Geosystems*, 6, Q05010, doi: 10.1029/2004 GC000877.
- Pike, C.R., A.P. Roberts, and K.L. Verosub (1999). Characterizing interactions in fine magnetic particle systems using first order reversal curves, *J. Appl. Phys.* 85, 6660-6667.
- Pike, C.R., A.P. Roberts, and K.L. Verosub (2001). First-order reversal curve diagrams and thermal relaxation effects in magnetic particles, *Geophysical Journal International*, 145, 721-730.
- Pike, C.R. (2003). First-order reversal-curve diagrams and reversible magnetization, *Physical Reviews B*, 68, 104424.
- Pike, C.R., C.A. Ross, R.T. Scalettar, and G. Zimanyi (2005). First-order reversal curve diagram analysis of a perpendicular nickel nanopillar array, *Physical Review B*, 71, 134407.
- Schlinger, C.M., D.R. Veblen, and J.G. Rosenbaum (1991). Magnetism and magnetic mineralogy of ash flow tuffs from Yucca Mountain, Nevada, *Journal of Geophysical Research*, 96, 6035-6052.
- Tauxe, L., T.A.T. Mullender, and R. Pick (1996). Potbellies, wasp-waists, and superparamagnetism in magnetic hysteresis, *Journal of Geophysical Research*, 101, 571-583.
- Winklhofer, M., Dumas, R.K., and K. Liu (2008). Identifying reversible and irreversible magnetization changes in prototype patterned media using first- and second-order reversal curves, *Journal of Applied Physics*, 103, 07C518.